PERFORMANCE EVALUATION OF FLEXIBLE FACINGS FOR SOIL NAILED SLOPES

Thesis submitted in fulfillment of the requirements for the Degree of

DOCTOR OF PHILOSOPHY

by

AMANPREET TANGRI

(176603)

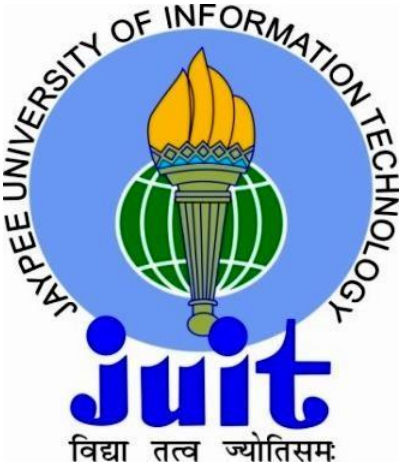

DEPARTMENT OF CIVIL ENGINEERING

JAYPEE UNIVERSITY OF INFORMATION TECHNOLOGY

WAKNAGHAT, SOLAN-173234, HIMACHAL PRADESH, INDIA

SEPTEMBER 2025

Contents

DECLARATION BY THE SCHOLAR

I hereby declare that the work contained in the Ph.D. thesis entitled **"PERFORMANCE EVALUATION OF FLEXIBLE FACINGS FOR SOIL NAILED SLOPES"** submitted at **Jaypee University of Information Technology, Solan, India** is an authentic record of my work carried out under the supervision of **Dr. Saurabh Rawat**. I have not submitted this work elsewhere for any other degree or diploma. I am fully responsible for the contents of my Ph.D. thesis.

Amanpreet Tangri

Enrollment No.:176603

Department of Civil Engineering

Jaypee University of Information Technology,

Solan-173234, Himachal Pradesh, India

Date:

JAYPEE UNIVERSITY OF INFORMATION TECHNOLOGY
(Established by H.P. State Legislative vide Act No. 14 of 2002)
P.O. Waknaghat, The. Kandaghat, Distt. Solan – 173234 (H.P.) INDIA
Website: www.juit.ac.in
Phone No. (91) 01792-257999
Fax: +91-01792-245362

This is to certify that the work reported in the Ph.D. thesis entitled **"PERFORMANCE EVALUATION OF FLEXIBLE FACINGS FOR SOIL NAILED SLOPES"**, submitted by **Amanpreet Tangri** at **Jaypee University of Information Technology, Solan, India,** is an authentic record of his original work carried out under my supervision. This work has not been submitted elsewhere for any other degree or diploma.

Date:

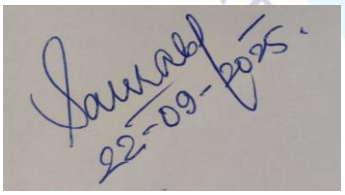

Dr. Saurabh Rawat
Supervisor -1
Associate Professor
Department of Civil Engineering Jaypee University of Information Technology, Solan Himachal Pradesh, India

Dr. Niraj Singh Parihar
Administrative Supervisor
Assistant Professor
Department of Civil Engineering Jaypee University of Information Technology, Solan Himachal Pradesh, India

ACKNOWLEDGEMENT

First and foremost, I wish to thank the Almighty God for providing me the opportunity, potential and all the strength to complete this task. With God's grace, I was able to complete my task with full dedication and sincerity. I would like to thank all those who supported me, helped me and guided me in every way they could do.

I would like to express my foremost gratitude and special appreciations to my Ph.D. supervisor ***Dr. Saurabh Rawat*** *for his tremendous encouragement, unconditional support, and guidance through his enlightening views on several issues related to my research topic.* ***Dr. Saurabh Rawat****, Associate Professor Jaypee University of Information Technology, Solan, Himachal Pradesh, India has always fortified me by his careful guidance and positive feedback during this entire study. He has supported and guided me to the right path, inspiring me for the successful completion of my research work.*

I am also thankful to my DPMC members ***Prof. (Dr.) Shruti Jain,*** *(Professor and Associate Dean (Innovation), Electronics and Communication Engineering Department, JUIT****, Prof. (Dr.) Ashish Kumar*** *Professor and HOD, Department of Civil Engineering, and* ***Dr. Saurav,*** *Assistant Professor (Senior Grade), Department of Civil Engineering for their valuable suggestions throughout my research work.*

Besides, I am also very thankful to my friends for helping me in numerous ways over the last seven years. I cannot forget the serenity of ***my parents, wife and kids*** *throughout my research work. It is only because of their support, love, and blessings that I could overcome all frustrations and failures.*

Finally, I would like to express my gratitude to all who were important in the realization of this work.

Thanks to all of you!

Amanpreet Tangri

LIST OF ABBREVIATIONS AND ACRONYMS

N_{60} - SPT N-value corrected for field procedures and apparatus

H- Height of wall

L – Length of Nail

B – width of Box

S_h- Horizontal Spacing of Nails

S_v- Vertical Spacing of Nails

C_u - Coefficient of Uniformity

C_c-Coefficient of Curvature

c - Cohesion

φ -Angle of internal Friction in degrees

β -Inclination degrees

d -Diameter in m

A - Cross section Area in m^2

α -Inclination of nail in degrees

EI - Flexural Rigidity in kN/m^2

AE/L - Axial Stiffness, kN/m

δ - Interface friction angle, degrees

N-Scale factor,

E_m - Elastic modulus of model

E_p- Elastic modulus of prototype

m- model

p- prototype

N1- Nail no.1 as so on for other nails

ΔR - Change in the resistance recorded

R- Resistance of the wheat stone bridge arms

$\sum c$ - Gauge factor

S- Strain gauge

D- Dial gauge

F- Strain Gauge at Facing

E - Young's modulus

ν -Poisson's ratio

ψ- Dilatancy angle

G- Shear modulus

R_{inter} – Strength Reduction Factor

E_{oed} - Oedometer modulus

F1- HDPE facing Net

F2- Polyester Geogrid

F3- Hex plastic Net

F4- Jute Geomesh

T_{FN}: Critical nail head strength

C_F: Flexure pressure factor

$M_{v,neg}$ and M_{vpos} : Vertical nominal unit moment resistance at the nail head and mid-span

C_s: Punching shear pressure factor

A_c: Soil contact area of cone-shaped block

A_{GC}: Cross sectional area of grout column

V_N: Nominal internal Facing punching mobilized stress.

E_s - Soil stiffness

I_m- Index

u- Pore water Pressure

P.M- Physical model Results

N.M- Numerical Modelling Results

List of Figures

List of Tables

ABSTRACT

Using steel components, a technique known as soil nailing retains soil while stabilizing steeply cut slopes and holding back the excavations. Soil nailing is a cost-effective method for building retaining walls from the top down and stabilizing pre-existing slopes. Steel tendons are drilled and grouted into the soil as part of this soil reinforcement procedure to form a composite mass that resembles a gravity wall. In soil nail slopes, a flexible structural facing is a middle alternative between soft and hard facing. They are frequently applied on moderately steep cut slopes with a slope angle of 33 to 70 degrees. The stress-strain behaviour as well as displacement in both the lateral and vertical directions were examined in the current study using a physical model that was built. Two type of nail arrangements were considered in the present research. The results of the FEM investigation were subsequently validated using the Plaxis 3D application. The results were compared, and it was shown that the soil nails can, in some cases, endure tensile loads and are helpful for stabilizing the slope. The current study investigated four flexible facing HDPE Facing net, polyester geogrid, Hex plastic net and Jute geomesh. The primary goal of the current research is to identify some replacement materials which could be resist the stresses in the field. Thereafter the results were compared with the rigid facing and check for various parameters such as lateral deformation, vertical displacement, nail forces, bending moment and Facing Punching mobilized stress. HDPE facing net was able to absorb higher surcharge load as compared to the other facing materials as HDPE has taken up 18.80%, 30.18% and 46.43% more surcharge than Polyester geogrid, Hex plastic net and Jute Geomesh respectively in rectangular arrangement. On comparison of Surcharge pressure for both the arrangement the increase in surcharge was 9.56%, 9.03%, 11.08% and 26.38% for HDPE facing net, Polyester geogrid, Hex plastic net and Jute Geomesh respectively for staggered arrangements. The facing strain increases with the increase of surcharge and are found to be higher in upper set of nails and similar trend is found with respect to height. The nail forces were higher in the case of HDPE facing and it was found to be 14.42%, 26.33% and 48.28% higher for Polyester geogrid, Hex plastic net and Jute Geomesh respectively in rectangular arrangement. The surface settlements during drainage were higher near the crest of slope as compared to other points and were higher for Jute geomesh in both cases by 8%, 13.04%, 21.73% and 56.52 % for hex plastic net, Polyester geogrid, HDPE facing net and rigid facing respectively for rectangular arrangement. The bending moment was noticed higher in HDPE facing slope as compared to other flexible materials as it was 4.88%, 5.66% and 27.70% for Polyester geogrid, Hex plastic net and Jute Geomesh respectively. The

Facing punching mobilized stress was found higher in Jute Geomesh and it was higher by 6.95%, 24.68% and 30.26% for hex plastic net, Polyester geogrid and HDPE facing net respectively. The facing displacements were lower in rigid facing by 18.18% as compared to HDPE facing net. The nail tensile forces were higher in rigid facing by 12.63% as compared to HDPE facing net. The bending moments in rigid facing were comparable with HDPE facing but higher than other facing materials. The Facing Punching mobilized stress was reduced by 54.69% on utilizing rigid facing as compared to Jute geomesh facing and 35.03% as compared to HDPE facing. The Flexible facing like HDPE facing net might be advantageous in cases when the slope is between 60 and 70 degrees in the field and could be considered in the conditions of temporary structures or structures of less importance and rapid development needs.

***Keywords**: Soil Nail wall, Plaxis 3D, Physical Model, Facing Material*

1. INTRODUCTION

1.1 General

This chapter gives an overview of the soil nail technique and the significance of its various components. The chapter bring out the issues prevalent with the conventional facing generally used for soil nailed structures. The chapter highlights the role of facing in the transfer of load and mechanism of a soil nail structure. The chapter ends with the objectives established for the present research work and the thesis organization.

1.2 Soil Nailing Technique

The concept of drilling hole, inserting passive metallic strips/steel bars, subsequent grouting with a final shotcrete layer as facing has been utilized for stabilizing weal slopes since the early 1960s[1]. The inserted passive reinforcement is commonly known as 'soil nail' and the technique is referred to as 'soil nailing technique'. The widely used soil nailing technique follows a 'top – to – down' construction methodology[2]–[5][6][7]–[10]. The step – wise construction of a traditional soil nail slope is shown in Figure 1.1

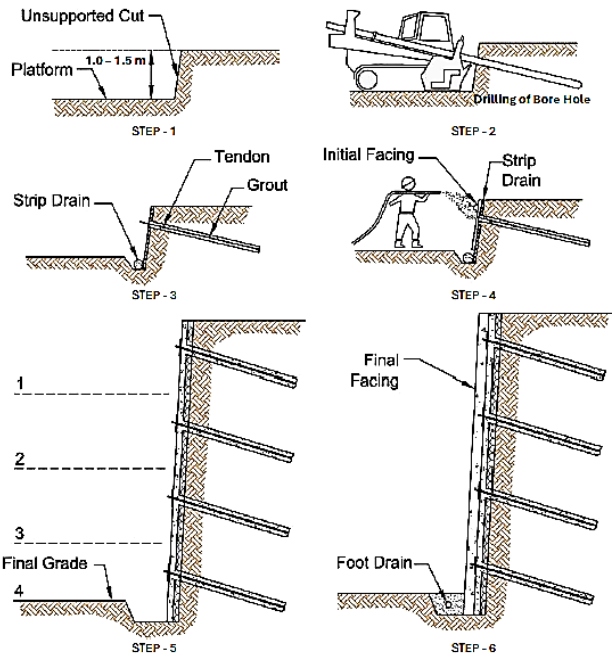

Figure 1.1 Stepwise construction of Soil Nailed Slope

Step – 1 includes the excavation of the first phase of top – to – down construction. The favourable soil condition for such excavation comprises of dense to very dense sand or gravel with 10 – 15% of fines. The presence of fines is significantly important to withhold the

unsupported excavated vertical or nearly vertical face of 1.0 – 1.5 m for one to two days. Alternatively, the presence of capillary water is also beneficial as it provides the necessary apparent cohesion., with a recommended value of a minimum of 10 – 14 kN/m^2 for an unsupported excavated height of 1.2 m [11]. Other such favourable site conditions for soil nailing are weathered rocks, fine – grained soils depicting SPT N_{60} – values ≥ 9 blows/30 cm, silty clays, sandy clays, and sandy silts. Soil nailing has also been identified as a successful technique for stabilizing slope of well compacted structured engineered fills consisting of a mixture of more than 90% of well-graded gravel and fine-grained soil with plastic index of less than 20 [11], [12][13][14].

Step – 2 comprises of drilling of bore holes using specialized drilling equipment. The bore hole drilling can be both cased and uncased strictly depending on the site conditions. The drilling equipment can be selected as rotary, percussion, auger, and rotary-percussion drilling depending on the ease of availability and site conditions.

Step – 3 deals with the placing of threaded steel tendons (nails) and its subsequent grouting. Fe 415 and Fe500 grade steel bars of diameter ranging between 20mm – 36 mm are generally used as soil nails. The maximum length of soil nail used for available diameter is about 12 m with the provision of extending the length using couplers. The design of soil nail length generally depends on the height of the unsupported wall (H) and taken as 0.5H to 0.8H[15]. Apart from the traditional soil steel tendons, hollow steel bars having with wall thickness of 7mm to 25 mm can also be used as soil nails. The soil nails are installed at inclinations varying from 0 - 15° with the horizontally to ensure flowing of grout through the entire bore hole depth and all around the steel tendon [11]. The inclined installation also serves another critical aspect of placing the steel tendon in area of maximum tensile strains developed during failure. Beyond 15°, the steel tendons are found to lie in zones with compressive strain, which ceases the mobilization of tendon – to – grout and grout – to – soil interface friction [16]. Prior to insertion in the drill hole, the steel tendon is protected against corrosion by one of the methods such as hot – dip galvanization, High density polyethylene (HDPE) or poly vinyl chloride (PVC) corrugated sheath covering or fusion bonded epoxy coating [11], [17].

Tremie grouting is carried out using clean cement grout under low nominal pressure of 0.3 to 0.6 bars or under gravity. The cement grout generally comprises of water to cement ratio ranging between 0.4 to 0.5. The minimum allowable 3- day and 28 - day strength in compression of grout is 10 N/mm^2 and 21 N/mm^2, respectively [11], [17]. In case of highly permeable granular soils, stiffer grout (slump of 30 mm) is also allowed. Post grouting, the soil

nail head becomes the most critical section susceptible to corrosion due to the partial filling of grout above and bottom of the nail. This section called as the 'bird's beak'[17] is grouted manually or during the facing placement.

In order to comply to the alignment of the inclination of the drilled hole and soil nail, centralizers are placed at regular interval of 3 m along the tendon length and 0.5 m away from both the ends of the tendon, prior to its insertion [11]. These PVC or steel centralizers ensure the placement of the tendon at the centre of the drilled hole, contributes in maintain uniform grout cover through the tendon length and facilitates the insertion of tremie pipe during grouting.

The construction step terminates with the placing of vertical geo composite strip drains. The strip drains are placed between adjacent soil nails and are unrolled from top to bottom as the installation progresses. Each strip drain is connected to a PVC outlet pipe at the bottom excavation lift which is further connected to the drain pipe running below the soil nailed structure or weep holes for discharging the accumulated pore water pressure.

Step – 4 revolves around the placing of initial facing. The initial facing generally involves shotcreting a layer of thickness 75 – 101 mm on the reinforced frontal surface of the soil nailing structure. The reinforced surface is prepared by placing welded wire mesh (WWM), horizontal and vertical reinforcement bars around the protruding threaded nail end. The process of shot creting is generally achieved by dry mix or wet mix shotcreting, with the latter being prominently utilized. Moreover, the wet mix shotcrete often results in only 5% loss of shotcrete rebound against 15% as recorded for dry mix shotcrete. Nevertheless, the rate of 'shootability' and 'pumpability' for wet mix is also greater in comparison to dry mix shotcrete. As per FHWA, 2015,[11] the rate of application per hour using dry mix shotcrete ranges between 1.15 – 2.3 m^3 which increases up to 1.5 – 3 m^3 for wet mix shotcrete. Additionally, wet mix shotcrete also provides more flexural strength and durability to the finished face in comparison to dry mix shotcrete under similar water/cement ratio of 0.4.

The quality of shotcrete is governed by the amount of cement used in the shotcrete and the in – situ density[11], [17].The percentage of cement content determines the 'shootability' and 'pumpability' of the shotcrete whereas the compressive strength depends on the in – situ density of the shotcrete. It is observed that the in – situ density which primarily reflects on the percentage air voids in shotcrete leads to a decrease of 15% in the compressive shotcrete strength for 1% air voids[11]. Furthermore, the brittleness of the shotcrete and the consequent crack propagation can significantly be arrested using reinforcement. The shotcrete and

reinforcement coupling are found to increase the toughness, ductility and impact resistance of the shotcrete facing.

The reinforcement comprises of Welded Wire Mesh (WWM) with specified aperture size and cross – sectional area which satisfies the norms of flexural and punching resistance. The WWM are generally available in rolls and hence the WWM panel size to be used is determined based on the site space constraints. However, a traditional thumb rule for selecting the panel width is based on the vertical soil nail spacing on the respective excavation lift. For lap splice between successive WWM panel between lift, an extra one full mesh panel is used[11] . Alternatively, a set of vertical and horizontal steel bars (Waler bars) of diameter ranging between 8 mm – 25 mm are used on either side of the soil nail to increase the flexural resistance of the initial facing. The procedure for initial facing is continued for the following excavation lifts with soil nails, till the required soil nail depth is completed as shown in Figure 1.1 (Step 5).

STEP – 6 The final construction step involved deals with the placing of a shotcrete layer of thickness of 152 mm – 304 mm over the initial facing which constitutes the final facing. The soi nails are connected to the initial facing by using a square shape steel bearing plate of size 200 mm – 255 mm [11]. The bearing plate is attached to the threaded nail end using a washer and a hex nut. For inclined soil nails, bevelled washers, spherical seat nuts and bearing plates with concave openings are used to perfectly match the inclination of the nail and slope.

The 19 mm – 25 mm thick bearing plate serves the purpose of distributing the nail forces to the initial facing and retained soil mass behind the soil nailed structure. The square shaped bearing plate is connected to the initial facing by using headed studs which are welded at the four corners of the plate. The 25 mm – 38 mm diameter headed studs eventually gets embedded in the final facing. These headed studs are contributing to development of interaction between the soil nail and final shotcrete facing layer.

1.3 Failure modes of soil nailed structure

Nevertheless, slope stabilization using soil nails poses advantages such as quicker installation, requirement of smaller right of way, multi – purpose installation equipment, construction without significant disruption to the prevalent traffic or surrounding structures, performs well in seismic conditions and high tolerance to the slope deformation in comparison to its counterparts such as retaining walls/anchored walls (FHWA. 2015)[11][18]–[20][21], [22]. However, the soil-nailed structures are verified for strength, serviceability, and extreme limits. The serviceability assessment is primarily governed by the reinforcing action of the soil nails by evaluation of the FOS (factor of safety) for global and internal stability[23]. Likewise, the

extreme limits are examined for seismic conditions, lateral slope deformation and settlement[24][25], [26]. The limit state for strength has two aspects: Geotechnical and Structural. The geotechnical limit state is dependent on the lateral sliding and pullout resistance of the soil nails, whereas the structural limit state is governed by the failure of nail under tension and facing failures[27][28]. The failure occurring in facing are mainly related to the flexural failure, punching shear failure and failure of headed studs under tension as shown in Figure 1.2, 1.3 and 1.4.

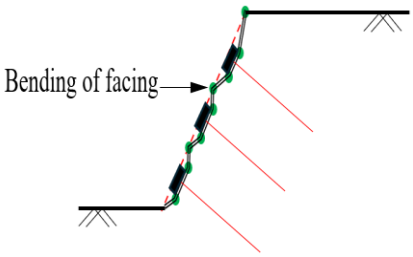

Figure 1.2 Flexure failure

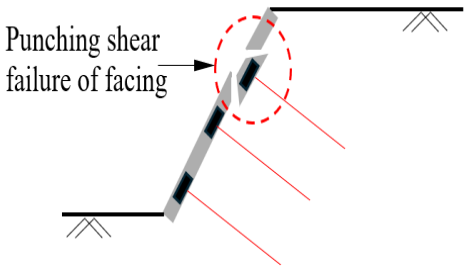

Figure 1.3 Punching Shear failure

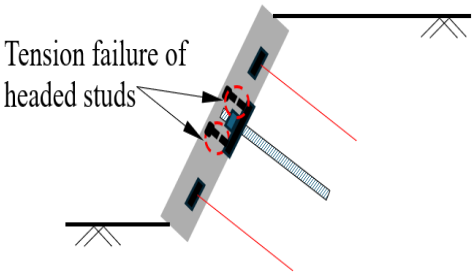

Figure 1.4 Tension Failure in headed studs

1.4 Load – Transfer Mechanism in soil nails

The primary role of a reinforcing element in soil is to provide tensile strength through the soil mass during failure. The maximum development of tensile stress in the reinforcing element can only be achieved in elements located in the zones of tensile strains during failure [16]. These locations in the soil nailed slopes can be harvested by installing the reinforcing elements at inclination of 0-30° with the horizontal and with length such that they intercept the failure plane[15][16][29]–[31]. The soil and the soil nails behave as a composite unit with their interaction being governed by friction. Therefore, the interface shearing resistance governed by the soil friction angle and generated tensile or compressive forces due to the normal stress plays a significant role[32]. Based on these stress states, the soil – nail interaction leads to the development of tension or compressive forces in the longitudinal soil nail direction and shear and bending in the transverse nail direction[16] [33]. The inclusion of soil nails, reduces the slope deformation by increasing the shear strength of the soil nailed slope and enhances the stability by mobilization of shearing resistance at the soil – nail interface [15], [34][35]–[37].

With the lateral slope deformation, the tensile stresses are mobilized in the soil nails which are a function of the tensile strength of the soil nail. A parabolic tensile stress distribution with its peak estimated to be occurring at the location of intersection with a hypothetical slip surface is

generally assumed. Likewise, the intersection points between the parabolic stress distribution and assume slip surface for all the subsequent nails divides the retained soil mass into active and passive zones[38][39][40], [41]. The slope movement near the soil nail head due to the active zone is resisted by the nail components and facing. This lateral deformation causes soil nails to displace both in the axial and transverse directions. The length of nail located in the passive zone provides the shearing resistance against this pulling force and is called as 'Pullout resistance'. However, the pullout resistance is smaller than the maximum soil nail tensile stress. The pullout resistance depends on the length of soil nail beyond the failure surface which is generally smaller than the nail length lying in the active zone. The maximum limiting value of mobilized tensile stresses in nail depends upon the maximum interface friction value of the soil – nail interface [42][43], [44]The transverse nail displacement mobilizes the shearing and bending forces in nail. The maximum limit for shearing and bending are basically equal to the bearing capacity of soil. However, due to the small slenderness ratio of nails, bending stresses are not considered during calculation [11].

The developed active earth pressure behind the slope face is primarily handled by the soil – nail interaction even in the active zone. Simultaneously, the facing with the nail bearing plates and headed studs provide the confinement against the slope deformation. The facing and its components add to the growing shear strength of the retained slope and mobilized tensile stresses along the nail. However, it is evident that the remaining tensile strains around the facing are significantly smaller than those developed beyond the facing along the nail length. Thus, facing is mainly considered for containment and protection role in a soil nailed slope. [45]–[48]

1.5 Problem Statement

The failure of a soil nailed slope is basically combination of internal and external failure. Though the external failure can be analysed using limit equilibrium method for safety against bearing and sliding, internal failure modes include the analysis of nail tendon – grout bond strength, grout – soil bond strength, nail tendon pullout resistance, facing and nail head strength. The backfill – facing interface is subjected to non – uniform lateral earth pressure during the lateral deformation of the slope. Moreover, the development of tensile nail forces significantly contributes to the global stability of the soil – nailed structure. The nail tensile forces generated at the nail heads are dependent on the facing element [49]and accounts to 60 – 70% of the active earth pressure at the backfill – facing interface [13], [50], [51]. In fact the

nail head tensile forces are used in designing of facing element[11]. Traditionally, shotcrete facing with WWM, vertical and waler bars provided sufficient confinement against slope deformation and erosion. Such facings classified as rigid/hard facing[52] are well suited for steep slopes or vertical cuts. Although the high facing stiffness contributes to improve the bending resistance but capitulates under punching shear failure. Moreover, without proper drainage, the behaviour of the shotcrete is significantly disturbed. Therefore, identification of alternative facing materials commonly termed as 'flexible facing' can be investigated for its response under flexural and punching shear failure, resisting lateral slope deformations, its effect on the development of nail tensile forces and eventually the slope stability of the reinforced slope. [53]–[55]

1.6 Types of Facing Elements for Soil Nailed Slopes

As per EN 14490:2010[52], facing elements for soil nailed slopes can be classified into three categories as:

- Hard Facing
- Flexible Facing
- Soft Facing

Hard Facing

The facing element classified as 'hard' is also known as 'Permanent facing'. The term 'hard' means that the facing element has sufficient rigidity to withstand the bending stresses and deformations due to the lateral earth pressure behind the facing[4], [33], [56].

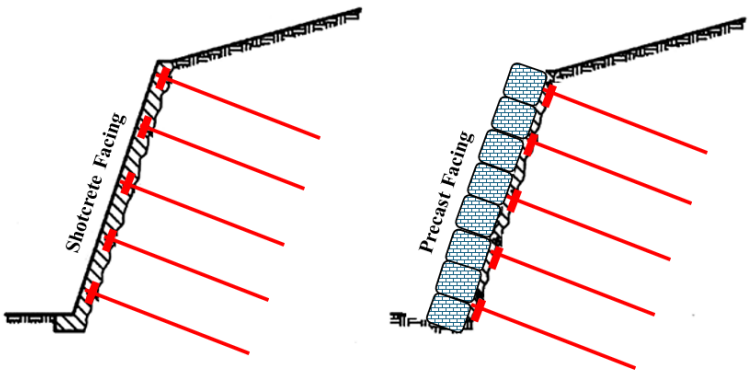

Figure 1.5 Constructed hard Facing (a) Shotcrete (b) Precast Panels

This type of facing is constructed by forming a layer of shotcrete on the frontal area of the reinforced slope with additional reinforcements provided in form of WWM, horizontal and vertical bars (Figure 1.5a). Alternatively, precast concrete panels used for facing also falls under this category (Figure 1.5b).

Flexible Facing

In this type of facing, a flexible material is placed on the outer surface of the soil nailing wall which helps in transferring the load from the nail surface to the nail head. The term "flexible" refers to a material having sufficient elasticity so that it can accommodate the deformation of the slope without reaching failure. The selection of flexible facing is dependent on the slope angle, soil frictional angle, height of the soil nailed slope and the nail head tensile force[57]–[61].

The conventional flexible facing type generally employed are High – Tensile Steel Wire Mesh with erosion control mats [52], [56], [62]–[65], steel wire mesh/ spiral rope nets, Geosynthetics mainly geogrid [33] or composite facing consisting of Galvanized wire mesh with geotextile [61].

Figure 1.6 Flexible high tensile wire mesh wall Installed at Z-Morh Tunnel, J&K, India

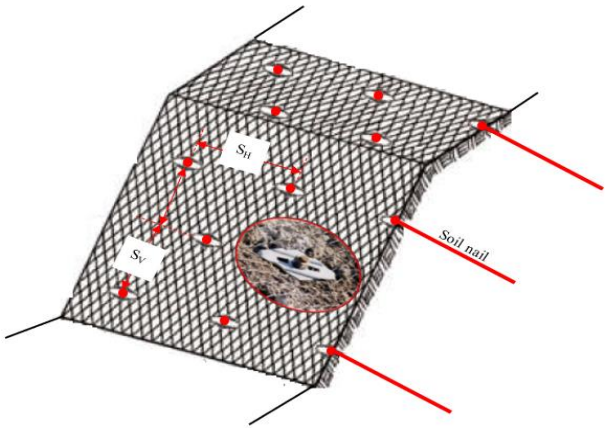

Figure 1.7 A typical flexible high facing High tensile wire mesh with nail components

Often flexible facing is also referred to as flexible structural facing[33] [66] due to its dependency on the size of bearing plate, stiffness of nail and spacing of nails. A typical flexible facing on an actual site application in shown in Figure 1.6 and flexible facing element is shown in Figure. 1.7.

Soft Facing

When the facing element is used for the sole purpose of erosion control, soil containment and promote vegetative growth without contributing to the any load transfer for slope stability is referred to as soft facing[52][33]. These facing elements are recommended for shallow slope angles varying from 24 - 30° [2], [11], [33]wherein the connected soil nails heads only contribute to fixing the facing on the slope face. The serviceability of these facings is entirely governed by the vegetative growth. The commonly used vegetation for such facing comprises of shrubs, grass, seeding using seeded geotextiles or hydro seeding [33] Figure 1.8. The available soft facing elements are coir mats, light metal mesh, cellular geosynthetics, geogrids, and geomembrane sheets.

Figure 1.8 Vegetative cover on soft facing at Birahi, Uttarakhand

1.7 Objectives

As mentioned in Section 1.6, several facing alternatives are available for soil nailed structures primarily governed by their contribution in the head nail tensile stresses during slope deformation. The conventional ‘hard facing’ is amongst the most common facing type due to is pronounced performance even in steep slopes. However, for moderate to shallow slopes of less sensitive regions, a provision of substituting ‘hard facing’ with ‘flexible facing’ can be

employed, provided its structural assessment is found to be satisfactory during internal stability. Based on this research idea, the following objectives are determined:

1. To study the effect of different facing materials (HDPE facing nets, Hex plastic net, Polyester Geogrid and Jute Geomesh) on the soil nail strains and facing strains with rectangular and staggered nail spacing under varying surcharge pressure through testing of lab-scale soil nailed model slopes.

2. To examine the effect of facing stiffness on flexural strength, facing punching mobilized stress behaviour of facing and retained slope deformation (Lateral and Vertical) through model testing.

3. To evaluate the performance of slope with different flexible facing materials through numerical modelling using finite element (FE) method (Plaxis 3D) and validating the numerical results against experimental data.

4. To compare the performance of different flexible facings with conventional hard facing based on results from experimental and numerical modelling.

1.8 Contribution

The contribution of the present research work can be evaluated from the fact that prevalent soil nailing design manuals such as FHWA, Geoguide 7, Geotechnical Engineering Office, 2008), EN 14490:2010 (2010), CIRIA 2005 [11], [17][16], [67][68]–[70][71]only focuses on accurate prediction of the ultimate capacity of the entire reinforced system, with limited calculations regarding the direct facing response. Moreover, the reported calculations are based on simplified earth pressure distribution specifically for 'hard' facing elements only. As per the Lazarte et al 2015, the main reason for limited facing design information available in the FHWA (Federal Highway Administration) manual for Design and Construction monitoring of soil nail walls can be attributed to the following statement '*our understanding of the magnitude of the face loadings developed in soil nailing application is not as good as our knowledge of the maximum loads developed within the nails'* is due to '*the quality of field monitoring data is poor'*. Nevertheless, the existence of provisos adds to the limitations of these methodologies and restricts the application of these existing design methods within the proven construction scenarios. These methods, thus have a limited competency in comprehension of behaviour of flexible facing elements.

The reported literature available on flexible facing elements is predominated by high tensile wire mesh with soil nails [61] at field scale and with combinations of wire mesh + geotextile [61], [72], aluminium facing [60], [73]–[75], perpex sheet facing [76], woven geomembrane [77] etc. Moreover, all these reported studies focused only on the horizontal deformation of the flexible facing and development of corresponding tensile forces in the nails.

Therefore, the assessment of the flexible facing elements in respect of strain development in nail, facing and under varying surcharge loading provides a new dimension to the overall soil – nail reinforcing mechanism. The flexural and facing punching mobilized stress evaluation of polyester geogrid, Hex plastic mesh, HDPE geonet and Jute geomesh reflects on the potential use of these alternative flexible facing materials in required site conditions[6], [78][78], [79]. The comparative study of the used flexible facing materials against the traditional hard facing also contributes in better comprehension of serviceability of flexible facing. The results and conclusions can also be helpful in developing design methods for flexible facing system in soil nailed structures.

1.9 Organization of Thesis

Chapter 1: The chapter outlines the general soil nailing technique with focus on the various forms of facing elements available. It covers the in – depth construction process for soil nailing of slopes with the adopted design criteria. The chapter dwells into the load transfer mechanism which is essential to bring out the significance of 'facing' in the reinforcing mechanism of soil nails. With the discussion on the novelty aspect of the present research work, the chapter enlists the objectives of the study. The chapter ends with the organization of the thesis.

Chapter 2: The chapter deals with review of the literature on large-scale field testing and small-scale laboratory model testing. It also provides information on earlier analytical, and experimental research done to comprehend the soil-nail relationship.
The chapter includes a summary of the literature review along with the research gaps that were looked into.

Chapter 3: This chapter focusses on material and methodology aspect. The discussion about the testing of various materials like soil, steel and flexible materials. The methodology is discussed to perform various tests using facing material and measurement of nail strain, facing strains, vertical deformation and lateral deformation. This chapter includes the procedure followed for numerical modelling using Plaxis 3D and various steps involved in the same.

Chapter 4: The findings from the model testing and numerical modeling are covered in this chapter. This section also presents a comparison and discussion of important findings from the results of model testing and numerical modeling. Additionally, this chapter offers validation using previous literature for both numerical modeling and model testing.

Chapter 5: The outcomes of physical testing and numerical modelling of various soil-nailed slopes using flexible and rigid facing materials are covered in the sixth chapter.

2. LITERATURE REVIEW

2.1 General

One method of improving the ground is to reinforce the soil mass with soil nailing. Steel bars are passively inserted into the soil mass at predetermined spacings as part of the soil nailing process. Soon after the New Austrian Tunnelling Method introduced the technique for rock excavation support in the 1960s, it became well-known in Germany, France, and the US. The use of soil techniques is expanding worldwide as time goes on. Using this technique, a borehole is drilled into the soil slope, and the cement grout is then placed into the borehole. After that, the wall face is shotcrete and the tendon head is secured with a bearing plate.[80], [81][37], [49], [74]

The soil-nail interaction, which determines a nail element's pullout resistance, is a crucial component of soil nailing. Numerous variables, including the type of soil, the applied surcharge pressure, and the nail geometry, affect the soil and nail interaction mechanism. Therefore, when these parameters change, so does the soil and nail interaction. As a result, the mechanisms underlying helical soil nails that vary according to soil type, geometry, and surcharge pressure become more intricate[42], [81]–[84].

It is advised to install a tensile member into the unstable soil in order to increase the soil's tensile strength. Thus, reinforcing action tensile members enhances the in-situ soil's overall shear strength, because a soil nail acts within two zones of soil that form during failure, it is referred to as a passive inclusion[85], [86].

The unstable soil in the active segment is disturbed and has a tendency to collapse, causing axial displacement along the soil nail that spans the active-passive zone. Equal and opposing resistance forces have been produced in the nail's passive region as a result of axial displacement in the active region. Nail members are therefore referred to as post-tensioned elements. Nail elements that are frequently used include spiral, helical, bamboo, fibre-reinforced polymer, conventional, and spiral soil nails. Soil nails are primarily divided into two groups according to how they operate and how they are installed. It consists of driven nails and grouted nails, also known as conventional nails[5], [87], [88].

One way to think of a nailed slope is as a composite structure made of facing walls, gout, nails, and soil. Due to the intricate interactions among these elements, which make soil nailing

research challenging, the majority of prior research has been focused on one or more of these elements.

2.2 Nail Parameters, Spacing and Orientation effects on Soil Nailing

A nail is a basic component of soil nailing, and determining the length and spacing of nails is a crucial step in the design process. It is well known that a nail force can reduce the primary strain in soil by bonding or causing friction with the surrounding soil. This improves soil stability and reduces soil displacements. Therefore, it is crucial to comprehend the mechanism underlying the interaction between soil and nail as well as how this interaction affects enhancing slope stability[75], [89]–[92].

In order to investigate how a variety of reinforcements affected the mechanical response of the soil to the applied stress, Jewell (1986)[15] conducted a number of direct shear tests on reinforced soil. He demonstrated that when the direction of the reinforcements matches the soil's minimum normal strain, the reinforcements are used most effectively. According to research by Bruce and Jewell (1986)[15], soil nails are installed horizontally or sub horizontally to act in tension, which improves the soil's shearing resistance. The reinforcement increases strength best when it is angled across a potential soil rupture surface, acting in tension. At other orientations, the bars offer less benefit and may even decrease the soil mass's shearing resistance if they act in compression.

Alston (1991)[93] conducted a study on building a Soil-Nail Slope Reinforcement Project in part of Eastern Canada Using Geogrid and Geocomposite in which soil nailing system was to permit the development of a slope with height of 18m among which 12m of slope was permanent and 6m was temporary. In the research work the soil nail system was designed based on NCHRP report which relied on tensile forces in soil only and no benefit for shear resistance of nails across a potential sliding surface was allowed. The minimum yield strength was ensured to be 415MPa for steel bar and diameter of steel bar was 22mm or 25mm depending upon height of slope. it was concluded from the present study that the unfaced portion of the permanent slope suffered surface deterioration and slumping, and the surface profiling was lost through a succession of minor slumps in the face[65], [86], [94].

Taek (2002) [95]considered two types of stainless stell bars for the nails which were 200mm long and 3mm in diameter and other one was 300mm long and 3mm in diameter, the study examined failure load by various front plate rigidities, displacements at the wall and tensile forces acting at the nail head. The failure load with 10-degree insertion angle was 11.18%

larger than the load at failure of zero-degree insertion angle. Chin (2004) [96]conducted study on various failure modes for soil nailing were discussed and were categorized into four types i.e nail tendon failure, pullout, face failure and overall failure or slope instability. The size of grouted hole was usually in the range of 75mm to 50mm, the tensile strength of nail in order to resist force and to stabilize the slope depends on diameter of the bar and the type of steel used. The smallest possible nail size considered was 25mm as smaller size may cause installation problems, the grout cover should be minimum 12mm but as far as practical purposes 25mm is recommended. Further from FHWA[11], it is recommended that 50% of the active force applied to the nail is derived from field observations of typical nail spacing, which varied from 0.75 to 1.8 meters.

Shiu and Chang[69] in 2005 presented Geo report no 197 and in the study's findings, a soil nail's inclination may have an impact on how strong it is. A rise in the inclination of the soil nails would result in a decrease of the reinforcing forces within the nails, which would diminish the stabilizing effect. Axial compressive forces may be activated in soil nails with a steep incline. The nailed structure's stability would be diminished by the compressive forces. The displacement characteristics of nailed excavations are influenced by nail length patterns. More can be done to reduce horizontal displacement when soil nails are positioned in the upper portion of a nailed structure during a staged excavation. The stability of the structure is improved more by those placed in the lower section. Shear and bending resistance of soil nails under working conditions do not significantly affect the system of forces that keep the soil-nailed structure stable. Shear and bending action may contribute more, but not significantly, even as failure conditions are approached. Compared to shear and bending, the efficiency of soil nails used in axial tension is significantly higher[68], [70], [97], [98].

Giacon[33] (2010) discovered that for orientation of soil nailing to be successful, that must closely match the primary tensile strain field of the soil. Nails are normally positioned in rows at a small inclination, below the horizontal of 5-20 degrees, with a maximum of 1-2 meters between the nails on the horizontal and vertical axes.

Three structures with identical soil and elemental parameters are represented by the first three models that were developed and implemented. (mechanical, geometric, and spacing characteristics), but with varying slope inclinations of 45°, 60°, and 75°, respectively.

According to Sanvitale et al. [4](2013), the nails were positioned in four horizontal and three vertical lines, with a 10.2 cm vertical and 13.2 cm horizontal spacing. The nails were composed of long, 6 mm-diameter aluminum tubes with a 1 mm thick layer of glued sand covering them.

The experimental results indicate that both flexional and axial stiffness affect a soil nailing system's performance during excavation and collapse.

Rotte and Viswanadham (2013)[60], [73]–[75] carried out the research work to investigate the impact of nail inclination and type of facing material on the deformation and stability of soil nailed slope. Two types of nail inclination were adopted i.e 10 degree and 20 degree with the horizontal plane. Three rows and three columns of nails were positioned with a 70 mm horizontal gap between them. The soil nail was a 200 mm long aluminum tube with an outer and inner diameter of 6 and 5 mm, respectively, from the results obtained it was found that nail forces were on higher side from a slope stabilized with soil nail inclined at 10 degrees than 25 degrees. Further the crest settlements for the nail inclination of 25 degrees were found to be 4.1% of height of slope and for nail inclination of 10 degree it was 2.6% of the height of slope.

Sanvitale (2013)[59] carried out research work on threaded bars in natural unstable slope, many tests were carried out using different facing types, which varied in stiffness and continuity, in an effort to increase overall stability. With a vertical spacing of 10.2 cm and a horizontal spacing of 13.2 cm, 4 horizontal and 3 vertical lines were nailed in place. A 1 mm thick layer of glued sand was covered by 32.5 cm long aluminium tubes that were used as nails. Based on the findings, it was determined that flexional and axial stiffness affect how well a soil nailing system performs during excavation and collapse.

Viswanadham and Rotte (2015) [74]conducted study on the nails made up of aluminium tubes 6mm in diameter and thickness of 0.5mm. A layer of epoxy coating of thickness 1.25mm was done by utilizing standard sand. The length of nail considered was 6mm with angle of inclination of 10 degrees with horizontal with spacing of 60mm*60mm. The present research focus on two types of facing material and based on the results the Slope facing, it was determined, is one of the most crucial elements of a soil-nailed slope and is useful in enhancing stability and deformation behaviour when exposed to seepage. Yazdandoust[99] in 2017 has conducted the study on seismic behaviour of soil structure which is mostly determined by how nails are arranged, including how nails are spaced apart, how nails are distributed in elevation, and how long nails are in relation to wall height (L/H). In the present research the nail spacing was kept as 0.2m, similar in both horizontal and vertical direction. It was found that shear modulus increases with increment in value of L/H ratio, that means the walls with longer nail will behave more rigidly as compared to shorter nails.

In the current study, a full-scale experimental soil-nailed wall 7.5 meters high was constructed in order to assess the environmental, financial, and mechanical performance of the novel construction method in comparison to the traditional shotcrete technique. Bui et al. 2020

[55]took into consideration that the vertical spacing between two horizontal rows of reinforcement should be 1.5 meters, and the horizontal spacing should be 2 meters. It was found that the new technique uses about 64% less concrete than shotcrete construction, which wastes a lot of concrete because of rebound on steel meshes, poor adhesion to the draining complex or the ground, and out-of-profile drilling brought on by soil excavation and ground disturbance during the installation of soil reinforcements. Additionally, the new method reduces the amount of steel rebar required for the facing by approximately 22%.

Razavi and Bonab (2016)[100] has studied the soil nailed wall under various service loading conditions. The behaviour is examined in order to examine the effects of the following i.e soil shear strength; nail length distribution; nail vertical spacing; and nail elasticity modulus. The findings might be helpful in designing soil-nailed structures. Three models with evenly spaced nail lengths are taken into consideration in order to examine the key aspects of the relationship between nail length and vertical spacing (SV). The vertical nail spacing for the "high," "mid," and "low" models ranges from 2 to 1·3 and 1 m, while the nail lengths vary from 7·3, 6·2, and 5·5 m, respectively. It is assumed that the nails are spaced horizontally by 1.5 meters. As can be seen, employing longer nails increases zone 1's extension while increasing zone 1's rigidity when using more nails.

Aluminum tubes with an outer diameter of 5 mm and a thickness of 1 mm were used in the current study to simulate the reinforced wall's nails. The impact of nail arrangement on the behavior of convex corner soil nailed walls was examined by Moradi (2020) [90]. The soil-nail models had an elastic modulus of 69 GPa and a yield strength of 100 MPa, respectively. On the models, 150- and 200-mm nails were used. The horizontal splaying of the soil-nails had a major effect on the deformation pattern of the walls. The soil nails were able to tolerate wall deformation as much along their axis as possible because of their axial resistance.

2.3 Laboratory and Field Testing

Physical models tested in laboratories offer more realistic conditions that account for the influence of unknown factors originating from the soil mass[101]. In this section various physical model developed for soil nailing would be discussed.

Taek (2002)[95] conducted the testing in the laboratory on a model to examine the impact of front plate rigidity on the soil nailed body by nail length, inserting angle of nail and location of surcharge load. The dimensions of apparatus were 130cm long, 60cm width and 60cm deep soil tube. The surcharge loading plate was 60cm long and 20cm wide. Alongside with this five LVDT’s and one 5-ton capacity load cell was used to measure the load applied. It was

concluded from the study that soil nailed body with various pate rigidity shows similar trends and in order to properly analyse the nail front plate intersections for different plate rigidities various lab and field test ae required with varying load and nail conditions.

Sanvitale et al (2013)[4] discussed about a model, 40 cm in height and 39.5 cm in width, with an 80° wall dip angle (Figure 2.1). To determine which stiffness—axial or flexional—mostly influences the soil nailing behaviour during excavation and the subsequent plate loading, six tests with different facing types were carried out. The models were brought to failure in three stages after they were fully configured: Applying a uniform load of 24 kPa on the plate; Excavating four wooden blocks one at a time, mimicking front excavation; and applying an increasing uniform load on the plate until it fails.

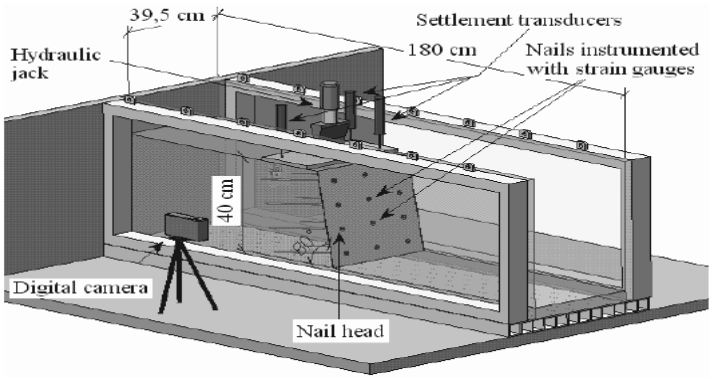

Figure 2.1 Schematic view of Physical Model

Pokharel et al (2011) [61]carried out testing on a box that has three fixed sides and a fixed base. On the front side, there are detachable steel channel sections that are 15 cm tall and fastened with nuts and bolts. The box measures 2.2 meters by 2 meters by 2 meters (L × B × H) of a normal soil nail wall featuring a nail distance of 5 feet by 5 feet (1.5 m*1.5 m) was the model for the physical test. To replicate the impact of an extra wall height above the unit under test, a surcharge was added. Based on the finite difference modeling, significant deformation was anticipated; as a result, a wire mesh (chain-link) form of facing was chosen since it was anticipated to result in the least amount of deflection among the flexible facing options. The figure 2.2 below depicts the front view of the geotechnical box and soil nail wall.

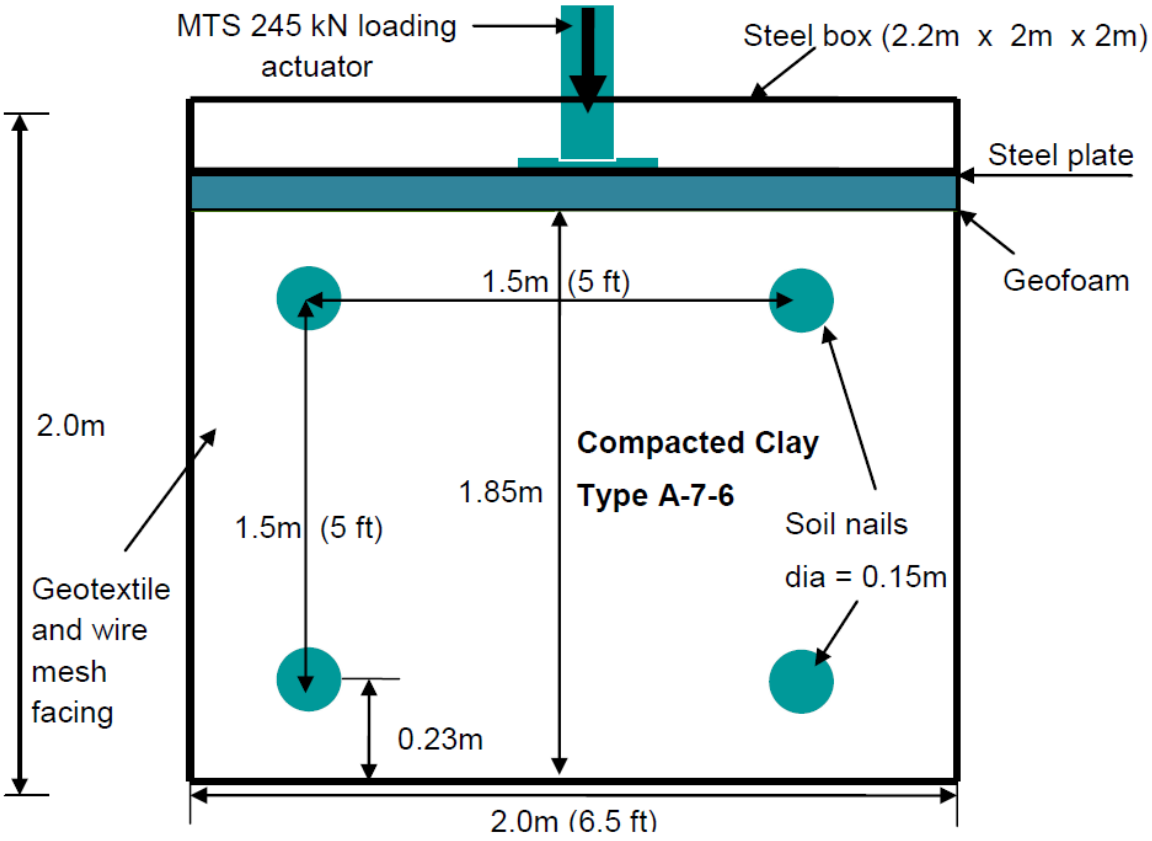

Figure 2.2 Front view of soil nail wall

Rotte and Viswanadham (2013) [73]created a slope model at normal gravity, a sturdy box with internal measurements of 760 mm in length, 200 mm in width, and 410 mm in height was employed. A seepage tank, a solenoid valve, and a pore water pressure transducer (PPT) within the seepage tank made up this system. A stand pipe was placed at the bottom of the seepage tank to keep water from overflowing the slope and to keep the water level there steady. To aid in downstream drainage, a toe drain was placed at the strong box's right end. The outlet was kept open for the duration of the test, allowing water that had seeped into the centrifuge chamber to escape[73]–[75], [102]. This configuration made it feasible and is depicted in figure 2.3 below:

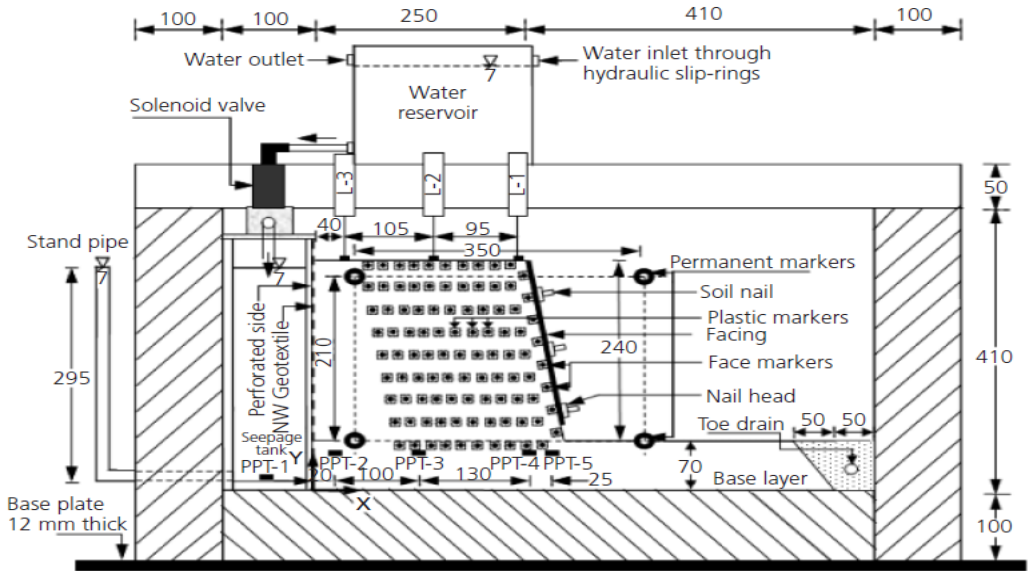

[73]

Figure 2.3 View of model soil-nailed slope

According to Viswanadham and Rotte (2015)[74], considered a box measuring 0.76 m by 0.20 m by 0.41 m for the experimentation. Deepa and Viswanadham (2009) discussed the remaining specifics of the strong box as well as the process to lessen friction effects and approximate plane strain conditions. During the tests, seepage of water through soil nailing slopes was enabled via a seepage simulator unit. On the inside of the Perspex sheet, a permanent marker grid measuring 350 mm by 210 mm was securely adhered. Using moist properly compacted soil at its maximum dry density and Optimum water content, layers of 30 mm thickness were used to build the 240 mm high model slope. Using the same soil, a 70 mm thick base layer served as the foundation for the slope model. The box setup is shown below

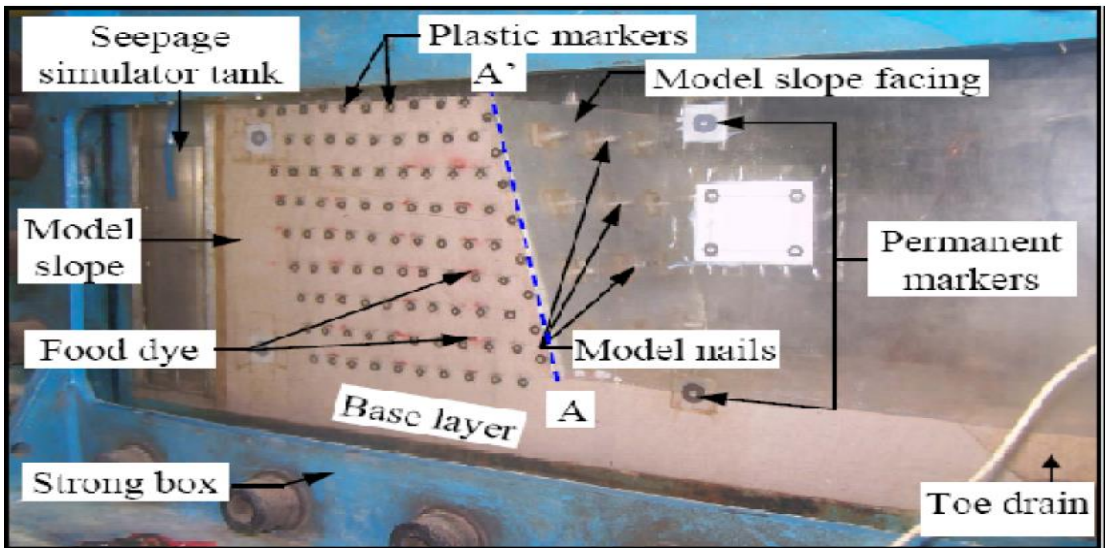

[102]

Figure 2.4 View of model soil-nailed slope

Rawat and Gupta (2017)[29] considered a model tank in their study measuring .60 m in length, .40 m in width, and .60 m in height is constructed using Perspex sheets with a thickness of 12 mm. Bolts hold the Perspex sheets to the iron angles. Iron strips brace the tank's sides to prevent sheets from deforming laterally while being tested. Slope deformation failure of the modelled screw nail soil slopes is tested by increasing the surcharge load at the slope crest. A steel plate with a plan area of 20 cm by 40 cm and a thickness of 4 mm is placed on the slope crest to guarantee an even distribution of load.[30], [31] The model for testing is shown in Figure 2.5 below

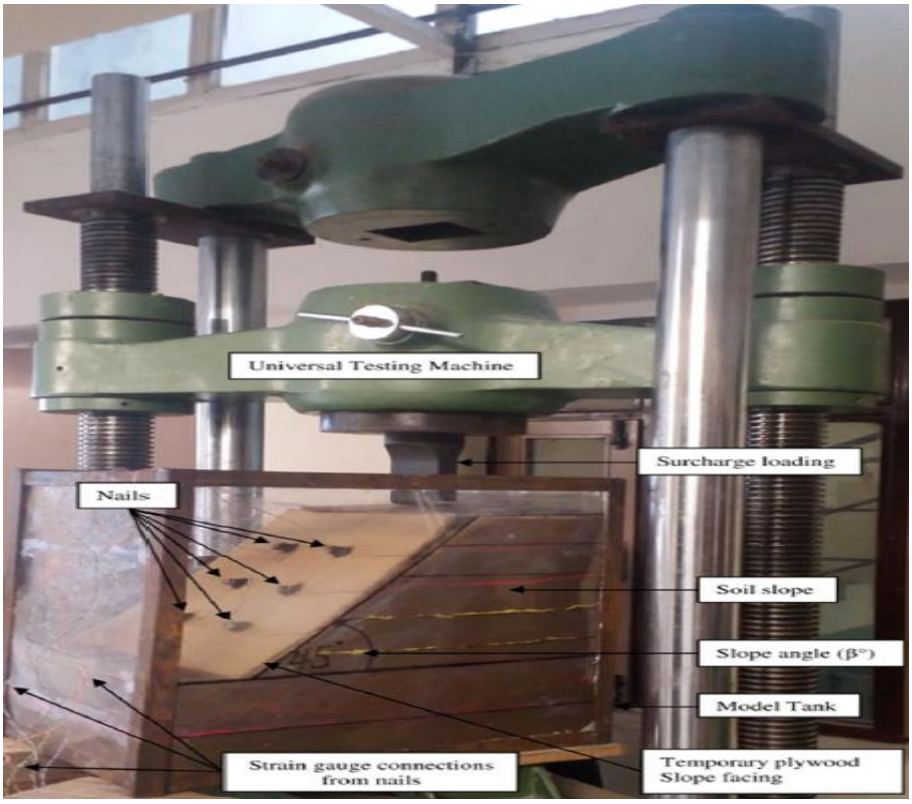

Figure 2.5 Soil Slope model set up

Moradi et al. (2020) [103] conducted study on the 130-g-ton beam centrifuge with a 2.7-meter radius—the geotechnical centrifuge at Tehran University—was employed. The basket offers a platform that is 0.8 meters wide and 1 meter long. possesses the ability to accelerate up to 1.5 tons of cargo under 100 g. The test model was constructed from 10-mm-thick stainless-steel plates with inner dimensions. 570 mm in width, 500 mm in height, and 800 mm in length. To make it easier to take pictures of the model while it is being tested in a centrifuge, a transparent Plexiglas sheet with a thickness of 40 mm is positioned on one side of the container. The centrifuge tests were carried out to assess the effects of two different soil-nail patterns on wall deformation as well as the behavior of a right-angled convex corner. Nail into a wall at a 45°

angle or perpendicular to the wall facing (PDD). The reinforced wall's ability to control horizontal deformation was not well achieved by soil nails arranged in a PDD pattern. In order to improve performance, the percentage of the nail length in the soil resistance zone behind the failure plane should be taken into account When figuring out the plan view nail pattern. The cross section of model is shown in following figure 2.6 below.

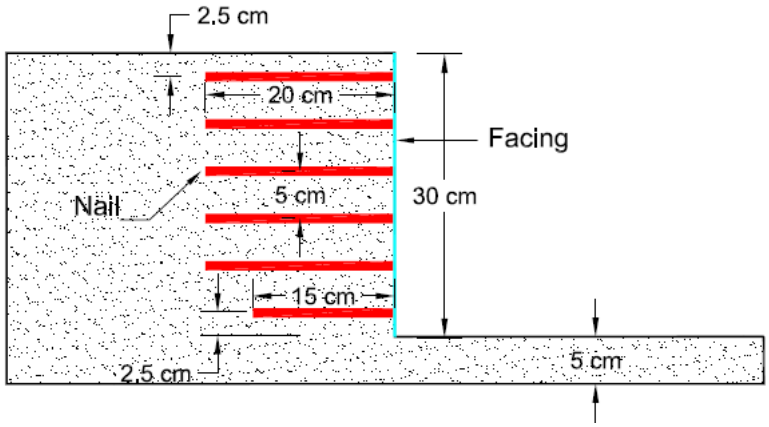

Figure 2.6 Cross section of Test model

2.4 Facing Material for Soil Nailing

Soil nails are not only used to stabilize the surface soil when they are used to build a new slope or stabilize an existing one. Head plates and/or a facing are used for this along with nails. It is necessary to implement and incorporate separate methods with the soil nail system in order to preserve the surface (and near-surface) soil. The internal failure mechanisms can be altered by the facing system, which can be soft, flexible, or hard, but facing type and slope angle are related (shallow angle can be constructed without a facing system, while steeper angles require hard facing).[104]–[107]

Generally, a facing is necessary, and when choosing one, one must take the site's limitations, the environment, and aesthetic standards into account. As was previously mentioned, the primary function of the facing is to stabilize the ground's surface and near-surface depth in the space between the nails. It offers the retained soil between the nail head locations lateral confinement. By shifting the soil load from the soil nails to the nail heads, flexible structural facings give the face of a soil-nailed structure long-term stability. The facing materials allow for more soil movement, so some slight bulging between the head plates is expected; however, as nail spacing gets closer together, the bulging becomes less noticeable[57], [58], [108], [109]. Commonly utilized materials include coated metallic meshes that are suitably engineered for the structural loads and durability requirements, in tandem with the head plates. As the failure

of the three-dimensional blocks between the nails can transfer potential out-of-balance forces to the facing, the facing needs to be built to withstand such forces. The flexible facing should be installed following the installation of soil nails but prior to the subsequent excavation stage in order to minimize degradation of the slope face. Similar to soft facing, in order to shorten the facing's span, intermediate or secondary pins are typically needed in between the nails. The design should specify the pins' length. The flexible facing needs to be fastened firmly at the top, ideally over the nails in the upper row[110]–[112].

Whenever a flexible structural facing is utilized, a vegetation layer is typically applied. The soil nail face slope, where the flexible structural facing is located, is prevented from degrading and softening by the application of a vegetation layer or soft facing. The installation of flexible facing has been shown in below figure by Barley et al. 1993[113]

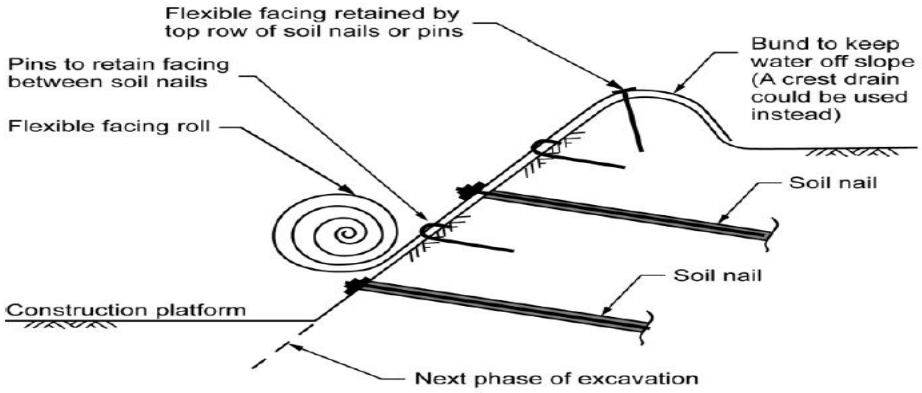

Figure 2.7 Schematic Diagram of installation of Flexible facing

Alston (1991) [93]There were three methods for facing the slope. In the first one a sand, topsoil, and the water slurry were injected behind the nonwoven geotextile facing in one system to act as a void filler and tension the membrane. The facing was held in place by geogrids fastened to the soil nails. In a second section of the slope, a geocomposite wall was built in front of the slope reinforced with soil nails, and geogrid was used to tie the wall to the soil nails. The third system was used on the temporary slope and comprised a single geotextile membrane that was woven and fastened to the soil nails using anchor blocks. Two winters and two spring thaws have shown that the reinforced slope is satisfactory.

The choice of flexible facing in a soil nail wall depends on various factors, including the soil conditions, expected ground movements, and project requirements. It is important to consult with a geotechnical engineer or a qualified professional to determine the most suitable facing system for a specific soil nail wall project. Singh and Babu (2009)[90] examined the soil nail walls' dependability analysis because basement construction uses soil nails. The stability of soil

nail walls under the influence of variations in soil properties was the main focus of the research. It was discovered that the soil nail wall's stability was significantly impacted by the shear strength parameters. Thus, a more accurate perspective for the evaluation of the soil nail wall was given by the reliability analysis[2], [98].

Pokharel et al (2011) [61]conducted the study in which Concrete was replaced with a flexible facing made of steel mesh. For surcharges of roughly 5 psi, the finite difference model predicted significant vertical and horizontal deformations. The flexible facing products fared well in strength tests; however, there were significant vertical and horizontal deformations in the facing, which were in line with numerical modeling. These findings suggest that the use of flexible facing in place of reinforced concrete should be restricted to non-critical structures where significant horizontal and vertical deformations are acceptable.

Sanvitale et al (2013)[4] has carried out six tests using different facing types to determine whether stiffness—axial or flexional—mostly influences the behavior of soil nails during excavation and the subsequent plate loading. Four facings covered the entire excavated front: A steel plate measuring 4 mm in thickness; b) a brass sheet measuring 0.25 mm in thickness; c) a steel mesh consisting of 1-mm wires welded perpendicularly at 6 mm intervals (MESH); d) a steel net consisting of 0.24 mm in diameter wires woven perpendicularly (NET). The remaining ones consist of two discontinuous facings made of PMMA rectangular tiles (produced by cutting a PMMA cover that was comparable to test as. The covering ratio in these circumstances that is calculated by dividing the total covered area by the total facing extension is equal to 95% (PMMA95) and 25% (PMMA25). The mechanical properties of these materials are mentioned in table below:

Table 2.1 Mechanical properties of various facing Materials

Model	Facing	Covering ratio (%)	Thickness/ Wire Diam. (mm)	Wire spacing (mm)	Young modulus E (GPa)	Axial stiffness EA/m (N/mm)	Flexional stiffness EJ/m (Nmm^2/mm)
a	PMMA	100	4	-	3.2	12800	17066.67
b	MESH	100	1	6	210	26180	3318.06
c	BRASS	100	0.25	-	126	31500	236.25
d	NET	100	0.24	1.02	70	3105*	22.66
e	PMMA95	95	4	-	3.2	-	-
f	PMMA25	25	4	-	3.2	-	-

From the results it was concluded from study that lack of continuity in the facing can limit the mobilization of shear stress along nails by keeping the front's flexional stiffness from causing

it to deform during excavation. Furthermore, horizontal front displacements can also be regulated if the facing exhibits low axial deformability but flexional deformability.

Rotte and Viswanadham (2013)[73] had considered two varieties of facing materials were chosen and put into modeling. These were an aluminum plate and a 230 mm by 198 mm sheet of plaster of Paris (PoP) that had been mixed with polyester fiber. It was found that a soil-nailed slope with fiber-blended PoP facing had high crest settlements and a longitudinal facing crack along the bottom row of nails for an identical slope and nail parameters. On the other hand, it was noted that the soil-nailed slope with aluminum facing was stable and showed very little deformation. Therefore, the type of facing material and stiffness affect how soil-nailed slopes that experience seepage deform. Viswanadham and Rotte (2015)[74] has considered two varieties of facing materials were chosen: aluminum sheet with a thickness of 2 mm and woven geotextile. Aluminum sheet was modeled as stiff facing and woven geotextile as flexible facing. Drilling into the slope facing was done using a 9 mm diameter hole bit in accordance with the nail arrangement meant for a soil-nailed model slope that was to be tested. The necessity of slope facing and the impact of slope facing stiffness on the performance of soil-nailed slopes exposed to seepage are the subjects of centrifuge model studies presented in this paper. As per the results it was concluded that with Sc/H = 0.226, a soil-nailed slope without facing saw 1.63 m of crest settlement. On the other hand, the maximum crest settlement on both the soil-nailed slopes with stiff and flexible facing was only 0.145 m, with Sc/H = 0.02. This suggests that one of the most crucial elements of a soil-nailed slope is the slope facing, which also helps to improve the slope's stability and deformation behavior when seepage occurs[60], [73]–[75]

Bui et al.,2020 [114]discussed about various projects carried out in recent years for various configuration sites and soil-nailing designs were examined in light of the process's industrialization. An ideal solution seemed to be to standardize the precast panel surface area to 3 square meters. Two horizontal rows of reinforcements were spaced 1.5 meters apart vertically and 2 meters apart horizontally in the geotechnical design of the soil nailing for the project's execution. The wall geometry and geotechnical conditions determine the length and tension of the reinforcements. So majorly the focus was on precast elements and their connections, so obviously they would be able to provide much safety to the structure as compared with the flexible material. The precast component is shown in figure below-

 [114]

Figure 2.8 Standard Panel

Table 2.2 Summary of various facings in Literature

Source	Wall Type	Facing Type	Number of Data	Nail Length (L)	Nail Inclination Angle	Nail Diameter (d)	Horizontal Spacing (S)	Vertical Spacing (S)	Facing Inclination
Wentworth (1994)	Swift-Delta S1	Shotcrete	5	6.4	15-25	127	1.4	1	90°
Wentworth (1994)	Swift-Delta S2	Shotcrete	5	6.4	15-20	203	1.8	1	85°
Peasmarsh	Geogrid	Shotcrete	5	12	15-25	127	1.5	1	75°
Guernsey	Geogrid	Shotcrete	5	15	15-20	127	15-175	1.5	75°
I30R-SA	Shotcrete	5	6	15	15-20	152	0.75	0.75	80°
I30R-SB	Shotcrete	5	12	10	15-25	203	0.75	0.75	80°
San Bernardino Left and Right	Shotcrete	8	6	15	15	152	1	1	85°
Cumberland Gap 1988	Shotcrete	5	12	12	15-20	152	0.75	0.75	85°
F-78 Albertson (Grids 24 & 33)	Concrete Panel	5	10	10	10	100	1.5	1	90°
Davis Wall	Shotcrete	5	15	10	15-20	152	1.5	1	80°
Oregon 13A-S2	Shotcrete	5	12	15	15-20	152	15-19	0.9-0.155	75°
Oregon 13A-S2	Shotcrete	5	10	10	10	100	1.5	0.9-0.155	85°
New York Wall	DPT Wall	Shotcrete	5	10	15-25	152-305	0.6	0.5	80°

Landau Associates Inc. (1939)	Geogrid	Shotcrete	2	8	15-20	152	1.5	1	75°
Menkiti and Long (2008)	DPT Wall	Shotcrete	5	10	15	152	1.5	1	80°
Holman and Tuzzo (2008)	New York Wall	Concrete Panel	5	15	15-20	150	1	1	85°
Wei (2013)	IH40 T/A & 7B	Concrete Panel	19	7	7 -8.5	150	1	0.5	90°
Sanvital et al. (2013)	1g small physical model	NA	8	0.32	20	6	0.13	0.1	80°
Viswarradhan & Rottos (2016)	Small-scale models	20mm thick	9	0.6	10	6	0.6	0.6	63.43°
Bucher et al. (2018)	Large scale R&D project	Diamond sheet	14	2	10	32	3	3	60°
Moradi et al. (2020)	Centrifuge model tests	Polycarbonate	6	0.15-0.20	5	0.5	0.05	0.05	45°

So as far as facing type is concerned, many of the researcher has focused on the shotcrete or conventional techniques and very few have dealt with the flexible facing materials so due to this region the present research work is focused on finding out alternate material which could be suitable for the steep slopes.

2.4 Numerical Modelling

In order to comprehend the interaction mechanism, stress distribution, and serviceability of the soil and nail element, numerical modeling techniques are widely used. Numerical models are established to assess the strength of soil nails based on laboratory and field tests. Many researchers conducted different parametric studies to investigate the numerical analysis for behavior of nails along with facing material[115], [116][117][118].

The study conducted by Giacon (2010) [33] was having primary goal to comprehend the behavior of a soil-nailed structure with a flexible facing in order to determine when and under what conditions it is a financially sensible solution. Because of this, it's critical to comprehend how each component of the structure functions to ensure the structure's stability. In order to do

that, analyses comparing various facing types were also conducted. While thousands of soil nail structures have been built all over the world, very few of them have been instrumented to guarantee appropriate performance and support design procedures (FHWA, 2015)[11]. Numerical modeling techniques like finite element and/or finite difference methods should be used to adopt a higher level of analysis in situations where greater confidence is needed. The degree of accuracy in numerical modeling depends on several factors, including the caliber of the data collected, the estimation of in-situ stress and soil stiffness, and the availability of reliable case histories for model calibration[119].

Lengkeek and Bruijn (2009)[5]In the present research work the concept of soil nailing is utilized in dike reinforcement. The verification of the results was done using Plaxis 3D, Foundation Modelling the soil nails as embedded piles. The design calculations of soil nailing were done using Talren and Plaxis 2D. As a result, it was concluded that this technique of soil nailing is a cost effective and feasible technique. Singh and Babu (2009)[98] studied the simulation of soil nail structure using the plaxis 2D. Soil nailing technique is majorly considered for soil stability. The efficiency of such structure depends upon resultant of interaction of soil- structure components such as soil, nails and facing. In this research plaxis 2D was used to study soil nail structure[98].

Jaya and Annie(2011)[120] has utilized the pseudo static approach for numerical investigation of nailed vertical soil wall. In this study the dynamic forces are being replaced by equivalent static force which is acting along the centre of gravity. It was studied by using plaxis 2D that on increment in the length of nail from 0.5m to 0.6m there was increase in the factor of safety by 7.34%.[120]. Siavash (2012) [121]studied the soil nail walls under seismic conditions in 3D. The numerical simulations were carried out for soil nail walls under vibration input. The results obtained were compared with statical loading. The analysis was compared with statical loading[24]. The analysis was performed by using FLAC 3D. The deformations of wall vary with wider range under static and dynamic loading. The tensile loads produced were less by 50% in static manner as compared to dynamic manner[121].Tang[122] (2019) The present study involves Plaxis 2D to generate geometrical models and Finite elements Grids. In the process of deep foundation pit excavation, the horizontal displacement of foundation pit was studied and was compared with simulation results which were very relatively close enough and it was studied that the results were satisfactory[122].

To mimic the behaviour of various soil nail slopes with steel wire mesh, a number of FLAC finite differences models were built. Giacon used FLAC3D was used for the soil nailed wall

numerical modelling. The majority of the times, flexible facing was the type of facing for which numerical modelling was conducted. To replicate the various behaviours of various slopes, seven models were created. These models included the effects of various facing types, the effects of various slope angles to the horizontal, and the behavioural effects of varying nail spacing. These findings suggest limiting the application of soil nail walls with flexible facing in sand to low- to medium-inclined walls where noticeable deformations are acceptable. Although it doesn't directly contribute to the wall's stability, flexible facing systems can be preferred over hard facing systems in certain situations due to their ability to support vegetation growth and consequently have less of an adverse effect on the environment. The equivalent static force acting along the wall system's centre of gravity takes the place of the dynamic force acting on the soil nail wall in the pseudo-static approach. Utilizing PLAXIS 2D, by Jaya and Annie (2011)[120] a finite element analysis of the soil nail wall was carried out to examine the behaviour of wall displacements and axial force on nails. The FS values of the soil nail wall increased by 7.34% when the length of the nails was increased from 0.5 m to 0.6 m.

Viswanadham and Rotte (2015) [74]has utilized PLAXIS 2D, a geotechnical finite element code, This study included a finite element analysis (FEA) of slopes reinforced with soil and nails, both with and without slope facing. The investigation that is ongoing is limited to a plane strain problem. Boundary conditions similar to those in centrifuge model tests were selected with regard to prototype dimensions. The analysis was conducted in three stages: the first three being gravity loading, plastic drained analysis, and safety analysis. FEA results show that both stiff facing and soil nails can improve the stability and deformation behavior of soil-nailed slopes. Moreover, it is found that the force mobilization pattern on a slope with stiff facing is different from that on a slope with flexible facing that is soil-nailed.

This may be explained by stiff facing interacting with nail heads to mobilize sufficient bearing strength. The results of physically observed centrifuge tests were found to be in good agreement with the slope models with and without slope facing using finite elements.
FLAC3D was used for the soil nailed wall numerical modelling by Pokharel (2011)[61]. Under 15 psi, several surcharge levels were modelled numerically. The failure surcharge determined by the physical test and the results of the 4 and 5 psi surcharge loading were nearly identical. Under long-term loading conditions, these observations are consistent with those from the finite difference modelling. It is evident from comparing the results that there was additional settlement between the nails, bulging between the nails, and some crumpling/sagging behaviour in the space between the upper nails for both the model and physical test, both of

which had significant deformations for a 5-psi surcharge. Phan and Gui (2019) [92]conducted a study to give the designer additional options so they can choose design parameters in a reasonable manner. Utilizing the La Son – Tuy Loan Highway improvement project in Vietnam as an example, a number of numerical analyses have been carried out to look at the previously mentioned factors. The findings of this study should help determine a more cost-effective building technique that would increase the effectiveness of using soil nails to reinforce the slope.

Krupa and Prasad (2020) [119] used PLAXIS to create finite element models to study bearing plate behavior in relation to horizontal fixity, vertical fixity, and total fixity at the nail and facing junction. When compared to the no fixity condition of the soil nail system, the results demonstrate that the development of axial forces along the length of the nail is significantly influenced by horizontal and total fixities and less so by vertical fixities. It is also mentioned that the axial forces inside the nails will decrease in the presence of both total and horizontal fixities.

Lehn (2020)[107] A first numerical study on an over-steepened slope is presented in this paper. The fundamental modelling techniques and the numerical system are explained. The importance of the soil's shear strength on deformation and load-bearing behaviour is examined using a 3D numerical model. As cohesion decreases, the entire slope stabilization system deforms more severely. The design methods used today compute the slope stabilization's ultimate limit state but do not predict deformation. As a result, there is no analytical method for confirming that such a system is serviceable. The numerical investigations presented in this publication represent the initial phase of an ongoing research endeavour aimed at validating and enhancing the analytical calculation methodologies.

To assess the likely impact of the facing on wall stability, two finite element models were created in OptumG3: a convex corner and a plane strain model by Moradi et al. (2020)[123]. The only structural component incorporated into the numerical models to examine its impact on wall behaviour was the wall facing. The test models of centrifuges had the same geometric dimensions. Tensile force mobilization in the facing's sides and soil confinement in the corner zone are responsible for the convex corner's increased stability. The substantial increase in wall stability at the convex corners caused by wall facing is indicated by the strong agreement between the experimental and numerical analyses.

In the study "Effect of Construction and Design Factors on the Behaviour of Nailed-Soil Structures" by Mauricio Ehrlich et al. (2021)[124], the authors investigate the effect of various construction procedures on the performance of soil-nailed structures, using a combination of

experimental data and numerical modeling. The research compares two main excavation procedures for soil-nailed walls. The first Procedure involves small-width incremental excavation. Excavation is carried out in steps, where each step involves soil excavation followed immediately by nail installation and shotcreting. This procedure results in minimal stress relief during excavation, thereby minimizing deformations and improving stability where as in second Procedure, each level is fully excavated before nail installation and shotcreting was performed. This method allows for greater deformation of the soil mass before reinforcement is applied, which leads to higher lateral displacements and mobilization of nail tension.

The study concludes that first Procedure leads to better performance, resulting in lower lateral displacements and more effective load distribution along the nails. Delayed nail installation i.e in second procedure promotes increased soil movement, which can negatively affect the overall stability of the structure.

2.5 Research Gaps

1. Previous reported literature on Flexible Facing - focussed only on assessing
   - Slope deformations (Lateral and Vertical)
   - Development of tensile nail forces
2. While previous studies have focused on the general performance of soil-nail systems, limited attention has been given to the evaluation of strains on the facing, which may play a critical role in the overall stability of the structure.
3. Limited studies have explored the role of facing stiffness in soil-nail systems, there is a significant gap in the literature regarding the specific impact of facing stiffness on the flexural and punching mobilized stress of flexible facings.
4. While the importance of drainage in stability of soil-nailed slopes has been investigated by previous studies such as Deepa and Viswanadham (2009), Idiculla and Dasaka (2019), with reported construction procedures for drainage with rigid facings given by Lazarte et al., (2003) and FHWA (2015). However, studies related to the influence of flexible facing systems on soil nailed slope drainage behaviour and consequently seepage-induced reinforced slope deformation remains virtually non-existent. Hence, assessing the impact of flexible facing on drainage aspect of a soil – nailed slope may be considered for investigation.

5. While the influence of soil nail spacing and varying surcharge on facing performance is recognized, further investigation is needed to understand the specific mechanisms and quantify their effects under different conditions.

3. METHODOLOGY

3.1 General

Essentially, this chapter addresses experimental setup, materials used and about methods adopted in the present study. Further it contains the details about fabrications, nail arrangements, material properties and various instruments used in the study. The testing was performed on various facing materials and were compared with the rigid facing. The methodology for determination of strain, pore water pressure and displacements has been considered in this chapter.

3.2 Material Testing

The following subsections provide a brief description of the materials used in this study.

3.2.1 Soil

The soil considered for the study was collected from Punjab province's Mohali region and testing was conducted to classify the soil. The initial testing was carried in order to classify the soil and determine various soil properties. The field moisture content was determined by oven drying test as per IS 2720 part 2, the specific gravity test was performed on oven dried soil by using pycnometer test as per IS 2720 part 3, thereafter light compaction test was performed in order to ascertain the characteristics of compaction, such as the maximum dry density (MDD) and the optimal moisture content (OMC). To ascertain the soil's grain size distribution, the sieve size analysis was performed. A series of sieves were arranged in descending order, the soil that was collected from the site had lumps, which were reduced by pulverizing it carefully so that only the lumps were broken and no particles were crushed. One kilogram of oven-dried soil is fed through the sieve stack that is clamped in the sieve shaker. For ten to fifteen minutes, the automated shaking is performed, and the mass retained on each sieve was recorded. As per the values of Coefficient of uniformity and coefficient of curvature the soil is categorized as poorly graded sand (SP). The value for cohesion and angle of shearing resistance were calculated by direct shear test. The Table 3.1 below lists soil characteristics, and Figure 3. 1 shows the analysis of the soil through a sieve.

Table 3.1 Soil properties

Properties	Values

Moisture Content (%)	11
Specific Gravity	2.56
Optimum moisture content (OMC) (%)	7.3
Maximum dry density (MDD) (g/cc)	1.98
Coefficient of Uniformity	5.6
Coefficient of Curvature	0.64
Unconfined Compressive Strength (kg/cm^2)	0.118
Cohesion (kPa)	2.1
Angle of Shearing Resistance (degrees)	37
Soil Classification as per ISCS	SP

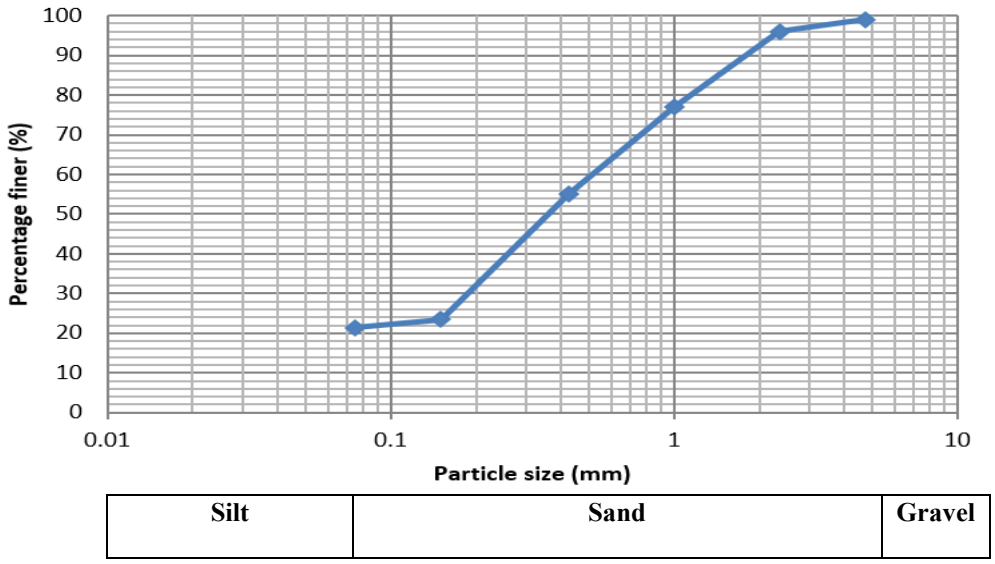

Figure 3.1 Grain Size Analysis of Soil

3.2.2 EDX and SEM testing on Soil

Soils are intricate mixtures of organic matter, minerals, water, gases, and living things. There are many variations in the size, shape, and chemical makeup of soil minerals. By examining a variety of microscopic traces, the scanning electron microscope (SEM) fitted with an energy dispersive x-ray (EDX) makes it easy to define the soil morphology and mineralogical composition of rocks or soils as well as to calculate the absolute surface area of each soil.

Every mid-energy X-ray that is gathered during a single analysis period is simultaneously displayed by the EDX detector system. The X-ray energy is represented as a spectrum, which is a plot of the number of counts against the X-ray energy histogram. Semi-quantitative and semi-qualitative data are both included in the spectrum. The area beneath the peak indicates the number of atoms of the element in the irradiated area. An element can be identified by its energy and position in the spectrum. In addition, X-rays are generated when the specimen's atomic nuclei's electrostatic fields slow down the electron beam.

SEM test is considered for understanding the basic elements of a soil and how they are arranged helps to comprehend its macroscopic characteristics. To comprehend the condition and evolution of a soil under diverse stresses and chemical environments, the soil fabric or microstructure is evaluated in many geotechnical applications. The EDX and SEM test results for the above soil are represented below:

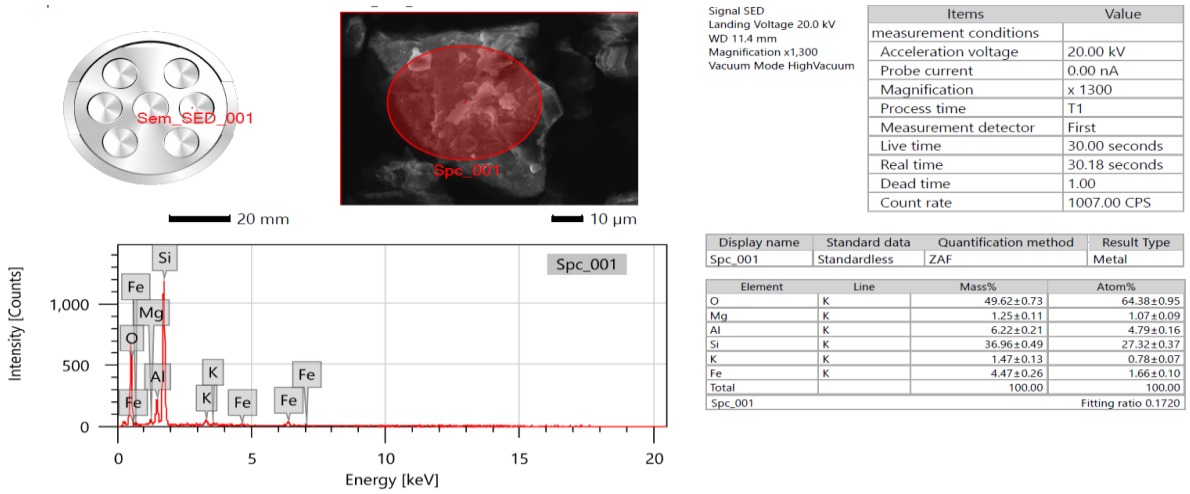

Items	Value
measurement conditions	
Acceleration voltage	20.00 kV
Probe current	0.00 nA
Magnification	x 1300
Process time	T1
Measurement detector	First
Live time	30.00 seconds
Real time	30.18 seconds
Dead time	1.00
Count rate	1007.00 CPS

Display name	Standard data	Quantification method	Result Type
Spc_001	Standardless	ZAF	Metal

Element	Line	Mass%	Atom%
O	K	49.62±0.73	64.38±0.95
Mg	K	1.25±0.11	1.07±0.09
Al	K	6.22±0.21	4.79±0.16
Si	K	36.96±0.49	27.32±0.37
K	K	1.47±0.13	0.78±0.07
Fe	K	4.47±0.26	1.66±0.10
Total		100.00	100.00
Spc_001			Fitting ratio 0.1720

Figure 3.2 EDX report of Soil Sample

Peaks that represent the energy levels for which the greatest number of X-rays have been received typically appear on an EDX spectrum. Since each of these peaks is specific to an atom, they all relate to the same element. The concentration of the element in the specimen increases with increasing peak height in a spectrum.

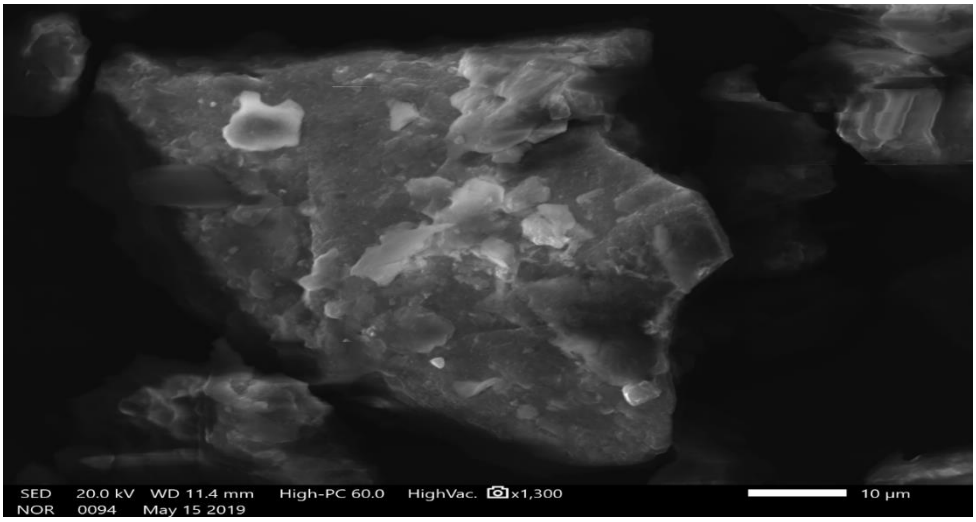

Figure 3.3 SEM Micrograph of Soil Sample

The soil is composed of micrometre scale grains which are fine particles having nanoscale structure. The particle sizes of soil samples seem to be heterogenous in nature as per the figure above and the scale considered was 10 µm

3.2.3 Steel Bars

The nails used in the study were made up of HYSD steel having a diameter of 10mm, the tensile strength of steel was tested using universal testing machine and its tensile strength was 458N/mm^2 as obtained from the graph in Figure 3.4 below, the length of nail was taken as 46 cm (0.7H Height of Soil Nail wall).

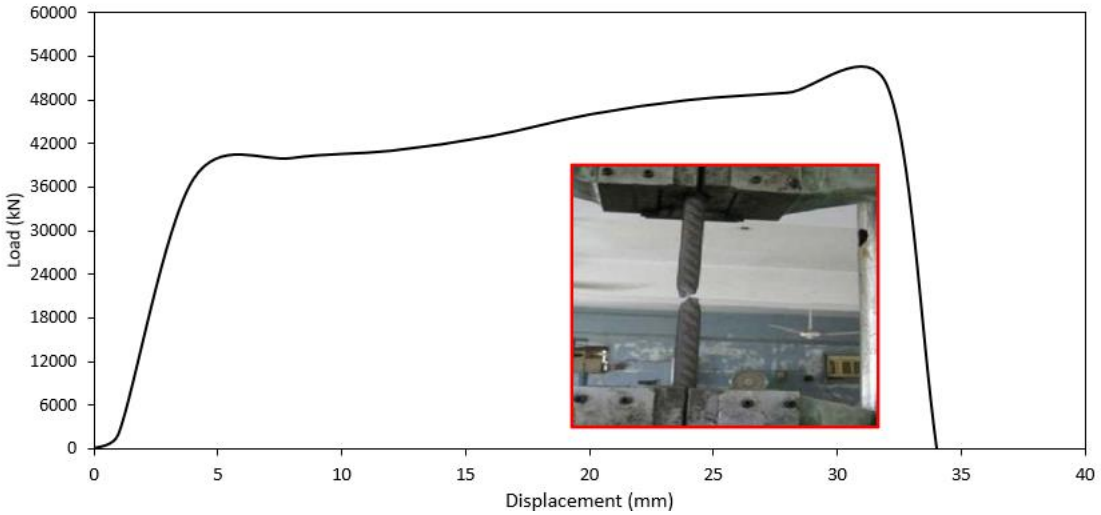

Figure 3.4 Tensile strength test for Steel bar

The nails were flattened at three points so as to place the flex sensor on the surface of bar and on the one end threads were formed so as to attach a bearing plate and a washer. The plate was

of square shape with dimensions as 5cm * 5cm and thickness of 6mm. Steel bars consisting of sensors with bearing plate and nut are shown in figure no.3.5 below. Each square plate is placed at the head of nail and the nuts are used to tighten the nail. These plates are utilized to transfer a concentrated compressive force between the structural elements. They are used to spread the pressure of the nut is evenly distributed on the surface so that the surface is not damaged. Make sure that the nut is pressed against a smooth surface, reducing the possibility of loosening due to its contact with the uneven surface.

	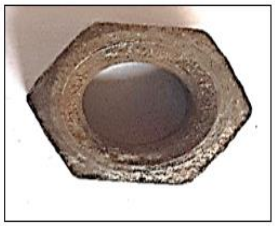	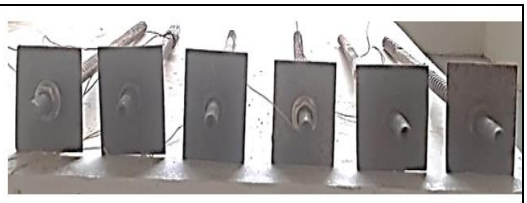
Nail head Bearing Plate	Hex nut for Soil Nail	Soil nails with nail head components

Figure 3.5 Steel nail head components

3.2.4 Facing Materials

In soil nailing, facing refers to a covering that is put on the slope's front face to prevent soil mass from being pulled out. There are three different types of slopes facing: soft, flexible, and rigid. In the present study four flexible materials were considered i.e. HDPE Facing net, Jute Geomesh, Hex plastic net and Polyester Geogrid. The tensile strength calculated by using Universal Testing Machine are represented below and the thickness of the materials were measured using vernier calliper.

Table 3.2 Tensile Properties of different facing Materials

Property	**HDPE facing nets**	**Jute Geomesh**	**Hex plastic net**	**Polyester Geogrid**
Tensile Strength	88 MPa	25 MPa	35 MPa	74 MPa
Thickness	5mm	4mm	3mm	2.5mm

A flexible facing material is frequently used for soil nail walls to offer protection and stability while allowing for wall movements and deformations. The materials considered are presented below:

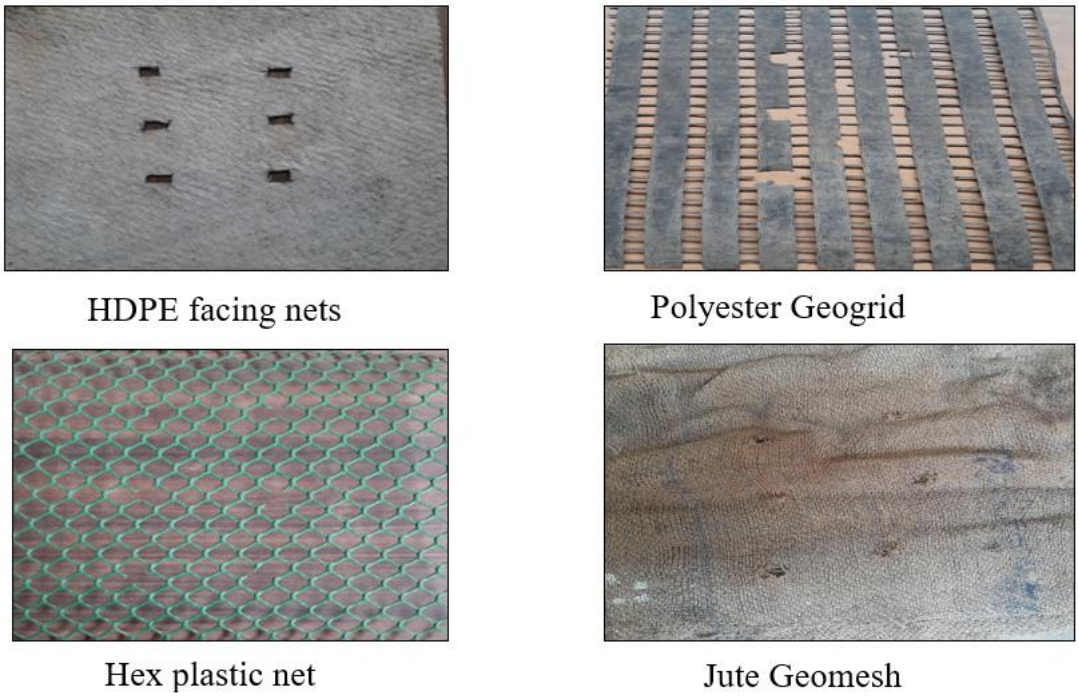

Figure 3.6 Flexible facing Materials

3.3 Fabrication of Model Test Tank and Soil

The soil mentioned above was filled in the physical model which was constructed using Perspex sheet. The dimensions of the model were taken Length as 70cm, breadth as 55cm and height of the model was 70cm. In order to avoid the boundary effect, the least tank dimension ae taken as 10 times more than the size of bar. Perspex sheet was used in the physical model along the sides of rectangular model as this sheet has a mouldable material, is lightweight, has high impact resistance, and has excellent optical transparency, and can be widely used in various fields the thickness of sheet was 8mm. The major benefit of using this sheet is to check the displacement of soil from the sides of slope[105], [125], [126]. The flex sensors were used to measure the resistance of the sensor and which was further used to calculate the strain. Figure No 3.7 below shows the physical model along with Perspex sheets.

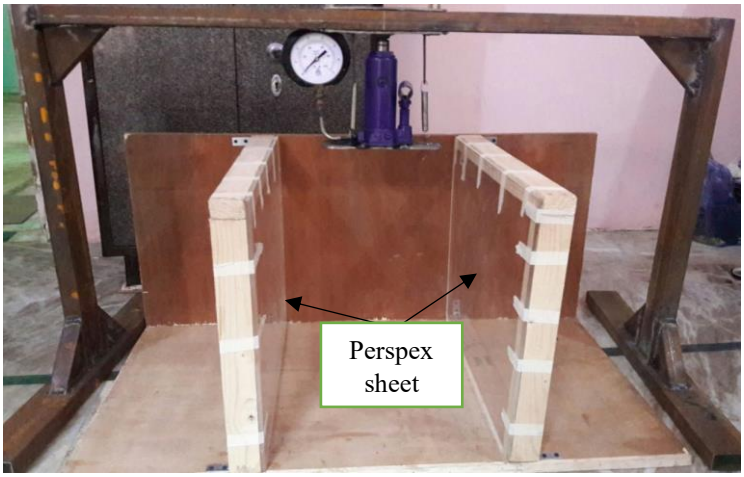

Figure 3.7 Physical model with Perspex sheets

The slope angle was considered 68 degrees for the present study. Six nails were considered in the rectangular arrangement for studying the stress- strain behaviour of soil along with the vertical and horizontal displacements and eight in a staggered pattern. The Horizontal and vertical spacing was kept as 15cm in rectangular pattern respectively as practically it would lead to simpler construction and quality control. Various investigators have considered the modelling by considering the ratio of length of nail to height of Slope(L/H) in the range of (0.32-1) which is in (46/70 = 0.65) present case and the ratio of vertical spacing to slope height (S_v/H) is in the range of 0.12-0.33 which is (15/70=0.21) in the present case for rectangular arrangement and as there were different set of spacing between nails in staggered pattern i.e (10/70=0.14) the above condition was fulfilled for the said pattern as well[47], [127].

3.3.1 Scaling of Model

The study model is made of a comparable material but has been scaled down to replicate the prototype's significant dimensions and features. The linear dimensions of the slope were reduced by a factor of N in order to correspond with the prototype conditions[125][128]–[130]. In reduced-scale physical modeling, the mechanical properties of critical components are often maintained at true scale to ensure realistic material behavior and reliable results. Properties like soil cohesion, friction angle, and particle size are intrinsic and cannot be proportionally scaled without altering the soil's shear strength and failure characteristics. Similarly, true-scale properties for structural components, such as soil nails and facing, ensure accurate replication of load-transfer mechanisms and stiffness. This approach aligns with validated practices, as emphasized by Jewell[131] and the FHWA Soil Nail Walls Manual (FHWA-NHI-14-007)[11], which highlight the importance of preserving realistic

mechanical behavior. By doing so, the model effectively reflects field conditions and provides meaningful insights into soil-structure interactions. The following table lists the scaling factors taken into account for key parameters in the modelling of soil nails.

Table 3.3 Scaling of Model flexural and diameter value

Quantity	**Prototype**	**Model**	**Actual Site Conditions**	**Scaled Down model**
Soil Parameters				
Cohesion *c* (kN/m^2)	1	1	-	2.1 kPa
Angle of internal Friction φ degrees	1	1	-	37°
Slope Parameters				
Height (m)	1	1/N	3m-14m	70cm
Inclination (β) degrees	1	1	-	68°
Soil Nail Parameters				
Length, L (m)	1	1/N	3m-6m	46cm
Grouted hole Diameter, d (m)	1	1/N	0.075m-0.15m	10mm
Cross section Area, A m^2	1	1/N^2	As per Dia.	78.60mm^2
Inclination (α) degrees	1	1	10-20°	10°
Flexural Rigidity, EI kNm^2	1	1/N^4	1030.40	0.103
Axial Stiffness, AE/L kN/m	1	1/N	48 490.48	2937
Interface friction angle δ, degrees	1	1	-	-
Surcharge Loading				
Surcharge Loading	1	1/N	-	-

N= Scale factor, $E_m = E_p$, m= model, p= prototype.

The value of N is taken as 10 for all the quantities mentioned above.

3.3.2 Tank Filling Process

The filling of soil in the tank was done in order to construct the slope at an angle of 68

degree. The uniform unit weight of soil was obtained by filling the tank by using pluviation technique. A moisture content of 7.3% was added into soil so as to obtain the required maximum dry density of soil i.e. 1.98g/cc. In this specific process, backfill compaction was not used. The pluviation method (gravity-based soil deposition) was employed to achieve the desired density without the need for mechanical compaction. To achieve uniform unit weight of backfill soil, sand is placed in the model test tank using pluviation (raining) technique. The backfill soil is allowed to fall freely through a specially fabricated sieve with holes of diameter 3 mm spaced at 25.4 mm center to center. The height of fall (25 cm) is decided after several trials where soil (sand) was dropped over the layer having 5 steel containers of known volume (98 cc) placed at the four corners of the model box and one at the centre. After achieving the desired height of 8 cm for the layer, the containers were removed and evaluated for mass of soil in the container. The minimum density achieved for each layer was calculated from the mass by volume relationship. The average minimum density was found to be 1.71 g/cc. The maximum dry density was attained from light compaction test in accordance to IS 2720-PART-7 (1980). The maximum dry density of 1.98 g/cc with an optimum moisture content of 7.3% was obtained. The target density was kept at 1.90 g/cc to achieve an overall relative density of 70% in each layer. However, due to the uncontrollable non – uniform flow of soil during pluviation technique in some layers, the relative density was found to vary with a margin of ± 2%. Once the entire slope of height 65 cm was constructed, the calculated amount of water equal to 28 litres was sprinkled on the slope crest and slope face using a gardening hand sprinkler of 10 litres capacity. Thus, the finished slope had a water content of 7.3% and relative density of 70±2%.

In order to fill the tank, first of all marking on the tank was done and temporary plywood slope facing is fixed at desired inclination angle. The nails were inserted as per the desired location and arrangements, during the insertion of nail the inclination was checked by measuring angle using proctor. The Flex sensor fixed on the nails and facing were having connection with the wires and the wires were visible at the front which could be attached to the multimeter to note down the value of resistance at a desired load. The procedure of filling the soil was repeated till the time the desired height was achieved.

3.3.3 Installation of Soil Nails

The nails were arranged in a rectangular pattern and six nails were used for the same. The spacing between the nails i.e horizontal and vertical is kept constant as shown below. Thereafter

the facing was applied at the front face of the model and on the application of load the strain was studied in different nails. The load was applied through the bottle jack and the resistance values were noted down for every nail and the symbol used for nails were N1to N6 which depict that N1 and N2 as upper set of nails N3 and N4 as middle set of nails whereas N5 and N6 as the bottom set of nails. The sensors were checked before placement of nail in to the soil via multi metre as they were reflecting readings on the screen of digital multi meter. Eight nails were considered in the staggered pattern and the spacing of nails are represented in the figure 3.8 below. The Nails were named as N1 to N8, similar to the rectangular pattern the nail numbers start from the top of the slope.

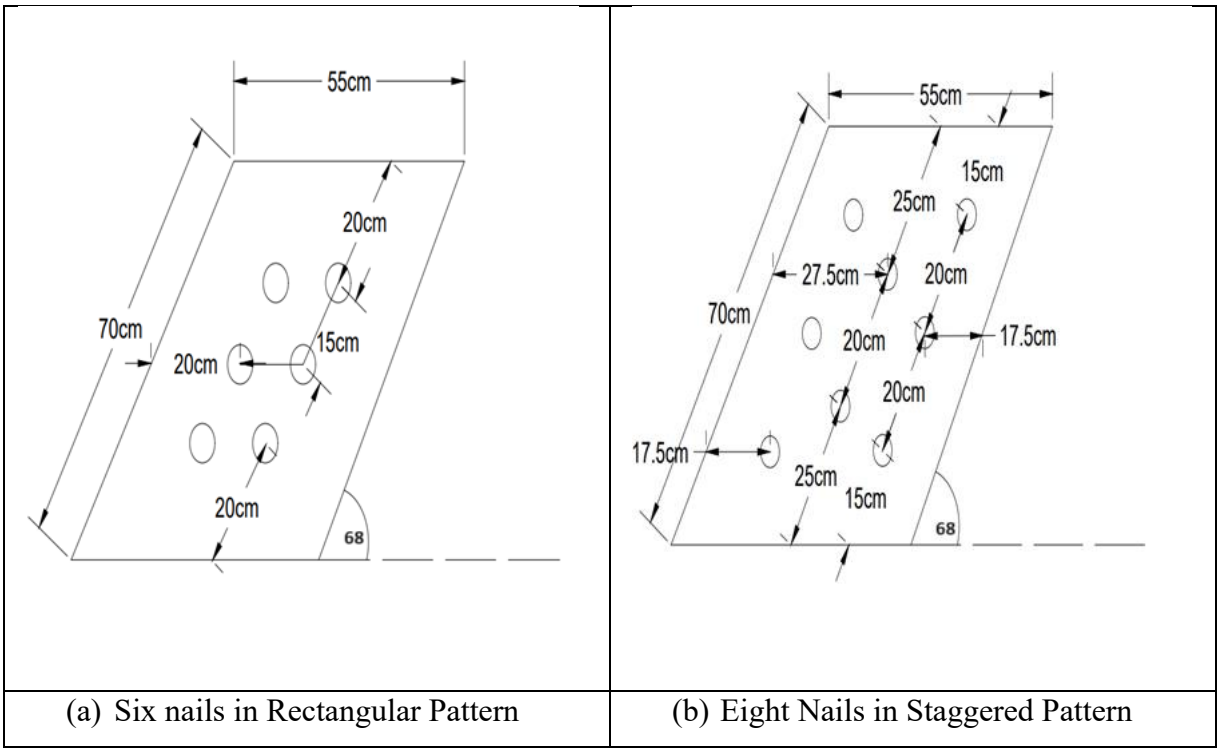

(a) Six nails in Rectangular Pattern | (b) Eight Nails in Staggered Pattern

Figure 3.8 Nail pattern for Rectangular and Staggered Pattern

3.4 Instrumentation of Soil - nailed model slopes

On application of load the stress was calculated by considering the load value from the bottle jack and the area is calculated by considering the top surface on which the load is applied. The sensors that gauge the degree of bending or deflection is called a bend or flex sensor. Typically, the sensor is adhered to the surface, and the surface can be bent to adjust the resistance of the sensor element. The application of load is carried out using a 44 cm × 55 cm bearing plate which was used for distributing the load as a uniform distributed load. The load was applied using a Hydraulic jack till the significant lateral deformation of the slope was observed. The installed dial gauges recorded the lateral slope deformation, with the LVDTs providing the

surface settlement values. The load cell connected to the hydraulic jack recorded the load applied. The developed strains at the nail were monitored using three flex sensors attached firmly on the nail at locations of 7.5 cm, 22.5 cm and 37.5 cm measured from the nail head as shown in Figure 3.10 and 3.11. Three strain gauges were also attached on the facing at location of 20 cm, 35 cm and 50 cm from the slope crest. The resistance readings were measured using multimeters and converted to strain using the relation as given in Eqn. 3.1.

$$Strain = \frac{\Delta R/R}{\Sigma c} \qquad \text{Eqn. 3.1}$$

Where, ΔR = change in the resistance recorded, R = Resistance of the wheat stone bridge arms, and $\sum c$ is the gauge factor having a value of 2.1 for 200 KΩ and a range of 2 to 2.5 as obtained from the manufacturer. The sensors were provided on the nail as shown below in figure 3.9.

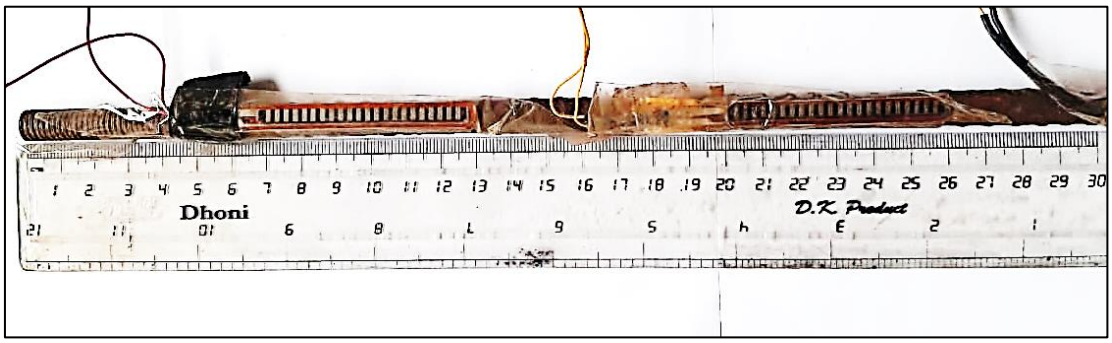

Figure 3.9 Mild steel nail

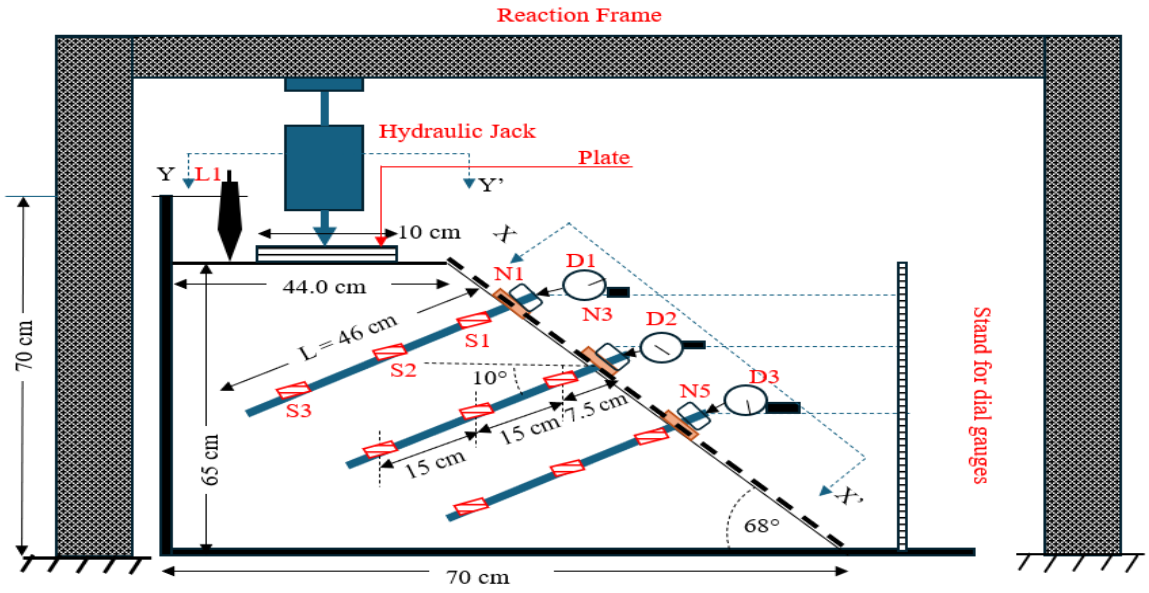

Figure 3.10 Schematic diagram of Model

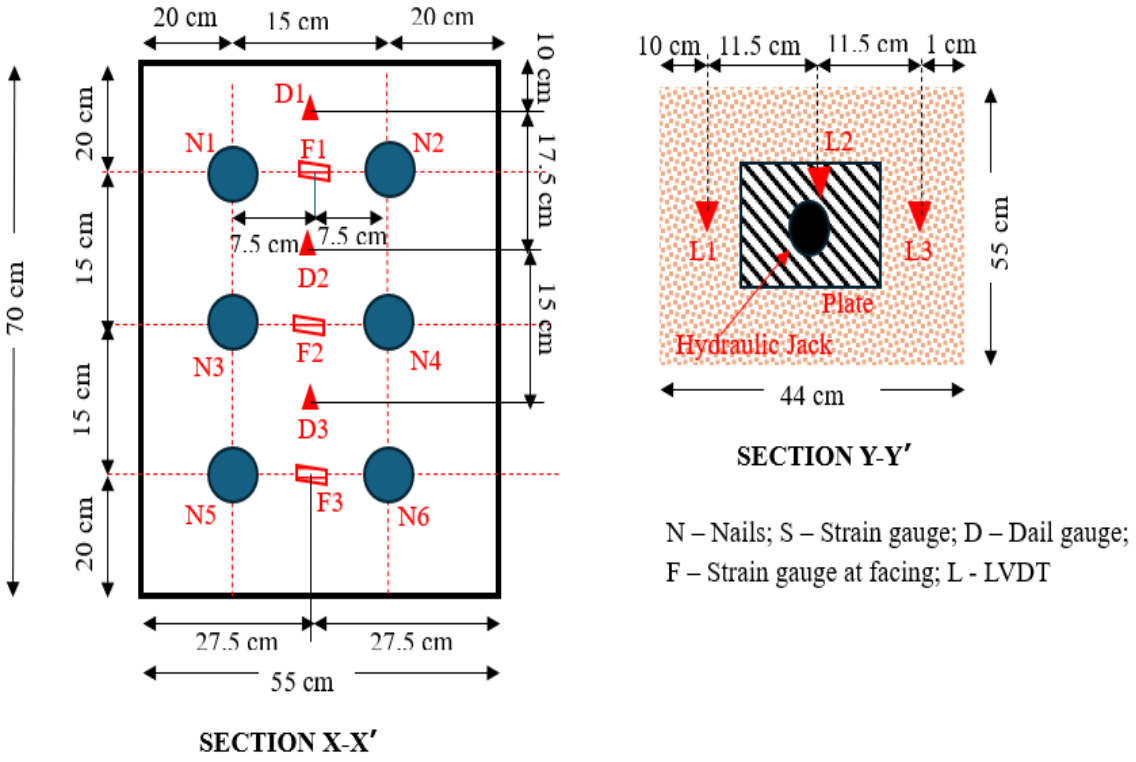

Figure 3.11 Section X-X' and Y-Y'

The figure below 3.12 depicts the step-by-step procedure for fabrication of model and testing process.

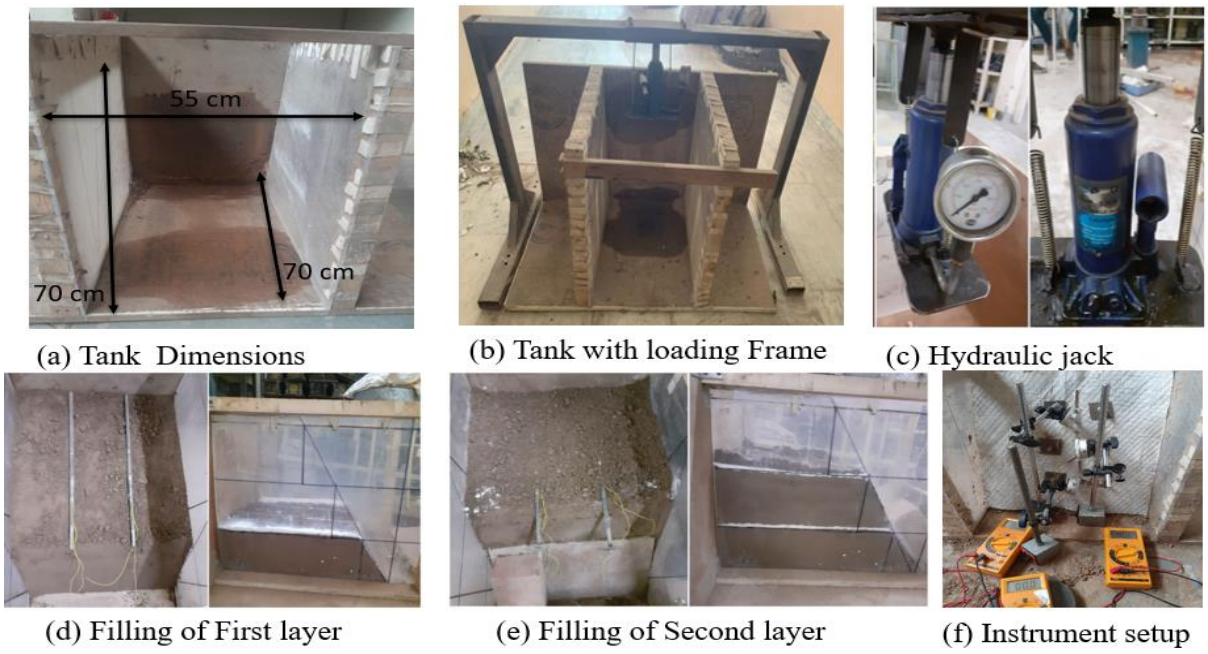

Figure 3.12 Fabrication of model and testing process

3.5 Facing Materials

The ability of inclined soil or rock slopes to tolerate or experience movement is referred to as slope stability; the opposite situation is known as slope instability or slope failure. A passive bar technique called "soil nailing" can withstand tensile, shearing, and bending forces while providing in-situ reinforcement. This method is applied to stabilize slopes and build retaining walls. In soil nailing, facing refers to a covering that is put on the slope's front face or surface to prevent soil mass from being pulled out. The present study focuses on finding out the alternative materials for Rigid facing, although Rigid facing due to higher stiffness and Rigidity can with stand high amount of stresses and usually considered at a slope of 90 degree. In regard to this if the slope is having angle with the range of 60- 70 degrees, there the utilization of flexible materials would be there, the present research focusses on comparison of various flexible materials with rigid facing.

3.6 Testing procedure for Drainage Assessment

The dimensions of water tank are considered as length 80mm, height 700mm, and width 550mm.This tank was constructed from 8mm thick acrylic sheets. The water tank's wall is perforated to allow water to pass through. To avoid any blockage from soil particles, the tank wall was coated with geotextile. To keep the seepage tank's water level constant and prevent the slope from overflowing, a stand pipe was connected at the bottom of the tank and kept at least 5 mm below the top surface of the model slope, allows for drainage on the downstream side, an outlet is situated at the right-hand corner. This outlet was kept open throughout the testing process so as to allow the seepage water out of the model setup as shown in figure 3.13.

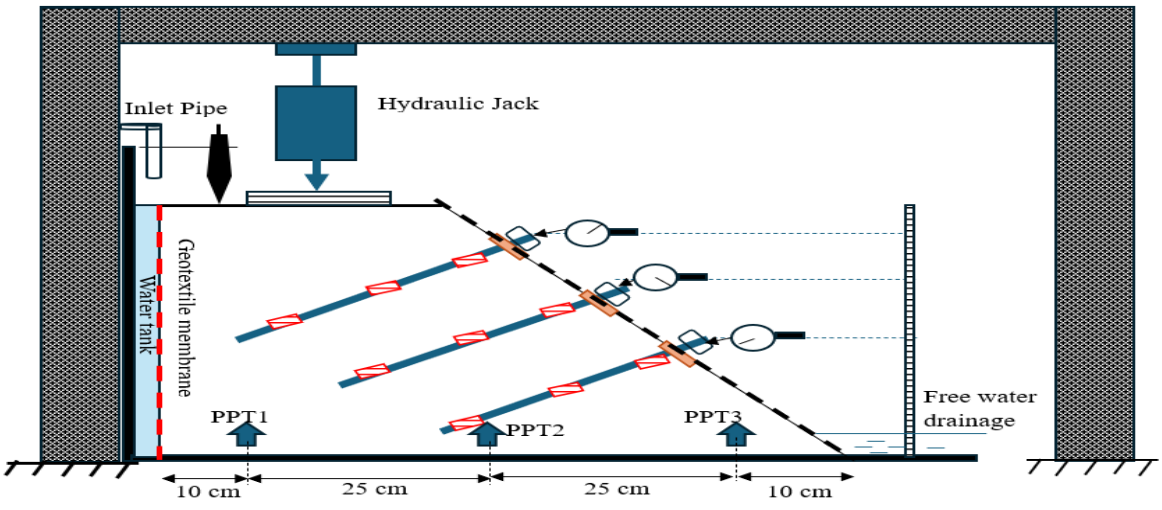

Figure 3.13 Instrumented Flexible facing model setup for drainage Assessment

Three PPTs (Pore Pressure Transducers) were used to measure the pore water pressure as the test progressed, and three LVDTs (Linear Variable Differential Transformers) were put on the top surface of the slope to measure the displacements. The surface movements at the top of the slope were calculated using the data from LVDTs.

3.7 Limitations of Physical Model

The physical modelling conducted during this study was developed as a representation close to the actual field conditions. However, certain limitations of the modelled reinforced slopes have been acknowledged as below:

1. Representative Nail Diameter

The physical modelling conducted in this study was performed using steel bar diameter of 10 mm, which represented a grouted soil nail of 100 mm in the field. As per FHWA (2015) and Juran et al. (1990), the recommended ungrouted soil nail diameter in the field usually ranges from 25 mm to 38 mm, leading up to 100 mm for a grouted full soil nail section. The employment of a larger diameter nail tendon of 10 mm in the present study was representative of the full grouted nail section in the field due to the practical constraints of carrying out the grouting process during nail installation in the laboratory set up. While this technique captures tensile load mobilization and global load displacement behavior reliably (Shiu and Chang (2006)), it introduces bending stiffness which has not been accounted in the present study.The representative soil nail diameter used for physical modelling have been scaled down from a typical grouted soil nail diameter generally used in the field.

2. Facing Strain, Nail Head Forces, and Deformation Response

The choice of a stiffer, full-section nail bar (10 mm) in the model directly affects nail head behavior, which in turn impacts the facing system. Increased stiffness near the nail head likely leads to reduced nail head displacement. This results in lower observed strain and deflection in the facing, particularly at the upper levels of the wall where tensile loads peak. The study by Eleutério et al. (2018) shows that strain distribution and deformation near the face are strongly influenced by the interaction between the nail head and the facing system, especially under differential settlements or concentrated loads. Higher bending stiffness in the nail bar can reduce local rotation at the nail head, which may lead to an underprediction of bulging in flexible facings in physical models. While the results of the physical model are reliable for relative comparisons, it is important to understand that actual facing deflections in the field could be more pronounced due to less stiff nail head connections.

3. Bending Moment Variation and Influence on Nail Performance

The increased stiffness of the nails in the physical model can improve bending resistance, especially in the upper third of the wall where flexural behavior is more pronounced due to constraints from face movement. However, studies by Jewell and Pedley (1992) and Juran et al. (1990) show that axial tensile forces dominate in most common soil nail wall designs, with bending moments contributing only locally near the nail head or within the facing zone. In this study, we maintained the nail inclination at 10°. Under this setup, as noted in Shiu and Chang (2006), bending and shear resistances can be conservatively neglected for global analysis. Nonetheless, the solid bar in the physical model may lead to an overestimation of bending contributions in shallower regions, which has not been accounted in the present study and is explicitly acknowledged as a limitation.

4. Punching Stress at the Nail-Facing Interface

A major concern with using full-diameter nails is the potential overestimation of contact stress at the nail–facing junction, often called punching stress. In field conditions, nail bars are usually embedded in grout or head plates that distribute the load to the facing panels. In contrast, the model uses direct contact between the nail and the flexible facing, which could lead to concentrated stresses at the contact points. The larger diameter and stiffness of the nail in the model may increase the local force transmitted to the facing, thereby underrepresenting the stress redistribution mechanisms seen in actual installations with broader load-spread zones.

5. Nail Pattern and Load Distribution Effects

Shahir and Delfan (2021) demonstrated that nail arrangement has a significant impact on internal forces and displacement patterns, especially in flexible systems. In the physical model, the larger diameter and associated stiffness of the nails may amplify the uniform load sharing, potentially reducing observable differences between patterns compared to what could happen in the field with more flexible elements. Moreover, the larger-diameter nails could lead to a more rigid load transfer mechanism, particularly near the face, which may underestimate the zone of influence or stress bulbs typically seen around individual nails in practice. While the patterns were carefully chosen to reflect realistic spacing, the effect of nail rigidity was not accounted when interpreting the pattern effects during physical testing.

6. Impact of Model Nail Dimensions on Bending Behavior

In this study, we used solid steel nails with a diameter of 10 mm. These represent a typical grouted nail system with a prototype diameter of 100 mm. The steel nail alone was chosen to simulate the function of a steel bar in grout, as modelling the grouting was difficult in the lab setup. This choice aimed to reflect the total stiffness of the nail system while avoiding issues related to grout quality, placement, or debonding. However, the authors acknowledge that using a solid steel bar instead of a grouted composite system could contribute to the increased nail bending stiffness which has not been accounted in the present study. For nominal diameter soil nails, Cheang et al. (2000) found that bending moments can develop near the wall crest or at shallow depths due to local deformations. Yet, these moments are minor compared to the main axial tensile forces acting on the nails. Similarly, Singh and Babu (2010) reported that the bending stiffness of soil nails has limited role in overall wall stability and affects only the facing deformation, particularly near the top of the wall. Increased bending stiffness can decrease nail head displacements, which impacts the stress transfer to the facing system. In their simulations, nails with higher bending stiffness showed less outward movement at the nail head, which could change how facing experience stresses and deformations. Therefore, in the physical model of our study, the overestimated bending stiffness could have created a stiffer interaction between the nail head and flexible facing, leading to an underestimation of local facing deflections compared to actual conditions. Assuming stiffer nails may limit the observable deformation or bulging in the facing, particularly at or near the top of the soil nailed slope, where maximum tensile forces and bending effects typically overlap.

However, as per GEO Report No. 197 by Shiu and Chang (2006), for nail inclinations between 10° and 20°, the effects of shear and bending are minimal and can be ignored for overall stability analysis. In the present study, a constant nail inclination of 10°was maintained, in accordance to the guidelines given by Shiu and Chang (2006). Additionally, in the numerical modeling (Plaxis 3D) both axial stiffness (EA) and bending stiffness (EI) was incorporated for simulating the behaviour of soil nails. This approach ensured a better understanding of nail–soil–facing interaction, particularly where the nail head's restraint significantly affects facing deformation.

7. Influence of Stiff Nail Element on Soil Deformation and Shear Mobilization

In this study, direct shear tests were conducted to characterize the soil–nail interface behavior and obtain key shear parameters for use in the numerical modeling of soil–nail walls. A modified direct shear test setup was adopted, wherein a representative segment of the soil nail (10 mm diameter, 40 mm length) was placed symmetrically within the shear box (20 mm in

the upper half and 20 mm in the lower half) to replicate the soil–nail interaction. This approach was selected due to its relative simplicity, the availability of equipment, and its ability to provide comparative shear strength estimates between soil–soil and soil–nail interfaces. The results indicated that the embedded stiff nail segment influenced the shear behavior of the soil, yielding slightly lower mobilized shear resistance and interface friction angle (δ) compared to the internal friction angle (φ) of the soil, and an apparent increase (~9.5%) in cohesion due to localized confinement effects introduced by the nail segment. Similar observations have been reported in earlier studies (Tei, 1993; Rawat, 2017; Sharma, 2021).

However, it is acknowledged that the direct shear test is a simplification that operates under two-dimensional conditions, where the rupture surface is pre-defined and assumed to be horizontal. In reality, soil–nail interaction occurs under three-dimensional conditions, with shear planes that evolve along the path of least resistance, making the mobilization of shear resistance highly dependent on the actual stress and strain states around the nail. Additionally, the area subjected to shear and normal loads may vary throughout deformation, making calculations based on a constant area only approximate (Sharma, 2021).

Ideally, a pullout test, conducted under three-dimensional boundary conditions, provides a more accurate and representative measure of soil nail interaction. Pullout testing captures the mobilization of shear resistance and load transfer characteristics along the length of the embedded nail, making it an essential tool for the design and performance assessment of soil nail walls (Juran and Elias, 1989 Pradhan et al., 2006). As observed by Wang and Richwien (2002), Direct Shear Test (DST) provides a shear interface measurement between soil and reinforcement but does not capture critical effects such as soil dilatancy and the tensile load–displacement behavior of the interface. Furthermore, Tei (1993) suggested that although pullout tests simulate field-like conditions more closely but are experimentally more demanding. The direct shear test, on the other hand, provides a simpler and more controlled laboratory method to evaluate soil-reinforcement interface characteristics under defined normal stresses. The variation in the Interface friction angles measured using DST and pullout tests is found between 5° to 8°, due to the localized failure mechanism and restricted mobilization of dilatancy and surface roughness (Tei, 1993; Palmeira, 2009). In line with Tei's conclusion and considering the objectives and experimental constraints of the present study, and due to equipment unavailability for pull out test, the direct shear test was adopted as a practical and widely accepted method for characterizing soil-nail interaction in sand.

8. Comparison of Rectangular and Staggered Nail Patterns

The Author acknowledges the limitations associated with comparing two variables nail pattern and number of nails simultaneously. Both the variation in pattern and the change in total number of nails are critical factors influencing the behavior of soil nail walls. Their combined alteration in the physical model indeed limits a direct one-to-one comparison of overall system behavior between the two configurations.

However, to address this methodological limitation and provide meaningful insights, the analysis in the present study was primarily focused on comparing the nail behavior at., lying at 35 cm from the slope crest for both the rectangular and staggered patterns. Therefore, Nail 3 and Nail 4 were considered for the rectangular pattern, while Nail 4 and Nail 5 were selected from the staggered pattern, all lying at the same vertical level from the slope crest. This approach was adopted to assess the varying nail configuration on the facing behaviour rather than the reinforcing action of the nails. Thus, the experimental results do not consider the influence of varying nail count on facing strain and force. Moreover, changes in nail layout influences the stress acting per nail. The denser nail arrangement leads to a reduction in load carried by each nail, particularly near the failure surface. In the staggered configuration, the effective reinforcement area per unit width of the wall increases, which affects not only the tensile forces but also the stress distribution across the nails and the facing. Nonetheless, the exclusion of the influence of difference in nail number, therefore, remains a major limitation of the study.

Furthermore, Shahir and Delfan (2021) have highlighted that ‘nail patterns with longer nails at the top of the wall reduce deformations and optimize performance, whereas nail spacing and quantity have a considerable effect on nail density and overall stability’. Further studies with comparable nail counts and varied lengths would be required to better isolate and quantify the individual effects of layout and quantity.

3.8 Numerical Modelling

For a variety of geotechnical applications, Plaxis is a multipurpose, 3D finite element program (FEM) that is used to analyze flow, deformation, and stability. In order to more precisely assess soil behavior and performance with regard to strain and deformation as well as soil stresses, the Finite Element Method (FEM) has been considered a very useful tool. With the help of this user-friendly graphical user interface, researchers can quickly develop a problem involving a geometry model and finite element mesh using this FEM-based program[3], [51], [132].

Numerical modelling techniques like finite element and/or finite difference methods should be used to adopt a higher level of analysis in situations where greater confidence is needed. The accuracy of numerical modeling is dependent on several factors, including the Caliber of the data collected, the estimation of in-situ stress and soil stiffness, and the availability of reliable case histories for model calibration.

Numerical modelling cannot take the place of observations made during construction. Predicting stresses and displacements is still a challenge, even with numerical modelling. Because the mobilization of tension forces is frequently not directly proportionate to facing deflections and construction stages, accurately modelling the grout/soil interface is also challenging.

The application of numerical modelling for the analysis and assessment of soil slopes has significantly improved as a result of the quick advancements in computer technology. In this current study, the FEM computer program PLAXIS 3D (2023) was utilized to analyse slopes, consisting of soil nails along with various facing materials, as various flexible materials were compared with the rigid facing.

This Major goal is to comprehend the behaviour of a soil-nailed structure with a flexible facing in order to determine when and under what conditions it is a sensible solution. Because of this, it's critical to comprehend how each component of the structure functions to ensure the structure's stability. In order to do that, analyses comparing various facing types were also conducted. While thousands of soil nail structures have been built all over the world, very few of them have been instrumented to guarantee appropriate performance and support design procedures (FHWA, 2003).

3.8.1 Working of FEM

The foundation of FEM is the idea of energy minimization. A body may take on multiple configurations when specific boundary conditions are applied, but FEM only considers the configuration that uses the least amount of energy[51], [53], [85]. Discretization is used to transform the Partial differential equation (PDE) into a set of matrix equations that can be solved using matrix algebra equations once the PDE for a phenomenon has been identified. These equations can be elliptical, hyperbola, parabola and these equations can be solved by either Finite difference method or variation method. The matrix equations are passed to the solver to solve after the object is split up into a mesh of elements known as finite elements. The computation of the ultimate outcome involves amalgamating the outcomes of every finite element. Inorder to calculate the results, the results of all elements are combined for all finite elements[14], [133].

Plaxis 2D and Plaxis 3D (x, y, z dimensions) function in a comparable way. There are five approaches to finish the modelling process. Geometry and calculation are the two distinct stages of the FEM analysis. While mesh generation, flow conditions, and construction stages are included in the calculation phase, soil properties and structural members (such as plates, walls, and beams) are included in the geometry phase. These are completed in the input program's first two-tab sheets, Structures and Soil. The final three-tab sheets (Mesh, Flow Conditions, and Staged Construction) of input program are where mesh generation and definition of calculation phases are completed. In PLAXIS 2D, there are two types of mesh elements i.e. 6 nodes or 15 nodes triangular elements, that can be used to model soil layers or other volume clusters. There are also 15 nodes wedge elements available in PLAXIS 3DF (3D foundations). 10 nodes tetrahedral elements were considered in present study.

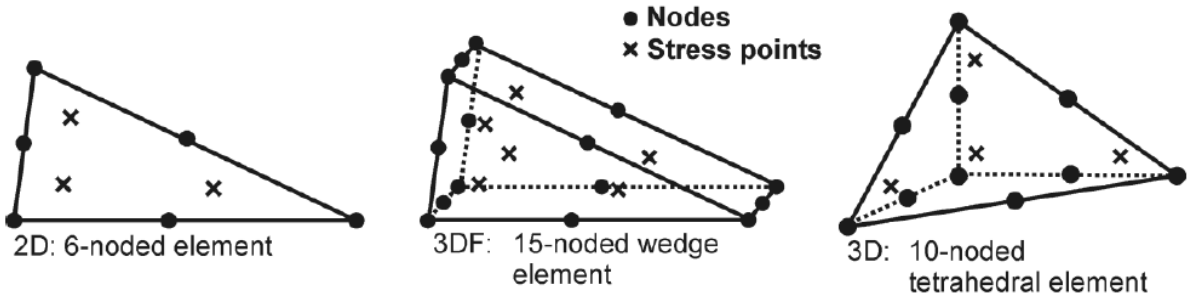

Figure 3.14 Finite elements in PLAXIS 2D, PLAXIS 3DF and PLAXIS 3D

3.8.2 Modelling in Current Study

After performing the testing on the physical model and obtaining the results from the model, the FEM analysis was performed for validation of the results using Plaxis 3D (2023) software[31], [100], [119]. The Boundary Conditions for study were selected similar to those considered in the physical model. The construction of model basically begins with the creation of geometry model. The model in Plaxis was constructed in three different phases. In the phase one i.e the initial phase. The slope was constructed and stress distribution were created. In the phase two the nail and facing was activated and displacements in phase one are rest to zero. In the phase three the loading is imposed and displacements in phase two are rest to zero, thereafter the calculation started and results were obtained. The major elements in the structure are soil, nail and facing materials. The PLAXIS 3D program utilizes fully automatic generation of finite element meshes. The model constructed in PLAXIS 3D was intended to simulate the physical model, not the full-scale prototype. This was done to ensure that the boundary conditions and setup reflected those used in the physical experiments, enabling direct comparisons between the physical test results and the numerical analysis.

In PLAXIS 3D, the staged construction sequence allows the modelling for a soil nail wall similar to the typical field construction procedure. The staged construction feature in PLAXIS was used to manage sequential activation and deactivation of model components. Excavation and nail installation are simulated progressively, with soil excavation followed by the activation of reinforcement elements (nails and facing). The relative density in terms of unit weight was incorporated for each layer, however the cohesion (c) and friction angle (φ) values for the soil were kept constant for the entire backfill soil in the Plaxis Model.

For investigating the effect of mesh sensitivity, three different mesh configurations namely coarse, medium, and fine mesh were adopted and the variation in the nail force mobilization, lateral deformation, and vertical surface settlement was recorded.

As can be seen from Table 3.4, the mesh sensitivity analysis depicted that using a coarser mesh led to a significant underestimation of nail forces by approximately 45.4% compared to experimental results. Additionally, predicted lateral deformation increased by 22% and vertical surface settlements increased by 28% when using a coarser mesh. Nevertheless, the computation time was significantly small. However, transitioning from a coarser mesh to a medium mesh drastically enhanced the computational time, the nail forces depicted an increase of 79.08% with reduction of 18.6 % in lateral deformation as compared to the

experimental results. However, overestimation of 14.67% in the vertical surface settlement compared to experimental findings was recorded, which can be attributed to the limitations in capturing localized deformation behavior with medium mesh alone. Using finer mesh for the entire system, increased the computational time significantly running it for several hours.

Table 3.4 Mesh Sensitivity Analysis

Parameter	FEM Reading (Coarser Mesh)	FEM Reading (Medium Mesh)	FEM Reading (Fine Mesh)	Experimental Reading	% Variation (Coarser vs. Experimental)	% Variation (Medium vs. Experimental)	% Variation (Coarse mesh to medium mesh)	% Variation (medium mesh to Fine mesh)
Nail Force at Interface	5.64 N	10.1 N	10.28 N	10.33 N	↓ 45.4%	↓ 2.2%	↑ 79.08%	↑ 1.78%
Lateral Deformation	26.84 mm	21.9 mm	21.92 mm	22 mm	↑ 22%	↓ 0.45%	↓ 18.6%	↑ 0.09%
Vertical Surface Settlement	19.2 mm	17.2 mm	16.5 mm	15 mm	↑ 28%	↑ 14.67%	↓ 10.4%	↓ 4.07%

With nail forces varying by about 1% to 2% and lateral deformation and surface settlement falling within 1% to 4% of the experimental values, the results for the fine mesh were found to be in very close agreement with the experimental data. There was only a slight improvement over the medium mesh: surface settlement dropped by about 4.07%, lateral deformation increased by about 0.09%, and nail forces increased by about 1.78%. This demonstrates that results are only slightly affected by mesh refinement beyond the medium mesh. It increased the overall run times by about three to four times, but at a high computational cost. As a result, even though the fine mesh offers marginally better accuracy, the advantages are outweighed by the additional computational effort. In this context, a hybrid meshing approach is justified, utilizing fine mesh elements in critical zones such as soil–nail interfaces and facing elements, and medium mesh elsewhere. This approach maintains an optimal balance between computational efficiency and result accuracy, aligning with best practices recommended in earlier studies (Chen and Poulos, 1997; Dasaka and Idiculla, 2019; Lazarte et al., 2015).

Therefore, in the present study, mesh optimization has been done by using fine mesh discretization for soil nails, facing elements, and interface zones critical for stress transfer. Medium mesh was used for discretization of the remaining reinforced soil slope so as to maintain a balance between accuracy and computational efficiency. Similar approach has also

been adopted as per the reported studies by Chen and Poulos (1997), Dasaka and Idiculla (2019), and Lazarte et al. (2015), wherein medium-density mesh was used for general soil regions and fine mesh for nail-soil interfaces.

The soil was defined by the bore holes which defines the soil stratigraphy along with ground surface level. The Mohr coulomb model was considered for study which includes five basic input parameters, namely a young's modulus E, a Poisson's ratio ν, a cohesion c, a friction angle φ, and a dilatancy angle ψ. However, because of its simplicity, it remains widely used in geotechnical modelling, especially for preliminary analysis or when more complex models are not necessary. In the context of this study, the Mohr-Coulomb model was selected over available soil models like Soft Soil Model, Hardening Soil Model, Soft Soil Creep, Hardening Soil with Small Strain, Modified Cam-clay because soil-nailed slopes are typically analysed to assess their stability against failure and Mohr-Coulomb model is the most effective in defining the failure criteria based on the Mohr-Coulomb failure envelope, making it appropriate for slope stability problems. The primary concern of the present study was to model the failure of the soil nailed slope as close as possible to the actual field conditions. The soil nail failure generally involves the shear failure and elastic behaviour of reinforced soil. While, the Mohr – coulomb soil model might not capture the soil strain-hardening or time-dependent effects, but it provides a good first approximation regarding the shear failure and initial stiffness of soil prior to failure. As per Brinkgreeve et al [119], this level of accuracy is sufficient for most of the practical soil nailed structure problems.

Moreover, the review of literature suggest that soil nailed structure problems using Mohr - Coulomb soil model has been carried out by Singh and Babu [2], Luo et al [28] Di flora et al [3], Sahoo et al [7], Rawat [29], Sharma et al [89].

The calibration of the constitutive model was done using the values cohesion (c); soil friction angle (ϕ) and soil elastic modulus (E) as obtained from direct shear test conducted under drained condition in the laboratory. A total of five direct shear tests were conducted in accordance to IS: 2720 (1986) for normal stress values of 50 kPa, 100 kPa, 150 kPa, 200 kPa and 250 kPa. The following average values were obtained over 5 direct shear test results which were used for calibration of the Mohr – Coulomb constitutive model is represented in Table 3.5

Table 3.5 Calibration of the Mohr – Coulomb constitutive model

Laboratory evaluation of soil properties		Calibration of Constitutive model (Mohr - Coulomb) in Plaxis 3D	
Property	Values	Property	Values
Relative density, RD (%)	70 ± 2%	Unit weight, (kN/m3) calculated corresponding to RD = 70%	19.8
Cohesion (c), kPa	2.1	Cohesion (c), kPa	2.1
Friction angle (φ°)	37°	Friction angle (φ)	37°
Shear Modulus, G (MPa)	30.54	Shear modulus G	30.6
Assumed Poisson Ratio (υ)	0.3	Poisson Ratio (υ)	0.3
Youngs Modulus, E (MPa)	79.40 ~ 80	Youngs Modulus (N/mm^2)	80
Dilatancy angle Ψ	7°	Dilatancy angle Ψ	7°
-	-	Oedometer modulus Eoed (Automatically calculated by Plaxis 3D)	107.69

The shear Modulus (G) was calculated under each normal stress of 50 kPa, 100 kPa, 150 kPa, 200 kPa and 250 kPa using the shear load vs horizontal displacement curve. The average G value and assumed Poisson Ratio (υ) = 0.3 (Noonan and Nixon, 1972) [134]was then used to obtain the Young's Modulus (E) of soil using the Eqn. (3.2) given as:

$$E = 2G(1 + \nu) \tag{3.2}$$

The dilatancy angle Ψ was calculated using the Equation (3.3) given as:

$$\Psi = \tan^{-1}\left(\frac{\Delta V/_H}{\Delta h/_L}\right) \tag{3.3}$$

Where, ΔV = Vertical displacement of sample; Δh = Horizontal displacement of the sample; H = Initial height of sample = 5.0 cm and L = Length of the shear plane = 6 cm.

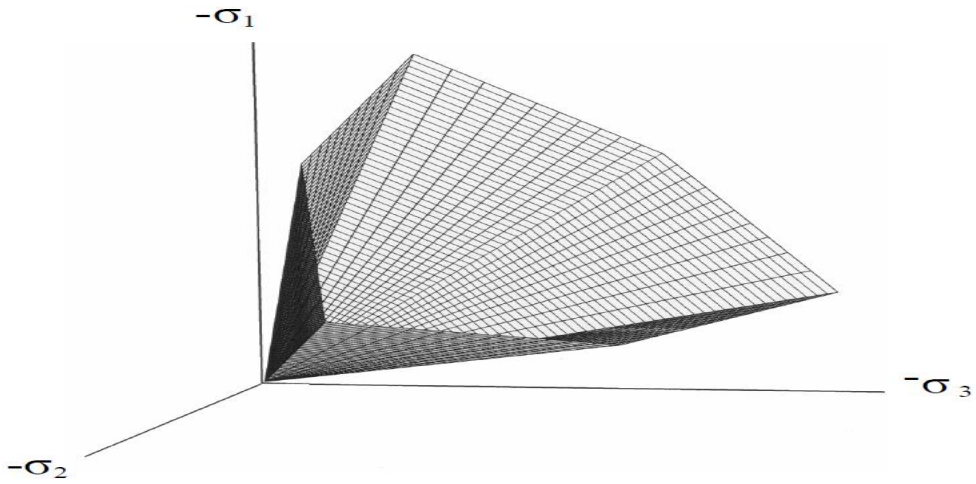

Figure 3.15 Surface in principal stress space for c-φ soil

The material used in the current study is poorly graded sand (SP) with a small cohesion intercept value of 2.1 kN/m^2. However, Fig. 3.15 shows the Mohr – Coulomb yield condition used by Plaxis during calculation (Brinkgreeve et al.,[119]. The yield condition consists of six yield functions when formulated in terms of principal stresses with two plastic model parameters (c and φ) appearing in these yield functions. At failure, all the yield function together represents a hexagonal cone in principal stress space as shown in Fig. 3.15.

The parameters of the M-C soil model were calibrated using the laboratory consolidated drained triaxial shear tests conducted as per IS:2720 (Part 12). The following values are calibrated for the M – C soil model:

1. Angle of internal resistance (ϕ) from failure envelope in q-p' space
2. Cohesion (c) from intercept
3. Young's Modulus (E) and Poisson's ratio (ν) from initial slope of σ-ε curve

The consolidated drained triaxial test was conducted at five different confining pressures (50 kPa, 100 kPa, 150 kPa, 200 kPa, and 250 kPa) reflecting to the expected field confining pressure.

The following results are obtained in q – p' space along with the plot for the same:

Table 3.6 Results from consolidated drained (CD) triaxial test showing axial stress (σ_1), confining stress (σ_3), deviatoric stress (q), and mean effective stress (p′)

σ_1 (kPa)	σ_3 (kPa)	q (kPa)	p′ (kPa)
220	50	170	107
375	100	275	192
540	150	390	280
760	200	560	387
965	250	715	488

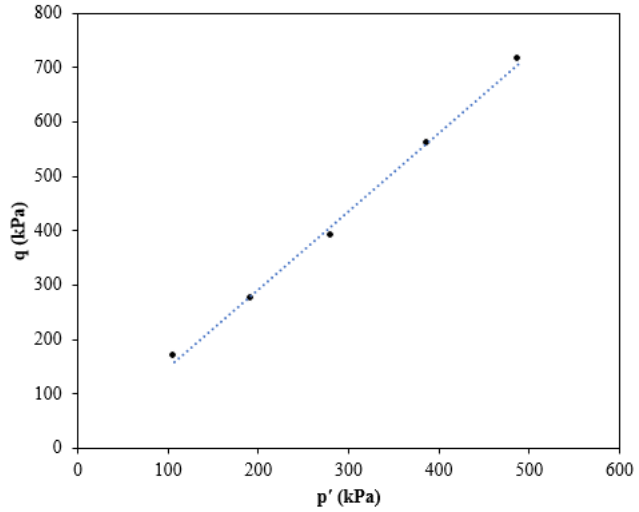

Figure 3.16 Plot of deviatoric stress (q) versus mean effective stress (p′) from consolidated drained (CD) triaxial test, showing the stress path in q–p′ space.

A plot of q vs. p′ was prepared from the above values, yielding the following equation (3.4) of the failure envelope:

$$q = 1.4385p' + 3.8761 \quad (3.4)$$

From this equation, the shear strength parameters were derived as:

c ≈ 1.92 kPa and φ'≈ 35.45°, which are consistent with the expected behaviour of the tested soil. The stress–strain (σ–ε) curve from the triaxial test is shown below in figure 3.17. The Young's modulus (E) was determined from the slope of the initial linear portion of this curve.

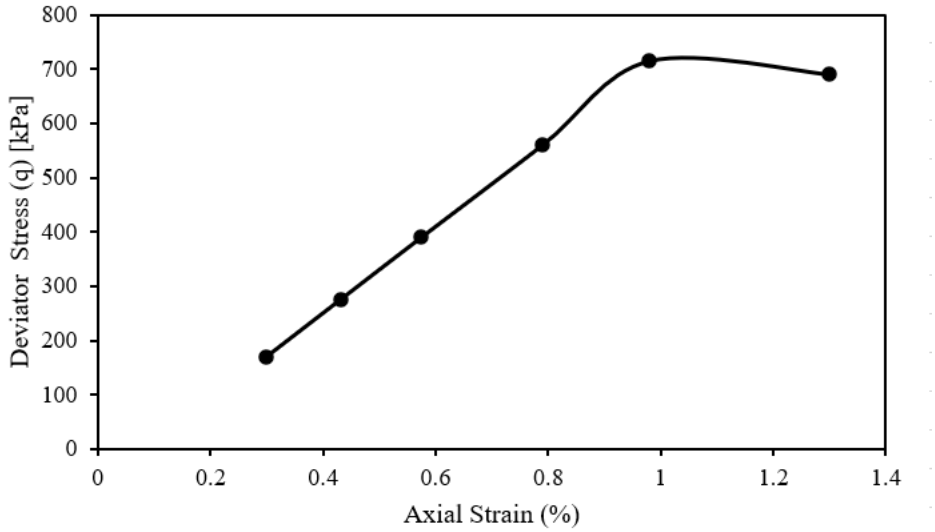

Figure 3.17 The stress–strain (σ–ε) curve from the triaxial test

The Young's modulus (E) was obtained from the slope of the initial linear portion of the stress–strain curve, yielding E ≈ 80.15 MPa. The Poisson's ratio (ν) was determined from the ratio of lateral to axial strain in the elastic region, giving ν ≈ 0.31.

The cohesion (*c*) and friction angle (*φ*) obtained from the CD triaxial test for the sand soil are within a reasonable range of the values determined from direct shear tests. The triaxial test results indicate c ≈ 1.92 kPa and φ' ≈ 35.45°, compared to c ≈ 2.1 kPa and φ ≈ 37° from the direct shear test. Consolidated drained triaxial test was conducted on the poorly graded sand (SP) at confining pressures of σ_3 = 50, 100, 150, 200 and 250 kPa, as presented in Table 3.6 and Figure 3.17. The results clearly show that the specimen reaches its peak deviatoric stress (q_{peak}) at an axial strain of approximately 1 %, which is characteristic behavior for poorly graded sands Similar observations have been reported for comparable sand types by Karni and Alshenawy (2006) who reported peak shear mobilization at axial strains of roughly 0.8–1.2 % across relative density of 95% and confining pressures 100, 200, 300 and 400 kPa for quartz sand Likewise, Cabalar et al. (2013) reported that the maximum shear resistance occurs at strains of about 1.0 ± 0.2 % for poorly graded sand tested under drained triaxial and shear conditions. Hence, the observed failure strain (~1%) is consistent with the published literature

The table for calibration of Mohr coulomb soil model is shown below in Table 3.7.

Table 3.7 Calibration of Mohr-Coulomb Soil Model

	Cohesion (c), kPa	Friction angle (φ'°)	Poisson Ratio (υ)	Young's Modulus

				, E (MPa)
Direct Shear test	2.1	37	0.3	80
CD triaxial test	1.92	35.45	0.31	80.15
Mohr-Coulomb Model in Plaxis 3D	2.1	37	0.3	80

Various steps involved in current Numerical modelling are as follows:

1. In the present research, beam is considered to be as a nail in plaxis specifically a horizontal beam with a specific value of bending stiffness and axial stiffness. The beam elements are considered to be three node line elements having six degree of freedom per node i.e. three translational and three rotational. The geometry input parameters to be considered are area of cross section (A), Unit weight (γ) of the beam material along with the stiffness properties (*E* – Modulus of Elasticity, ν- Poisson's ratio, and moments of inertias)
2. The plate elements were considered for modelling the Facings, plate elements are a form of wall elements which consists of 8 node quadrilateral elements consisting of six degrees of freedom. During degeneration walls are composed 6 node triangular plate elements which is compatible with 6 node triangular plate elements. The geometry parameters include thickness of the facing d, unit weight of wall material (γ) and (*E* – Modulus of Elasticity, ν- Poisson's ratio, and *G*- Shear modulus) as shown in figure 3.18.

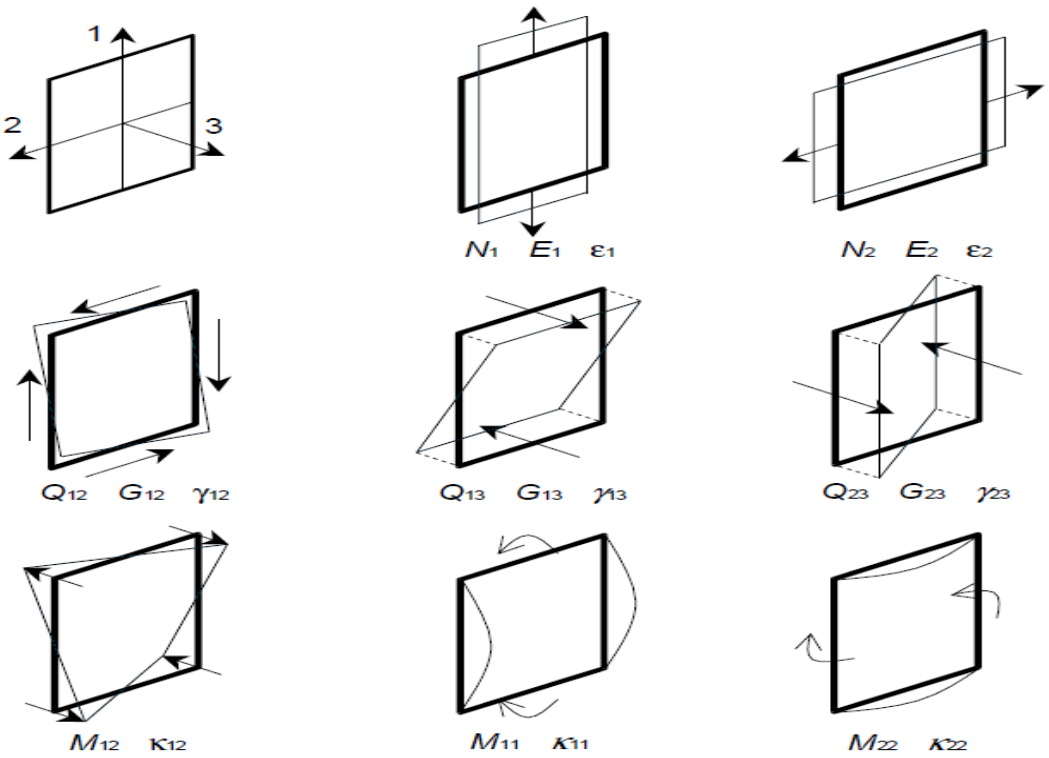

Figure 3.18 Wall's local system of axes and various quantities [119]

3. Interface elements play an important role in Plaxis, there are two types of interfaces in the present study i.e. Soil nail interface and nail facing interface. Each interface consists of 16 node interface elements. Virtual thickness, an imaginary dimension assigned to each interface, is used to determine the stiffness properties of that interface. The average element size is typically 0.1 meters, and virtual thickness is equal to that amount divided by the virtual thickness factor. The properties of interface are calculated by using strength reduction factor R_{inter} at the interface and the equation 3.5 mentioned below:

$$c_i = R_{inter}\, c_{soil}$$

$$\tan\varphi_i = R_{inter}\tan\varphi_{soil} \leq \tan\varphi_{soil}$$

Eqn. 3.5[119]

The interface properties (cohesion and friction angle) used in the Plaxis model were calibrated based on Direct Shear Test (DST) results. The 6 cm x 6 cm plan area and 5.0 cm depth DST set – up was filled with a soil at relative density of 70% using pluviation technique.

Prior to backfilling, a small representative segment of the soil nail (10 mm diameter, 40 mm length) was positioned centrally within the shear box, placed symmetrically such that 20 mm of the nail length was embedded in the upper half and 20 mm in the lower half of

the box.

The presence of a stiff nail bar embedded in the soil during the direct shear tests does influence the stress and strain behavior of the surrounding soil. This observation has also been supported in the study by Tei (1993), Tei (1993) noted that such reinforcement elements tend to confine the soil locally, restricting both vertical and horizontal deformations. Because of this confinement, the natural movement of soil particles is limited, especially in dense sand, where interlocking and dilation play a key role in mobilizing shear resistance. The stiff bar essentially alters the failure mechanism, leading to a reduction in the mobilized shear stress at failure. In the present test, this was reflected by the lower interface friction angle (δ) recorded for reinforced soil – to – reinforced soil interface in comparison to the soil – to – soil interface internal friction angle (φ). Consequently, the reduction in shear strength mobilization due to the presence of a rigid inclusion in the shear zone is observed.

The introduction of the nail element in the presented test led to a 6.67% reduction in interface friction coefficient, indicating constrained shear mobilization due to the stiff inclusion. However, the cohesion increased by about 9.5%, likely due to enhanced confinement and interaction between the soil and nail surface.

The modified DST set – up was adopted from Tei [135]. The representative bar sample has a modulus of elasticity (E_n) of 210 GPa and Poisson's ratio (ν) of 0.3, which was determined from the tensile strength test conducted on the nail bar sample representative of the nail model used in the model testing. The final set – up consisted of a represented sample of the nail tendon embedded in soil, with 20 mm of bar length in the upper box and lower box respectively. Five sets of DST(s) for each condition with soil–soil (without nail) and soil–soil (with nail) was conducted. The results for both the testing conditions are shown in Table 3.8.

Table 3.8 Shear parameters obtained from soil – soil (with and without nail) direct shear test

Interface	Angle of Internal friction	Interface Friction Coefficient	Cohesion (c) in kN/m^2
Soil - Soil (without nail)	φ =37°	tan (φ) = 0.75	2.1
Soil - Soil (with nail)	δ = 35.3°	tan(δ) = 0.70	2.3

The soil–soil (without nail) depicts a higher angle of internal friction than soil-soil (with nail) as presence of the nail restricts particle movement, reducing interparticle interlocking and dilation, which are key contributors to shear resistance. Additionally, part of the shear plane may slide along the surface of the nail, where the roughness is typically lower than that of soil particles. The nail also creates localized stress concentrations and boundary effects that alter the stress distribution along the shear plane, further reducing shear resistance. These combined effects explain the slight reduction in the interface friction angle (δ) compared to the internal friction angle (φ) So, a lower soil–nail interface friction angle (δ< φ) is observed. In the absence of pullout test results for soil nails, the coefficient of friction for pullout test (P*) can be determined by the interface friction coefficient friction obtained from the direct shear test (*tan δ*). The relationship to obtain the coefficient of friction for pullout test (P*) for soil – to – nail interface is adopted from Wang and Richwein given as Eqn. (3.6):

$$P^* = \frac{tan\delta}{1 - \left|\frac{2(1-\upsilon)}{(1-2\upsilon)(1+2K_0)}\right| (\tan\delta \tan\psi)} \qquad \text{Eqn. (3.6)}$$

where, υ = Poisson's ratio of soil taken as 0.3; K_o = Earth pressure coefficient at rest which is calculated by the Jaky's formula as (*1- sinφ*); ψ = Dilation angle of soil calculated by (φ - 30°). Using Eqn. (3.6), the coefficient of friction from pullout for soil nail is calculated as P* =0.72. This value has been used as R_{inter} value during the model simulation in Plaxis for soil – to – nail and nail – to – facing interfaces.

The slight increase in cohesion from the soil-soil (without nail) to the soil-soil (with nail) condition is mainly due to the localized confinement provided by the nail, stress redistribution near the nail, and the possible contribution of nail-soil interlocking. The input values for various materials are represented below in Table 3.9 and Table 3.10.

Table 3.9 Input values for Soil and Soil nail

Soil		**Soil nails**	
Property	**Values**	**Property**	**Values**
Soil model	Mohr - Coulomb	Element	Beam
Unit weight (kN/m^3)	19.8	Diameter (mm)	10
Youngs Modulus (N/mm^2)	80	Length (cm)	46
Poisson Ratio (υ)	0.3	Youngs Modulus (N/mm^2)	210000
Cohesion (c), kPa	2.1	Tensile Strength (N/mm^2)	458
Friction angle (φ)	37°	Unit Weight (kN/m^3)	78.5

Dilatancy angle Ψ	7°	Poisson Ratio (υ)	0.3
Shear modulus G	30.76		
Oedometer modulus E_{oed}	107.69		

Table 3.10 Input values for various Facing Materials

Property	**Conventional Facing**	**HDPE facing nets**	**Jute Geomesh**	**Hex plastic net**	**Polyester Geogrid**
Element	Wall plate	Wall plate	Wall plate	Wall plate	Wall plate
Thickness (mm)	5	4	3	2.5	5
Poisson Ratio	0.3	0.33	0.4	0.108	0.15
Tensile Strength (MPa)	-	88	25	35	74
Density (g/cc)	1.7	0.9	1.4	0.98	1.3
Modulus of Elasticity (MPa)	25	1500	2000	1600	6000

4. The bottom of the model was fixed in all directions ($u_x = u_y = u_z = 0$ with slope back free in z direction and fixed in x and y direction. The model conditions were used for simulation for validating the scaled – down experimental results. Since lab scale models allow the control of factors such as nail and facing installation effects, which are also difficult to simulate in Plaxis 3D, simulating a prototype soil nailed wall was avoided. Additionally, the findings of the simulation can further be used as a firsthand approximation when simulating full-scale prototypes with incorporation of installation effects. Similarly, the reported literature, FHWA GEC No. 7[17] also recommends using scaled-down models to study soil nail wall behaviour with appropriate adjustments made to account for scaling effects. Yoo and Kim [95] has also highlighted that reduced-scale tests offer valuable insights into nail force distribution and wall deformation, which can be applied to prototype designs. The modelled slope is shown in figure 3.19 below:

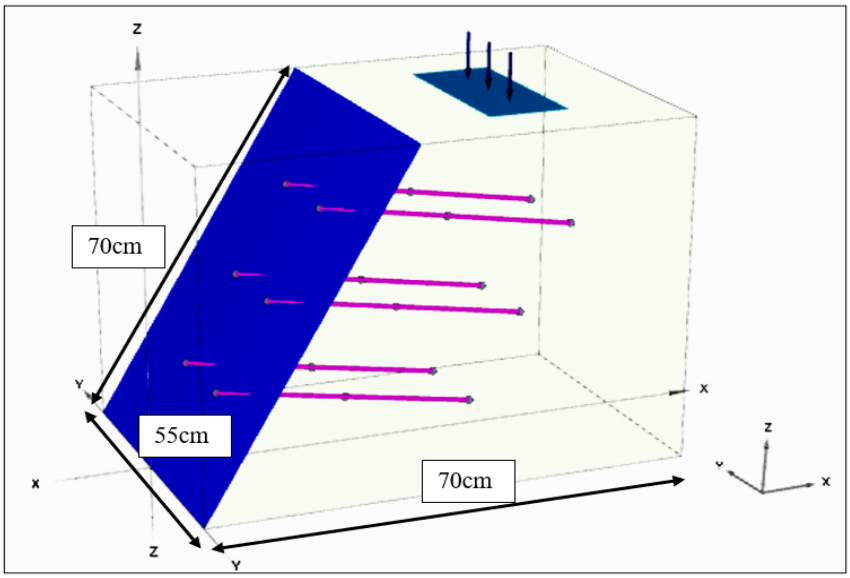

Figure 3.19 Modelled Slope

5. The in-situ stresses were developed by gravity loading and the loading was applied in the form of uniformly distributed load similar to the maximum load taken by the physical model for a specific facing.
6. The mesh is created in two dimensions once the model's geometry has been established and the material's properties have been assigned to the various soil layers. By discretizing a complicated object into distinct cells that can be assigned the governing equation, meshing makes it easier for the solver to simulate physical behaviour. If the 2D mesh is considered adequate, a 3D mesh is created. In 3D, the soil elements are essentially composed of 15 node wedge elements that are produced from 6 node triangle elements. Because of non-horizontal soil layers, some 15-node wedge elements may degenerate to 13-node pyramid elements or even 10-node tetrahedral elements.

7. However, when the entire model was meshed using fine mesh, the computational time was significantly increased. Based on the mesh size variations, regions with significant stress concentrations (e.g., around the nails, facing, and at the soil-structure interface) were only meshed using fine mesh with medium mesh for beam elements used as nails and plate element used as facing which helps ensure that the localized behaviours are well-represented. Similarly, reported literature by as Chen and Poulos [136], Dasaka and Idiculla , Lazarte et al. [11] has also advocated the use of medium-density mesh for general soil regions and fine mesh for nail-soil interfaces to better capture stress transfer mechanisms.

   The details of meshing in the current study are presented in a tabular form below:

Table 3.11 Components of Soil nail wall and Meshing

Structure	Plaxis	Mesh Generation	Mesh type	No of Elements
Nail	Beam	3-node line elements	Medium	250
Facing	Plate	6-node plate elements	Medium	250
Soil	Borehole	10-node tetrahedral elements.	Coarse	100
Interface	Through Nodes	16-node interface elements	Fine	500

The number of soil elements and nodes were about **11088 and 17806** respectively.

The Figure below 3.20 represents mesh generation in the current study.

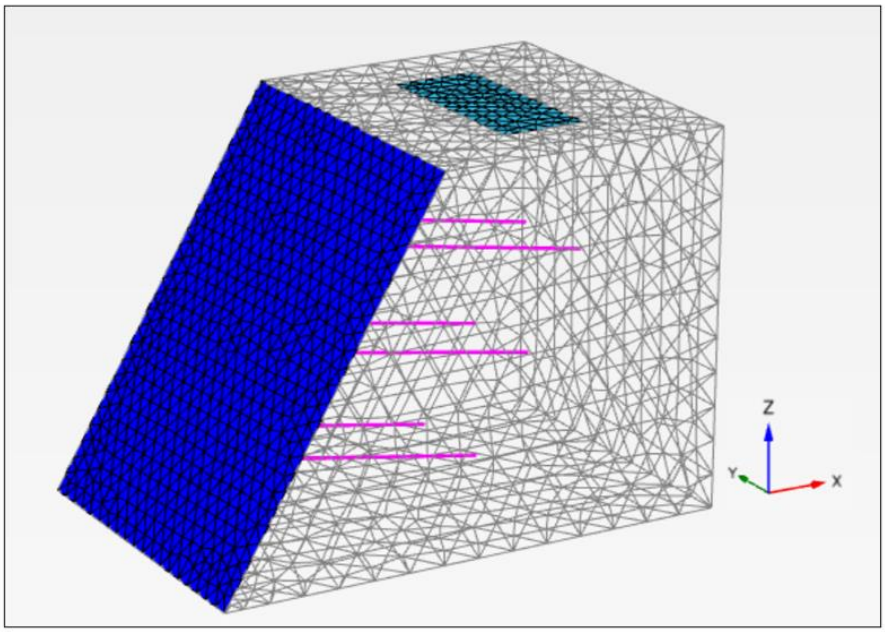

Figure 3.20 Mesh Generation

8. The calculation phases were divided into three parts i.e
   a. Initial Phase
   b. Activate Structural Elements
   c. Loading

In the first phase, or the first stage. Stress distribution and the slope's construction were completed.

Phase one displacements are rest to zero, and the nail and facing were activated in phase two. Phase three involves imposing loading and setting phase two displacements to zero. Following this, the calculation was initiated, and the results were obtained.

9. The type of calculations that were considered for first stage were gravity loading and for the second and third stage were plastic calculations. By applying soil weight through gravity loading, a real finite element calculation can be used to determine the initial stress state. According to small deformation theory, an elastic-plastic deformation analysis is performed using plastic calculation. In the majority of real-world geotechnical applications, this kind of calculation is appropriate.

10. The phi/c reduction method, which Plaxis employs for safety analysis, involves reducing the strength of the soil materials by a factor of ΣMsf until a stable value of ΣMsf is reached or the maximum number of calculation steps are reached.

3.9 Limitations of Numerical Modelling

The Mohr-Coulomb (M-C) constitutive model was selected for the present study due to its widespread application, simplicity, and proven effectiveness in capturing shear failure mechanisms and global limit state behavior in soil nail walls. Its bilinear elastoplastic formulation provides a satisfactory estimation of tensile forces and overall stability, making it well suited for design-focused analyses where global safety is the primary concern (Singh and Babu, 2010; Sahoo et al., 2016; Rawat, 2017; Sharma et al., 2019). However, it is acknowledged that this model has limitations when representing behavior closer to service conditions. The M-C approach assumes constant stiffness (E_{50}) throughout the elastic range until the yield surface is activated, whereas actual soil stiffness is highly strain-dependent and varies with both load level and unloading–reloading conditions. As a result, the M-C model tends to over-predict deformations at low stress levels and can under-predict deformations when the factor of safety is low, making it less accurate for long-term serviceability analyses (Gouw, 2014). Moreover, its inherent simplification of unloading-reloading behavior ($E_{ur} = E_{50}$) can lead to unrealistically high heave or settlement estimates, as actual unloading–reloading stiffness is often two to five times higher than the loading stiffness (Gouw, 2014).

Although the Mohr–Coulomb model correctly predicts global stability, Ardakani et al. (2014) found that it significantly overestimates deformations, lateral wall displacements and excavation base heave were noticeably higher with Mohr Coulomb compared to HS and HSS models. The Hardening Soil formulation reduced these deformations, while the HSS model incorporating small-strain stiffness yielded the least displacement often 10–20% lower than HS making it more reliable for assessing serviceability behavior in soil–nail

walls. It is acknowledged that for analyses focusing on serviceability constraints such as surface settlement, long-term deformation, and excavation-induced heave, more advanced constitutive models like HS and HSS are better suited (Brinkgreve et al., 2015; Gouw, 2014). These models offer improved prediction of strain-dependent stiffness and stiffness degradation with stress level. Although the Cam-Clay model both original and modified can capture critical state behavior and volumetric strains effectively, its formulation is most appropriate for normally consolidated or lightly over consolidated fine-grained soils. The Drucker–Prager (D-P) model, which provides a smooth approximation of the Mohr–Coulomb yield surface, is another useful alternative. It is particularly advantageous in three-dimensional simulations, such as in PLAXIS 3D, as it avoids numerical issues associated with the angular corners of the Mohr-Coulomb yield criterion. The D-P model allows a more continuous representation of the effects of intermediate principal stress and is better suited for stress states that involve complex loading paths. While the D-P and Mohr-Coulomb models produce similar results in plane strain for sandy soils, the D-P model can offer improved convergence and more stable results in 3D analyses, especially when modeling stress redistribution near soil–nail interfaces. Therefore, for sandy soils and for the purpose of capturing both stress-dependent stiffness and realistic deformation response, the HS and HSS models remain the more appropriate advanced constitutive models for future research. Moreover, the choice between plane strain and axisymmetric formulation can also influence the results, and it is essential to align the modeling approach with the actual geometry and boundary conditions of the problem (Gouw, 2014).

For future research works, it is suggested to implement these advanced models to investigate facing nail interaction, capturing critical facing behavior such as cracking initiation, strain localization, and progressive stiffness degradation. Localized strains, load transfer, and bending effects within the facing all have a significant impact on the interaction between the facing and the nail. The Mohr-Coulomb soil model's linear-elastic-plastic formulation is limited in capturing the localized strain concentrations and progressive deformation that occurs at the facing-nail junction.

4. RESULT AND DISCUSSIONS

4.1 General

The current section provides a detailed discussion of the outcomes from the different experimental objectives that were introduced in Chapter 1. Various results obtained from the physical model testing on various nail arrangements and flexible materials are presented. The stress strain behaviour of nails under different nail arrangements, their deformations, effect of each nail set on facing, Nail Forces, facing strains, pore pressure measurement, surface settlements were studied through physical testing. So based on the experimental results obtained important observations are revealed. Further the physical model results were compared with the Numerical Modelling results.

4.2 Results of Soil nail strain for Facing materials in rectangular pattern

As mentioned in the previous sections various flexible facing material for soil nail slope were considered in the current research work. The testing was done on the physical model set up in two different patterns i.e. rectangular consisting of six nails and staggered consisting of eight nails. The nail patterns were described in earlier sections with the diagram. Flexible material considered in the present study were HDPE facing net, Polyester Geogrid, Hex plastic net and Jute geomesh. The results obtained are depicted below for rectangular pattern in the graphical forms and thereafter the comparison is drawn out of them in order to find out suitable flexible facing material.

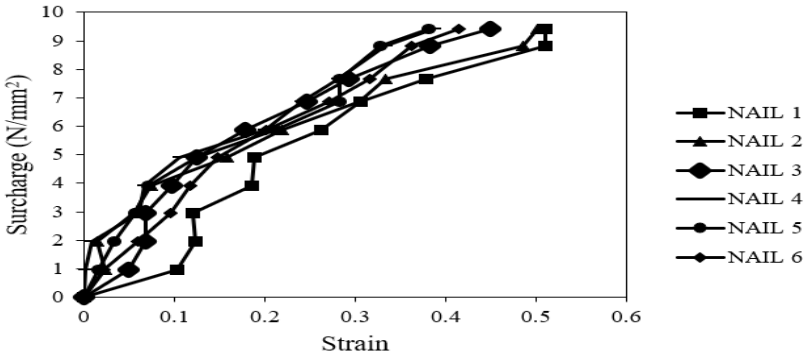

Figure 4.1 Variation of nail strain with Surcharge Pressure for HDPE facing net

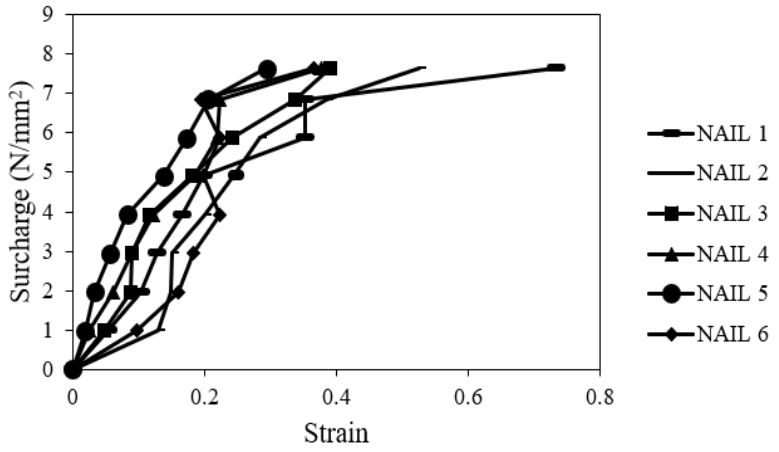

Figure 4.2 Variation of nail strain with Surcharge Pressure for Polyester Geogrid

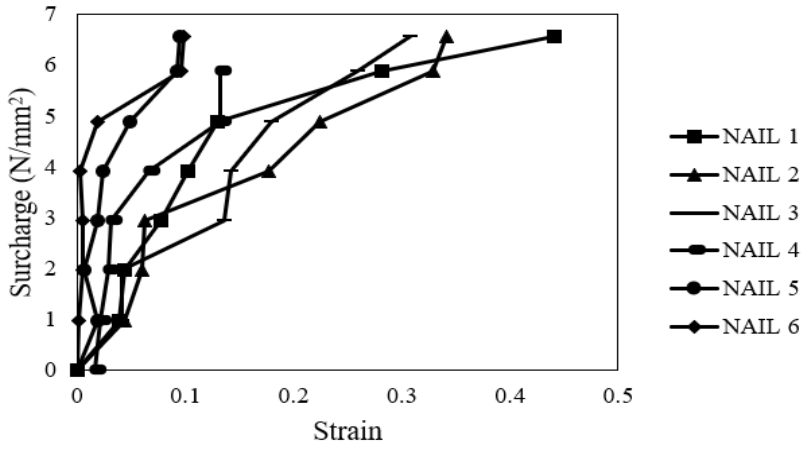

Figure 4.3 Variation of nail strain with Surcharge Pressure for Hex plastic net

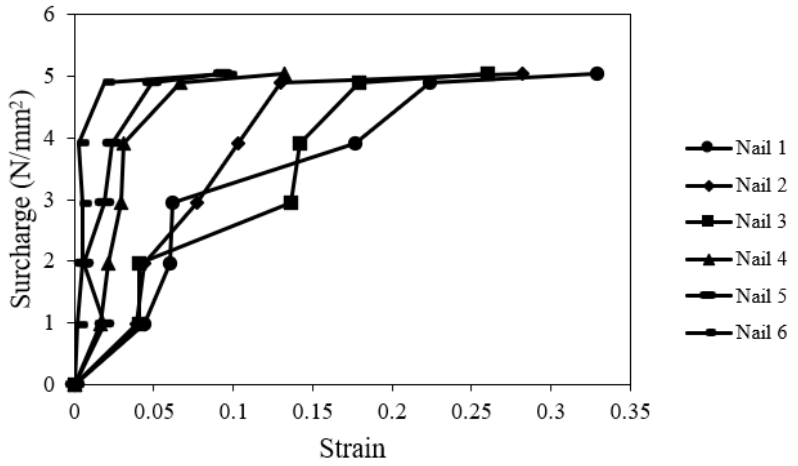

Figure 4.4 Variation of nail strain with Surcharge Pressure for Jute Geomesh

The results obtained for various flexible materials, depicted above for rectangular pattern from Figure 4.1 to 4.4 it can be concluded that the maximum stresses for a rectangular pattern are taken up by HDPE facing net and minimum by Jute Geomesh facing material, this could be majorly due to stiffness of flexible material. Moreover, the usual trend is followed in all the facing is that maximum strain is in upper set of nails mainly nail 1 and nail 2. This is due to the proximity of the external load (with limited width, i.e., non-infinite distributed loading), the upper portion of the soil nailing mass experiences higher overburden stress than the lower layers. The external load also induces greater lateral movement at the top nails compared to those at the bottom, leading to higher loading in the top nail layers.

The comparison of surcharge pressure was also studied for rectangular pattern for the above-mentioned flexible materials, the figure 4.5 below shows the variation of surcharge pressure.

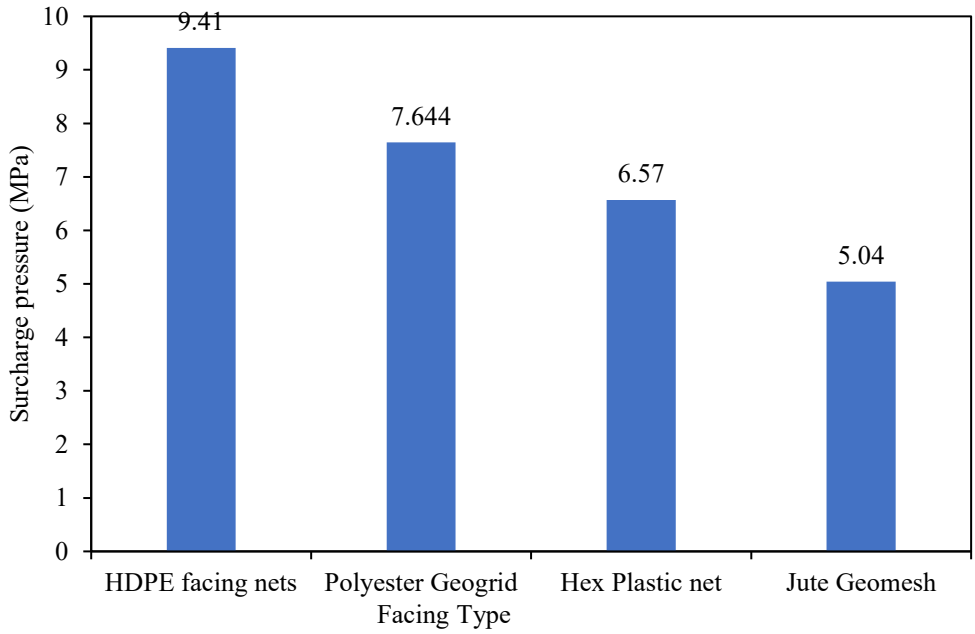

Figure 4.5 Variation of surcharge pressure for Flexible materials

As depicted from above figure HDPE facing net is able to absorb more surcharge pressure as compared to other materials due to its higher tensile strength and the maximum surcharge pressure was taken up by HDPE Facing net for both the nail arrangement. HDPE has taken up 18.80%, 30.18% and 46.43% more surcharge than Polyester geogrid, Hex plastic net and Jute Geomesh respectively in rectangular arrangement.

4.3 Average strain in each Row set for rectangular Arrangement

The comparison was conducted between various set of nails with respect to strain i.e how various rows of nails behave on the application of stresses. As in the rectangular pattern, there are six nails that basically forms three row sets i.e. Nail1 and Nail 2 considered as set 1, Nail 3 and Nail 4 as set 2 and Nail 5 and Nail 6 were considered as set 3 or lower set. So, the comparison was conducted for flexible materials and are represented in figures below:

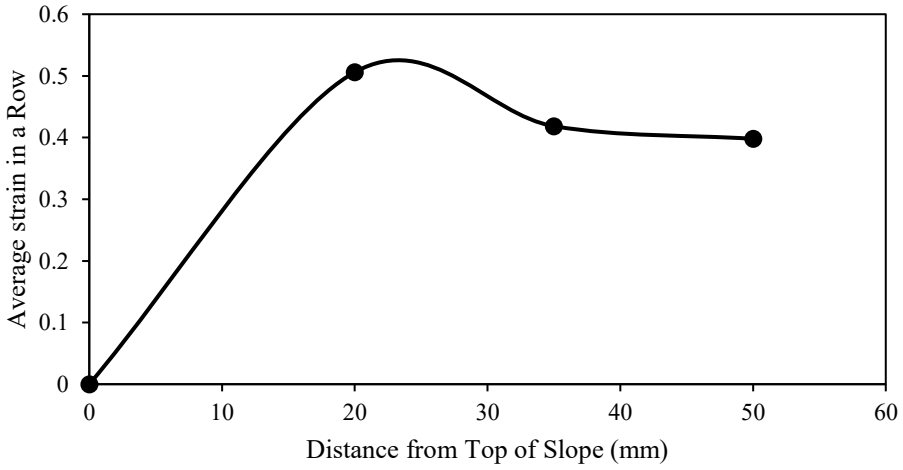

Figure 4.6 Average Strain for HDPE facing net

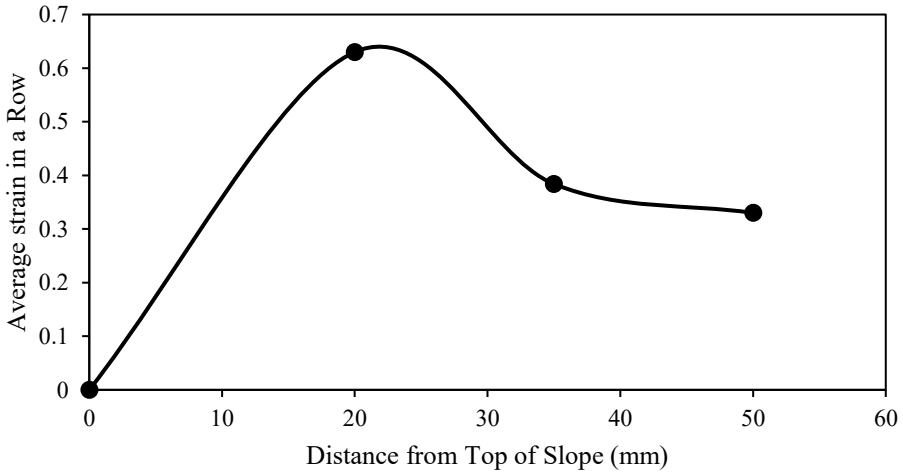

Figure 4.7 Average Strain for Polyester geogrid

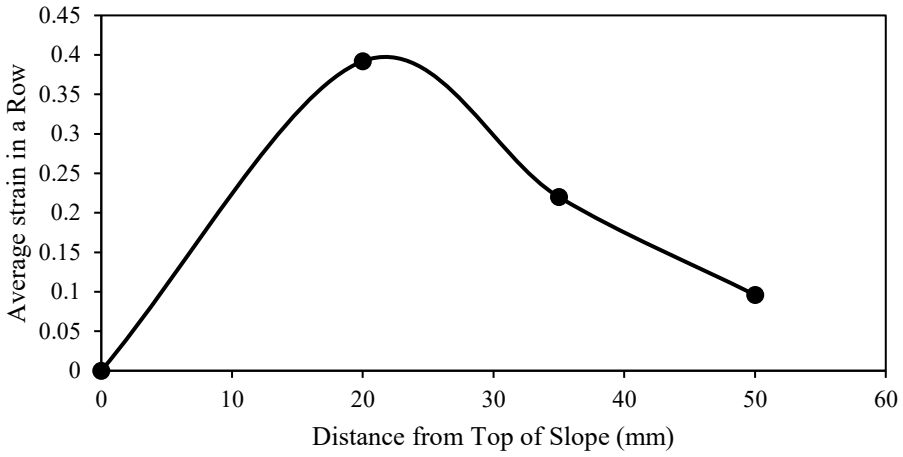

Figure 4.8 Average Strain for Hex Plastic net

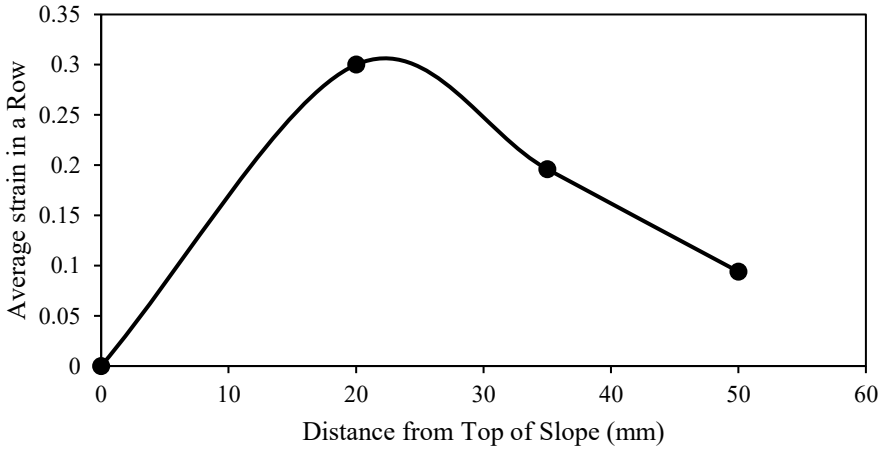

Figure 4.9 Average Strain for Jute Geomesh

As per the figures, where it is observed that the first set of nails undergo the maximum strain as compared to the other as they absorb maximum stresses the behaviour of soil nails can be understood as a function of their passive nature in response to the deformation of the reinforced soil mass. Due to the proximity of the external load (with limited width, i.e., non-infinite distributed loading), the upper portion of the soil nailing mass experiences higher overburden stress than the lower layers. The external load also induces greater lateral movement at the top nails compared to those at the bottom, leading to higher loading in the top nail layers.

4.4 Results of Soil nail strain for Facing materials in Staggered pattern

The testing was done for staggered pattern in the similar manner as done for rectangular pattern with the major difference in spacing and arrangement of nails. Flexible material considered in the present study were HDPE facing net, Polyester Geogrid, Hex plastic net and Jute geomesh.

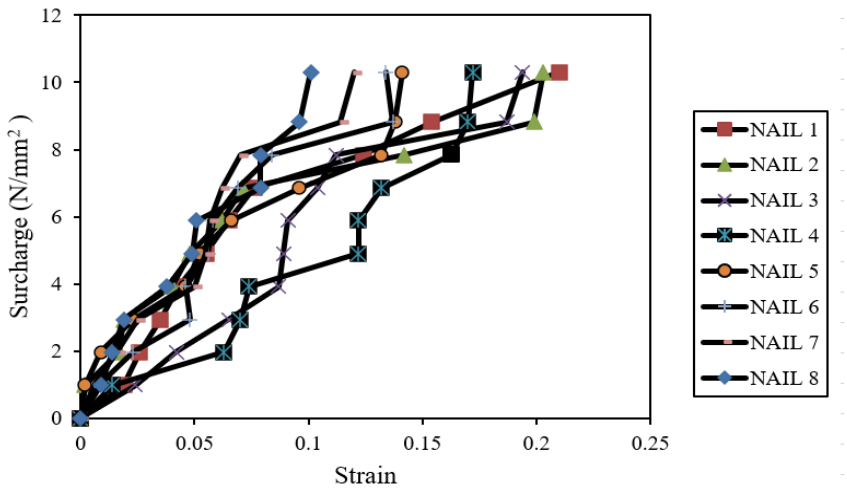

Figure 4.10 Variation of nail strain with surcharge pressure for HDPE facing

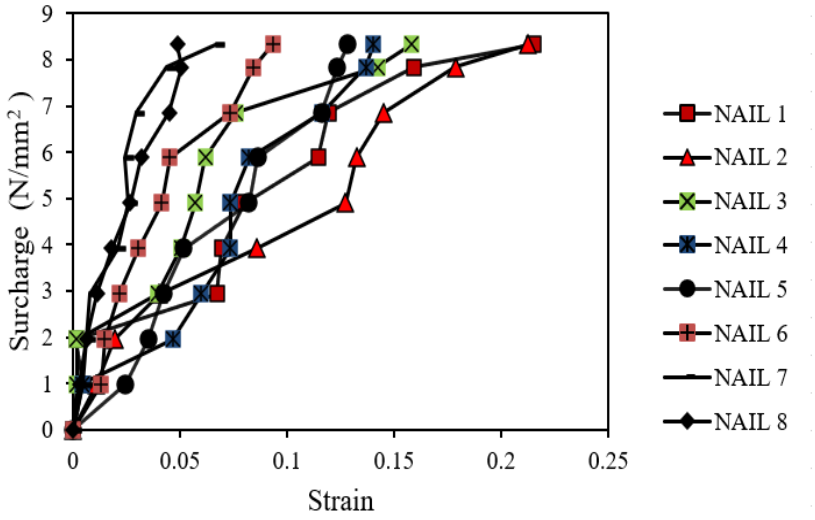

Figure 4.11 Variation of nail strain with surcharge pressure for Polyester Geogrid

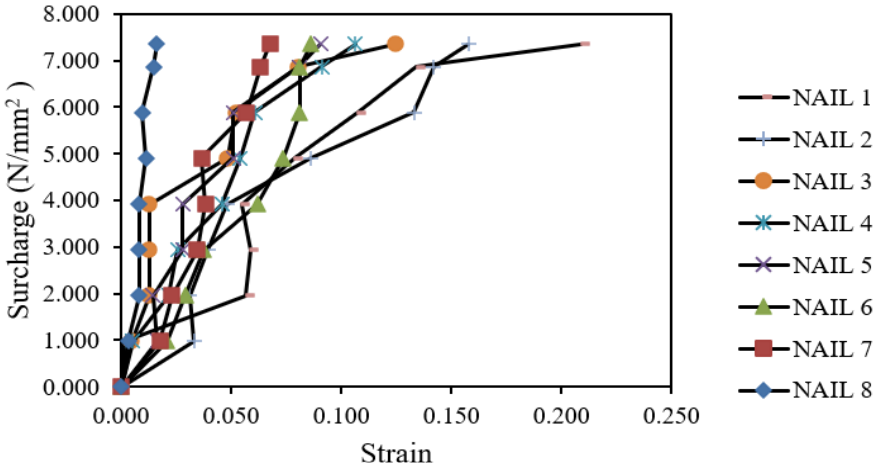

Figure 4.12 Variation of nail strain with surcharge pressure for Hex plastic net

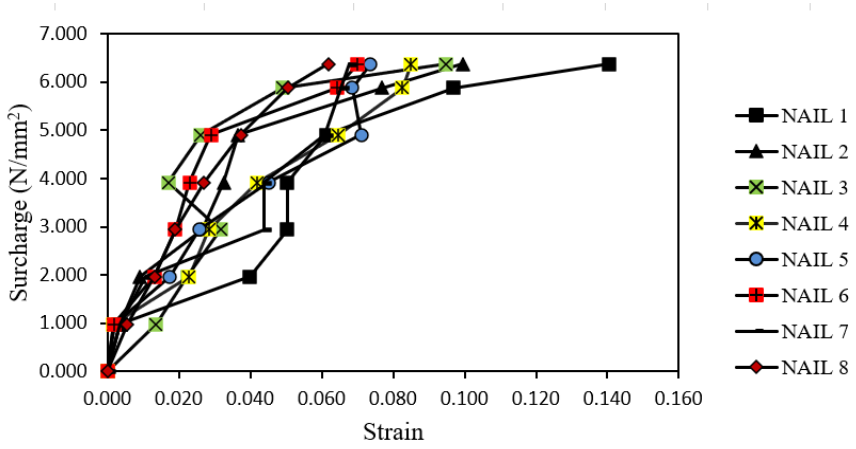

Figure 4.13 Variation of nail strain with surcharge pressure for Jute geomesh

The results obtained for various flexible materials, depicted above for staggered pattern from Figure 4.10 to 4.13 it can be concluded that the maximum stresses for a staggered pattern are taken up by HDPE facing net and minimum by Jute Geomesh facing material, this could be majorly due to the higher tensile strength of the material and stiffness of flexible material. Moreover, the usual trend is followed in all the facing is that maximum strain is in upper set of nails mainly Nail 1 and Nail 2. This is due to the fact that because of the nature of load transfer mechanisms, higher flexibility and deformation of the wall near the top, and increased lateral earth pressure at shallow depths, the upper nails in soil nail walls undergo higher strains.

The comparison of surcharge pressure was also studied for staggered pattern for the above-mentioned flexible materials, the figure 4.14 below shows the variation of surcharge pressure.

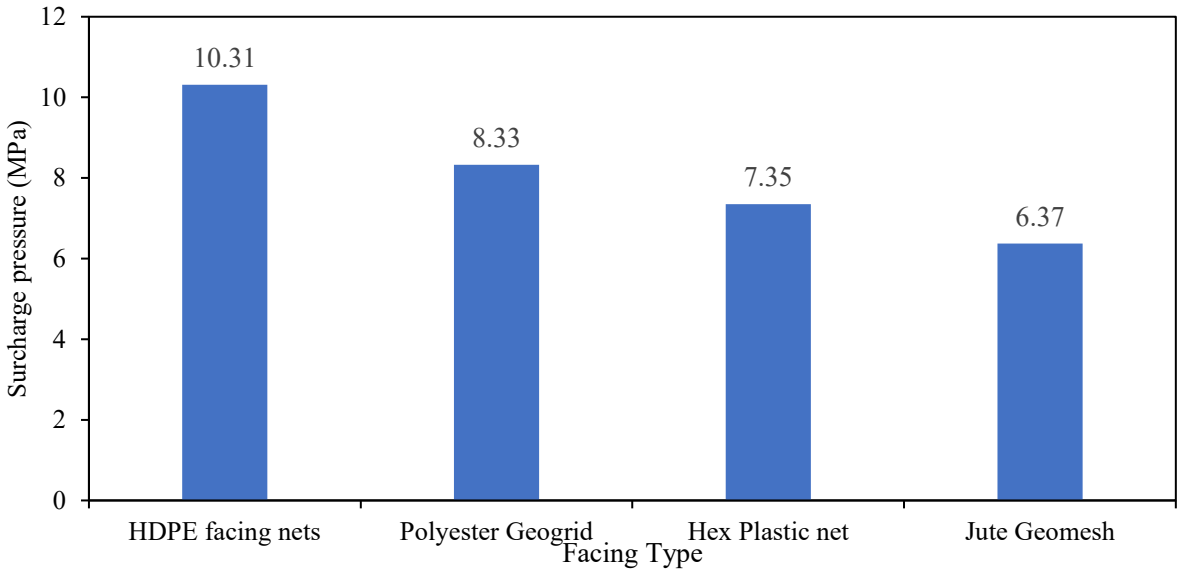

Figure 4.14 Variation of surcharge pressure for Flexible materials

As depicted from above figure HDPE facing net is able to absorb more surcharge pressure as compared to other materials due to its higher tensile strength and the maximum surcharge pressure was taken up by HDPE Facing net for both the nail arrangement. In case of staggered Pattern HDPE has taken up 19.20%, 28.70% and 38.21% more surcharge pressure than Polyester geogrid, Hex plastic net and Jute Geomesh respectively.

Further the comparison was considered for surcharge pressure in both the nail arrangements in order to find out the percentage increase in the surcharge pressure. The figure 4.15 below depicts the same.

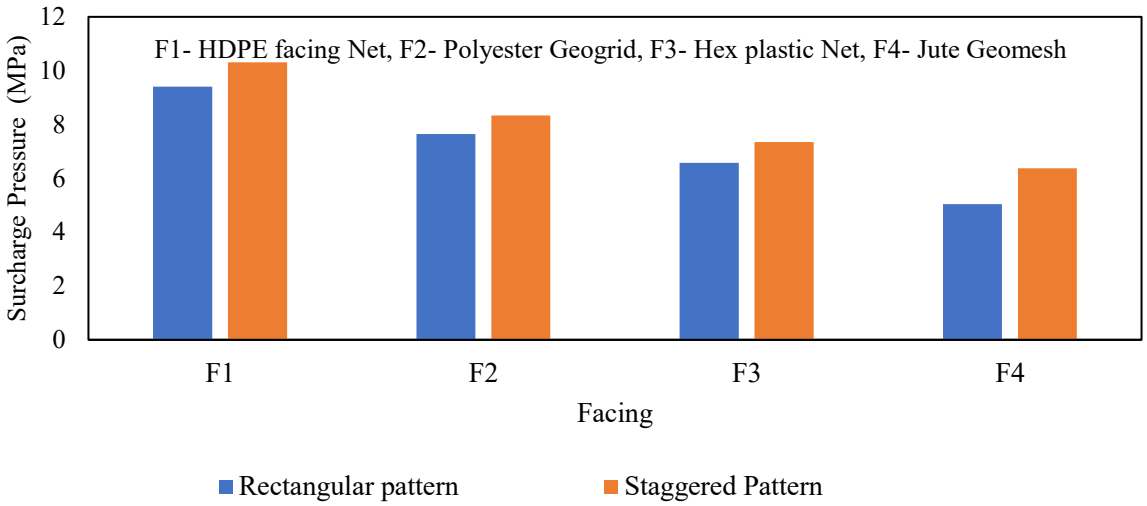

Figure 4.15 Variation of Surcharge Pressure for both Arrangement of Nails

As per the results depicted in the above figure, HDPE facing net facing is able to take up higher surcharge pressure due to its higher strength and stiffness for both the arrangements. On comparison of Surcharge pressure for both the arrangement the increase in surcharge was 9.56%, 9.03%, 11.08% and 26.38% for HDPE facing net, Polyester geogrid, Hex plastic net and Jute Geomesh respectively for staggered arrangements. There is an increase in surcharge pressure in case of staggered pattern, that is due to the fact that there is more no. of nails in staggered pattern and they are closer as compared with rectangular pattern.

However, we would like to clarify that the comparative analysis presented in our study was focused on comparing the behaviour of nails lying at equal distance from the crest of the slope in both the patterns to eliminate the influence of varying number of nails. Both aspects i.e. the change in nail pattern and the variation in the number of nails have been addressed as outlined below:

1. **Effect of Pattern**

Staggered nail arrangements are known to improve load distribution and increase the interaction area between reinforcement and soil, reducing unreinforced zones and stress concentrations on the facing. This has been reported in literature (e.g., Jewell, 1996), showing that staggered patterns offer greater redundancy and uniform soil reinforcement coverage, thus reducing deformation and strain.

2. **Effect of Number of Soil Nails**

   The total number of nails clearly contributes to overall slope stability by increasing the resisting force.

4.5 Average strain in each Row set for Staggered Arrangement

The comparison was conducted between various set of nails with respect to strain i.e how various rows of nails behave on the application of stresses. As in the staggered pattern, there are eight nails, Nail 1 and Nail 2 is considered as set 1, Nail 3 as set 2, Nail4 and nail5 as set 3, Nail 6 as set 4 and Nail 7 and Nail 8 as the 5th set. So, the comparison was conducted for flexible materials and are represented in figures below:

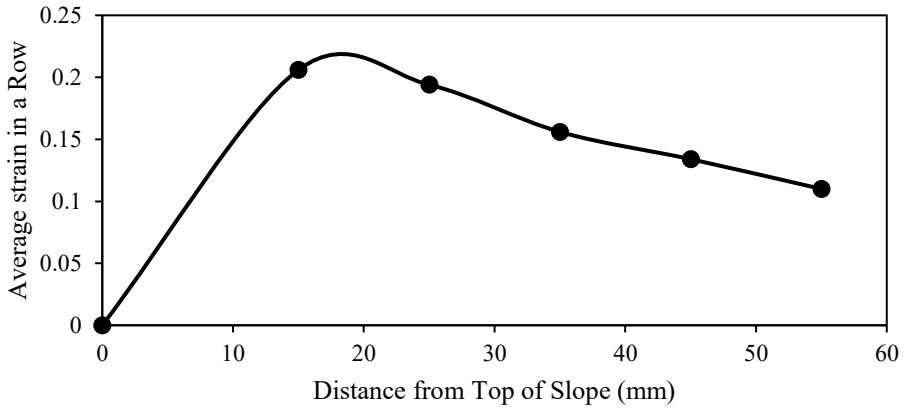

Figure 4.16 Average Strain for HDPE facing net

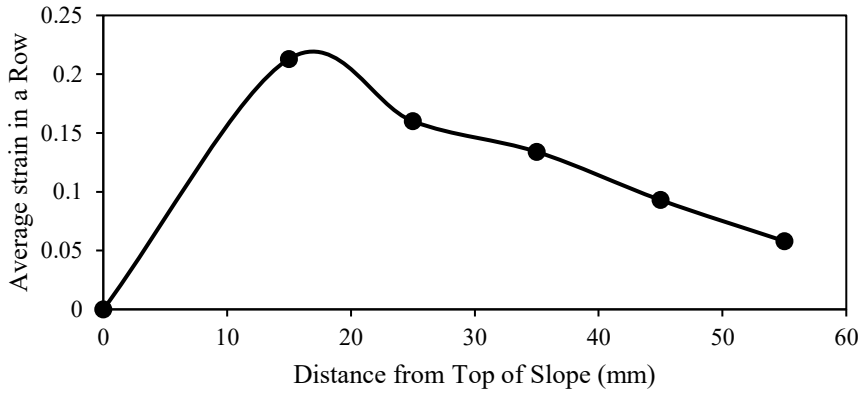

Figure 4.17 Average Strain for Polyester Geogrid

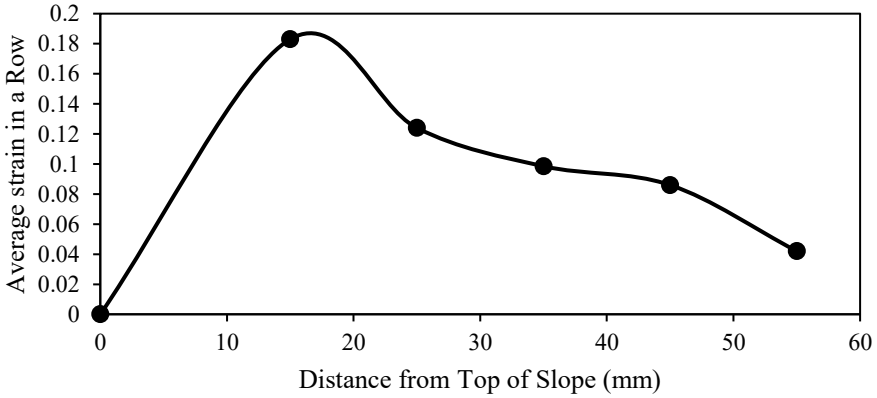

Figure 4.18 Average Strain for Hex plastic net

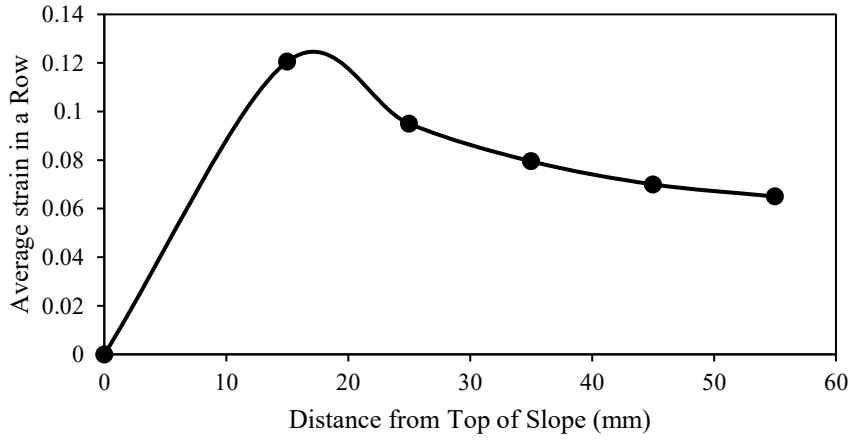

Figure 4.19 Average Strain for Jute geomesh

As per the figures 4.16-4.19, where it is observed that the first set of nails undergo the maximum strain as compared to the other as they absorb maximum stresses the behavior of soil nails can be understood as a function of their passive nature in response to the deformation of

the reinforced soil mass. As the soil experiences loading and deformation, the nails engage and mobilize their capacity, effectively distributing the loads throughout the system. Failure occurs only when the cumulative stress on all the nails approaches their respective capacity limits. Thus, the beauty of soil nails lies in their ability to work collaboratively, transferring loads seamlessly throughout the system, ensuring stability and safety until the entire nail system reaches its failure threshold.

4.6 Tensile Nail Forces in Rectangular Pattern

The pull-out capacity per unit length determines the rate at which tensile nail force begins to increase. The maximum value that establishes the nail tensile strength is reached at a certain point, which isn't always the failure surface. After that, it once more begins to decrease at the same rate until it reaches the nail head, which establishes the facing capacity. The pullout capacity, tensile capacity, and facing capacity are the three limiting conditions that set the value. so similar trend is followed in the present testing results, the nail forces were measured at the distance of 75mm, 225mm and 375mm from the nail head, the nail forces were higher for 225mm distance from the nail head. The figure 4.20 below shows the results for the nail forces for at various points.

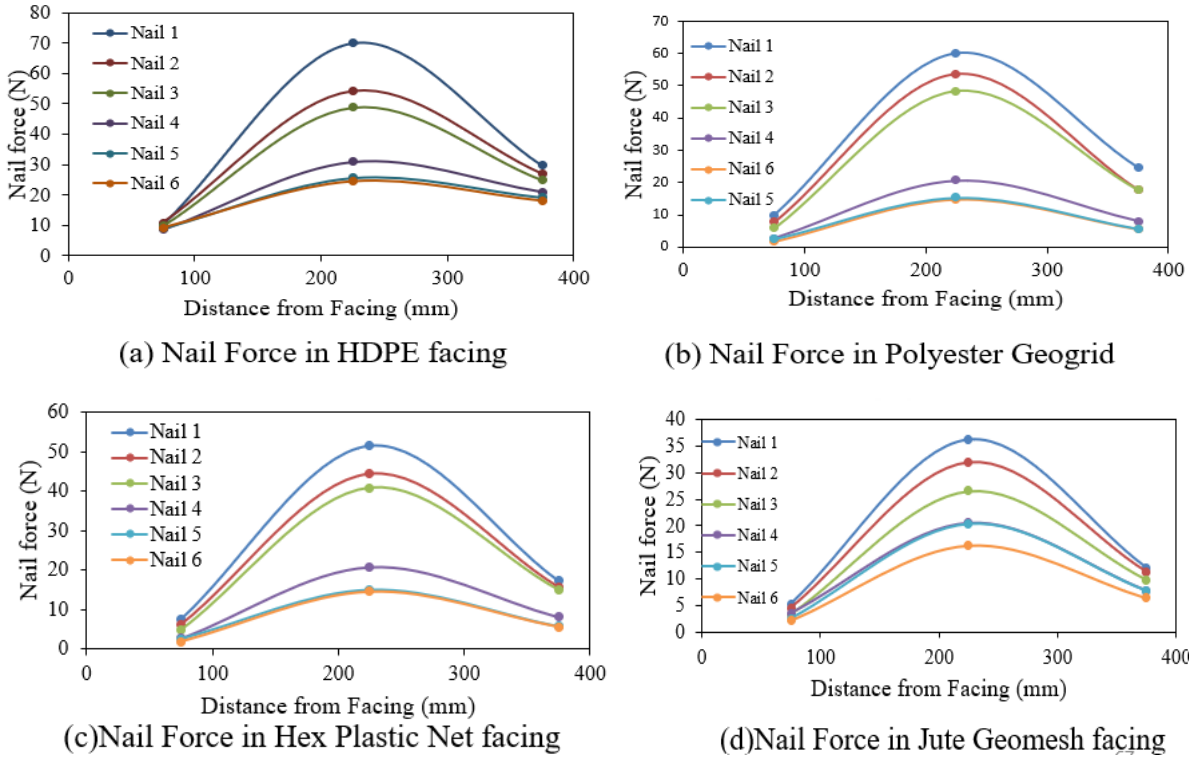

Figure 4.20 Variation of Nail forces in Rectangular Arrangement

So, from the above figures related to the tensile nail force it is found to be higher at distance of 225mm from nail head and it is due to the distribution of stress along the nail's length when it is subjected to bending forces. The nail forces were higher in the case of HDPE facing and it was found to be 14.42%, 26.33% and 48.28% higher for Polyester geogrid, Hex plastic net and Jute Geomesh respectively in rectangular arrangement.

4.7 Tensile Nail Forces in Staggered Pattern

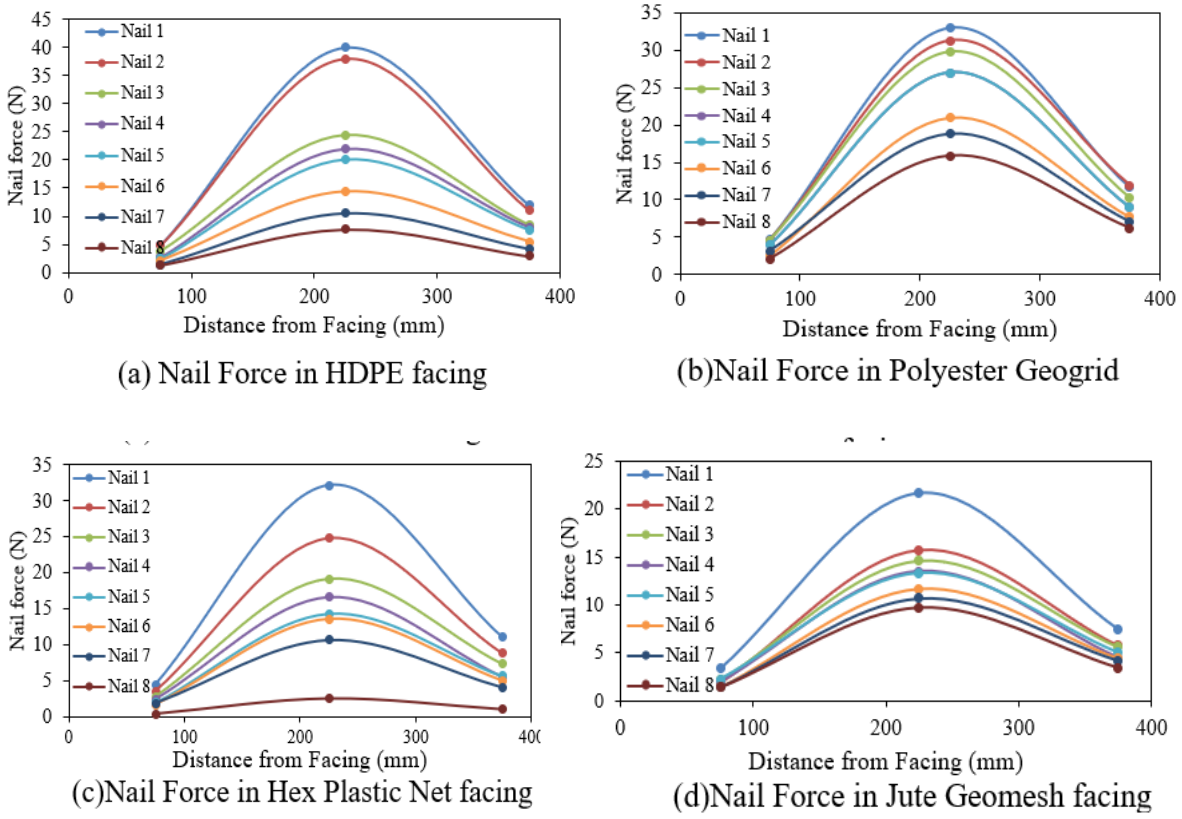

Figure 4.21 Variation of Nail Forces in Staggered arrangement

So, from the above figures related to the tensile nail force it is found to be higher at distance of 225mm from nail head and it is due to the distribution of stress along the nail's length when it is subjected to bending forces. In the present study the bending stiffness has been treated as an insignificant factor based on the findings reported by Jewel and Pedley[15] which emphasized that the shear force developed in the nail up to failure is insignificant compared with the axial forces. Moreover, similar observations were reported by Kenny and Kawai [137] where nails with highest bending stiffness, only effected the displacements in the upper half of the slope near the wall crest. Other researchers, Singh and babu,[2]; Hajialilue-Bonab & Razavi,[100] also reported to neglect the bending stiffness during the reinforcing action of the nails. Thus, the effect of bending stiffness has been neglected as a

contributing factor in the model tests. The diameter of the nail (10 mm) considered in the presented study intends to represent both the steel bar and grout-filled borehole system representing a grouted nail of 100 mm. Jewel and Pedley (1990)[15] suggested that under the common construction practice for soil nailing, grouting around the steel bar increases the surface area and consequently the axial force and shear forces increases. Nevertheless, the nail bar sags between the widely spaced centralizers causing practical difficulty in maintaining the steel bar centrally within the grout body. This leads to increase in the bending stiffness on the side of the potential shear plane where the bottom of the grouted hole is under tension and derives the advantage of bearing the compressive stress by the grout. However, on the opposite side of the potential shear plane, where the bottom of the grouted nail is under compression, no benefit either in bending stiffness or ultimate plastic moment capacity will be offered by the grout. Therefore, it was recommended to assume that grouting lead to no benefit in relation to bending forces or bending stiffness. Furthermore, for routine design of soil nailed structures, the assumption that grouted reinforcement has the same overall bending stiffness as the bar alone and the effective diameter of the soil nail equals to the diameter of the grouted hole.

Therefore, in the present study, diameter corresponding to the pre – drilled grouted bore hole is taken as the nail diameter. However, in the numerical analysis using Plaxis 3D, both the axial stiffness (EA) and bending stiffness (EI) has been used for simulating the soil nails.

Furthermore, many previous studies have also suggested to neglect the effect of bending of soil nail as compared to its tensile resistance. Babu and Singh (2009)[138] report that the development of bending moments and shear forces in nails is considerably less significant compared to axial (tensile) forces. Similarly, Elias and Juran (1987)[81] observed that the contributions of shear and bending strengths account for less than 10% of the overall stability of soil nails, which is why conventional design practices tend to conservatively disregard these components. Eleutério et al. (2018) further emphasize that while failure modes involving bending can occur under concentrated deformations near the failure surface, the overall influence of bending moments on nail performance is minimal under typical stability conditions, as also noted by Jewell (1990) and Clouterre (1991)[139].

Nevertheless, the inclination of soil nails used in the physical model is kept constant at 10° with the horizontal. As per the recommendation of Geoguide report No. 197 (Shiu and Chang[69], at inclinations between 10° to 20° with the horizontal, contribution from the shear and bending resistances mobilized in the nails is not significant and may be discounted.

The nail forces were higher in the case of HDPE facing and it was found to be 17.55%, 19.55% and 45.72% higher for Polyester geogrid, Hex plastic net and Jute Geomesh respectively in staggered arrangement.

4.8 Variation of Facing Strain with Height

The variation of facing strain was studied for both the nail arrangements as the strain vary with the increase in height of facing. As in the earlier results, the strain was found to be higher in upper set of nails for various flexible materials.

The strain measurement was done at three points on the facing as depicted in the figure as well and the results were compared for various facing materials and both the arrangements.

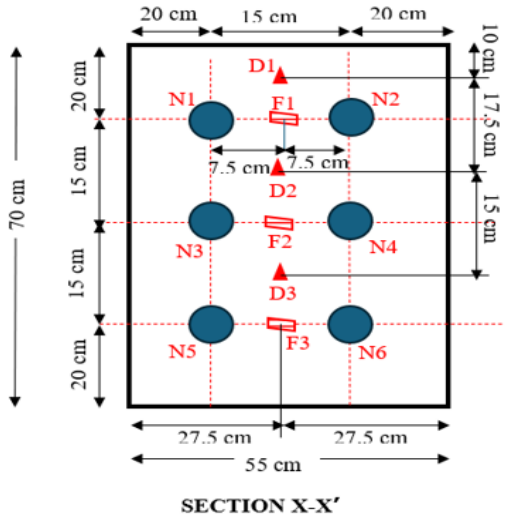

Figure 4.22 Positioning of Strain gauges

Where F1 – Strain Gauge at Location 1 on the facing i.e. 20 cm from top

F2 – Strain Gauge at Location 2 on the facing i.e. 35 cm from top

F3 – Strain Gauge at Location 3 on the facing i.e. 50cm from top

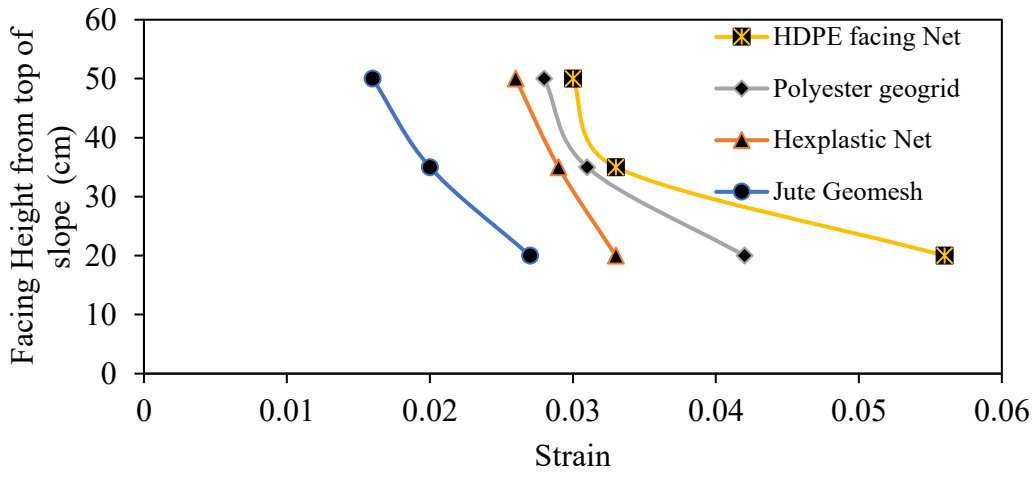

Figure 4.23 Variation of Strain with facing height for Rectangular Arrangement

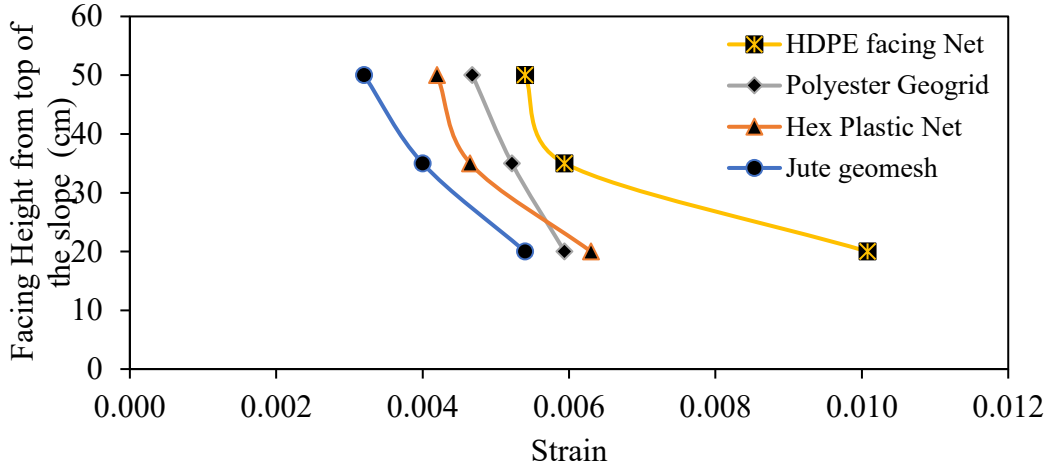

Figure 4.24 Variation of Strain with facing height for Staggered Arrangement

The upper set of strain gauge experience higher stresses than the lower set, the strain is higher in the upper strain gauge of facing because of the shape of the wall and the loading circumstances, the upper nails are frequently exposed to greater lateral loads, the proximity of the surcharge load contributes significantly to the increased mobilization near the top of the wall. However, the nails function as passive elements, with the mobilized forces in the nails linked to the stress-strain behavior of the reinforced soil mass. Therefore, in the case study model, the increased mobilized tension in the nails located near the top of the wall is attributed to the lateral displacements induced by the proximity of the surcharge load. The maximum strain is found to be in HDPE facing net for both the cases due to its higher strength and ability to withstand higher load.

4.9 Facing Strain due to variation of Surcharge

The variation of facing strain was also studied with the variation in surcharge, the three points selected in the above point were considered for surcharge variation as well. In general, with the increase in surcharge there is increase in facing strain as well but the strain was higher at the point which is near to the top of slope. The results for three points for facing stain are mentioned in figures below:

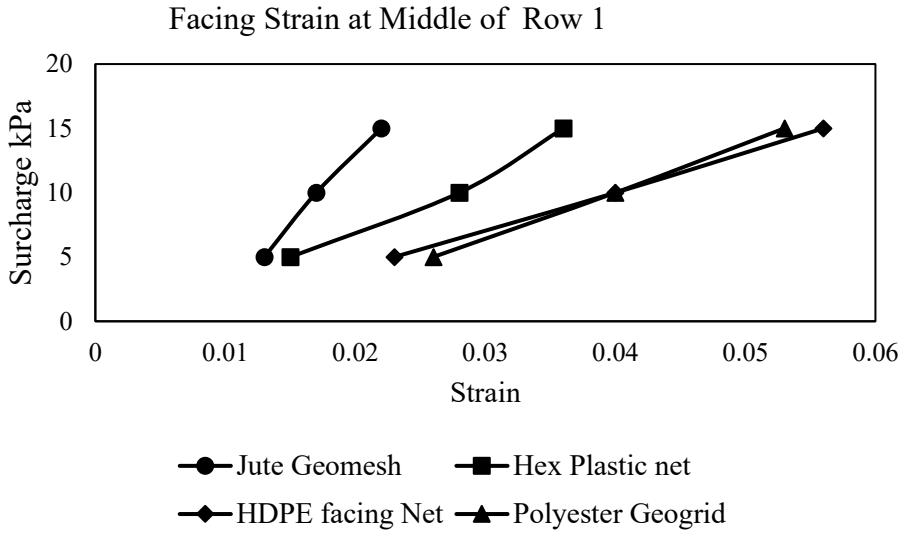

Figure 4.25 Facing strain at Middle of Row 1

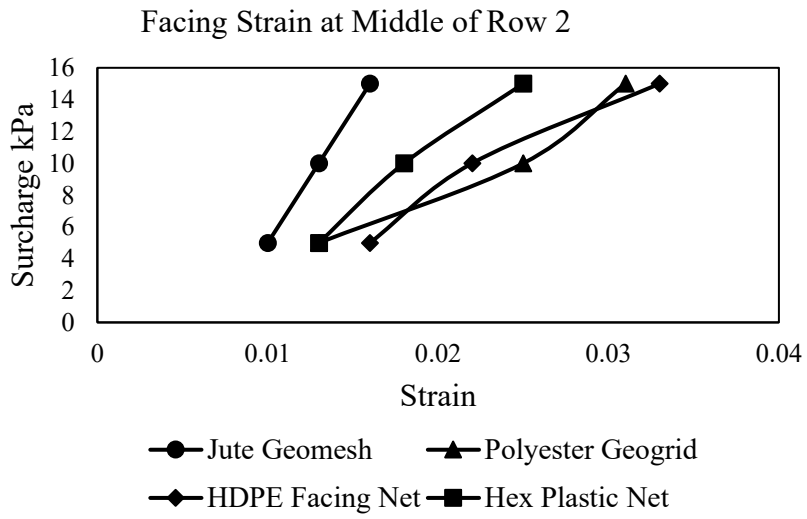

Figure 4.26 Facing strain at middle of Row 2

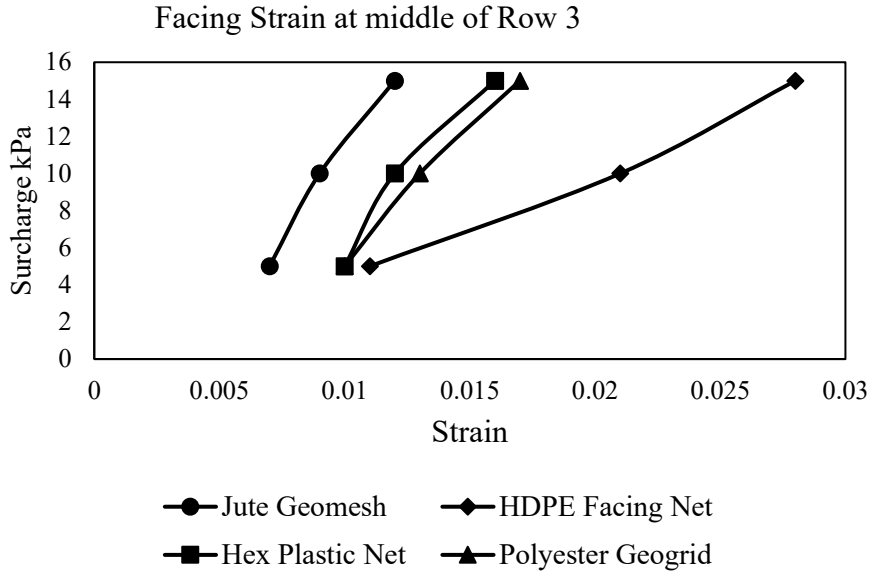

Figure 4.27 Facing strain at Middle of Row 3

The larger and more concentrated lateral pressure exerted by the surcharge load, the resulting flexural and shear stresses, and the behaviour of the soil-structure interaction near the top of the wall are the main causes of the higher facing strains in the upper set of a soil nail wall caused by surcharge variation. These elements work together to produce a situation where the top of the wall facing is subjected to greater strain than the lower parts.

4.10 Facing forces variation along the Soil nail wall

The variation in facing forces follows a pattern similar to the strain distribution. The facing forces are generally higher near the top of the soil nail wall and decrease progressively toward the bottom of the slope. Due to the proximity of the external load (with limited width, i.e., non-infinite distributed loading), the upper portion of the soil nailing mass experiences higher overburden stress compared to the lower layers. Additionally, the external load induces greater lateral movement and facing forces at the top of the soil nailing structure. The facing forces are higher in the upper part of soil nail wall and deceases towards bottom of slope. The figures below represent the variation of facing forces for both the arrangements.

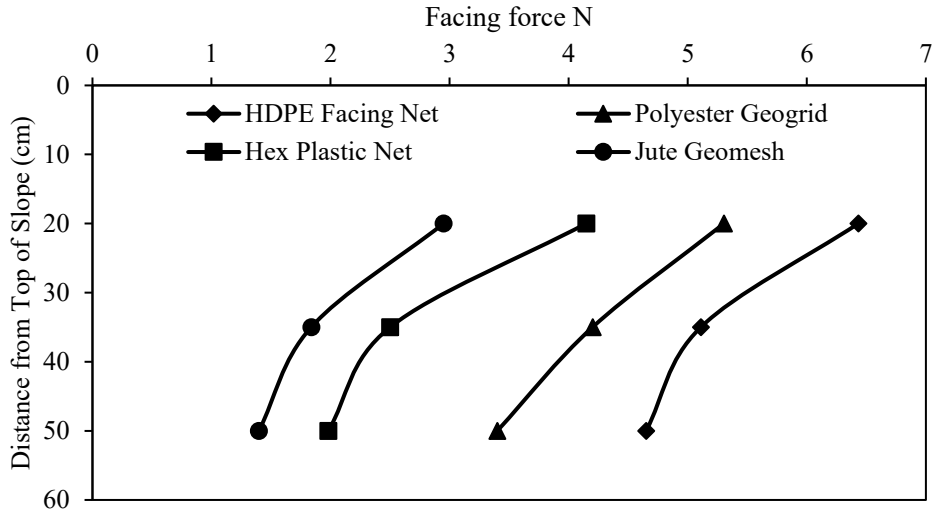

Figure 4.28 Facing Force variation in Rectangular Arrangement

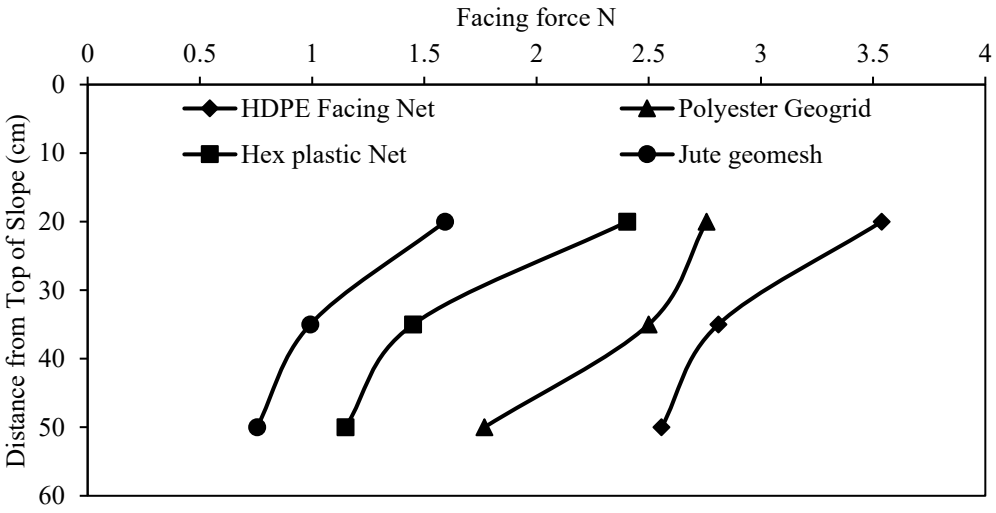

Figure 4.29 Facing Force variation in Staggered Arrangement

In the figure 4.28 and 4.29 it is observed that higher forces are in the upper set because the soil is less confined and more prone to movement close to the surface, increasing the lateral earth pressure on the facing. Higher facing forces in the upper rows result from this. Moreover, the higher forces are in the HDPE facing net as compared to other facing because of its higher strength and ability to take up higher forces than other materials. The facing forces were found to be higher in the HDPE facing net, they were higher by 17.53%, 35.54% and 54.15% as compared Polyester geogrid, Hex plastic net and Jute Geomesh respectively in rectangular arrangement. In case of staggered pattern, the facing forces in rigid facing were higher by 22.09%, 32.01%, and 54.95% for Polyester geogrid, Hex plastic net and Jute Geomesh respectively.

4.11 Effect of Nail Arrangement on Facing Strain and Facing Force

To make a comparable estimate regarding the impact of rectangular and staggered nail arrangements on the facing strain and facing force, the set of nails (for rectangular pattern - Nail 3 & Nail 4; for staggered pattern - Nail 4 &Nail 5.) at 35 cm from the slope crest are only considered. The closer spacing in the staggered configuration means that each nail experiences lower individual forces compared to the nails in the rectangular pattern. The results for the same are depicted below:

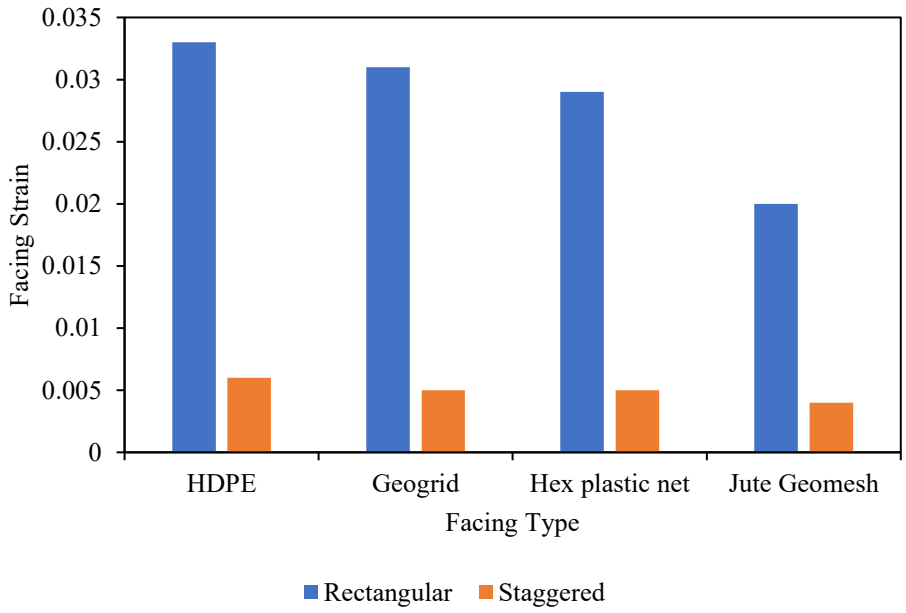

Figure 4.30 Comparison of Facing Strain for various Facing materials in Rectangular and Staggered arrangement

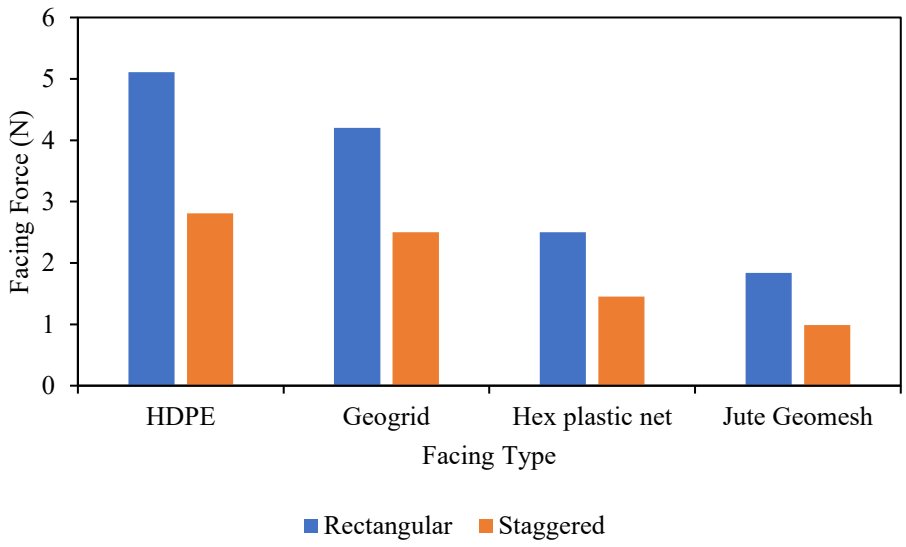

Figure 4.31 Comparison of Facing Forces for various Facing materials in Rectangular and Staggered arrangement

As can be seen from Figs. 4.30 and 4.31, facing strains and facing forces are higher in rectangular pattern due to uneven load distribution, limited redundancy, and larger unreinforced zones. In the rectangular pattern, nails are aligned in straight rows, creating gaps where soil displacement occurs, leading to concentrated stresses on the facing. This causes the facing to resist more load, resulting in higher strains.

In contrast, the staggered pattern offsets nail positions, allowing for better coverage, more uniform load distribution, and improved interception of potential slip surfaces. The staggered arrangement enhances redundancy, reduces displacement, and lowers the strain on the facing even when both patterns lie at the same distance from the top of the slope.

4.12 Bending Moment variation for various facing with reference to Nails

The installation of steel bars is carried out after drilling of boreholes and subsequent grouting around the soil nail tendons. The grouting facilitates a two – way interaction; steel bar – to – grout and grout – to – surrounding soil. The interaction in the form of interface friction creates the steel bar grouted pre – drilled hole to act as a single unit or can be represented as a nail tendon with enlarged diameter. Since in the present study, the actual installation of soil nail tendons with grout was difficult to physically model, and therefore diameter of steel bar tendons adopted was corresponding to the grouted diameter which is equivalent to the pre – drilled bore hole. Nevertheless, steel bar of 100 mm has been adopted corresponding to the cumulative diameter (soil nail tendon + grout = drilled bore hole) which lies within the range of 75 mm to 150 mm as adopted in the field. Thus, with a scaling factor of N = 10, the adopted 10 mm nail tendon corresponds to a grouted soil nail of 100 mm in the field.

Furthermore, the physical model was developed with careful attention to the flexural rigidity (EI) and axial stiffness (AE/L) (i.e. mechanical similitude) of the soil nail tendons for simulating the structural behaviour of actual nail tendon as realistically as possible at the lab – model scale. By adopting the grouted soil nail rather than the soil nail tendon alone, the approach closely reflects the field installation process, wherein the nail tendon tensile behavior supersedes the relatively minor contribution of nail tendon bending and shear forces (FHWA, 2003; Clouterre, 1991; Jewell, 1990; Babu and Singh, 2008).

Understanding the distribution of earth pressures, strengthening the facing to withstand bending stresses, and utilizing in-depth analysis techniques like FEA to guarantee the wall

can deform safely under load are all important design considerations. In order to control bending moments and guarantee the stability and lifetime of the soil nail wall, appropriate material selection, reinforcement detailing, and construction techniques are essential.

The bending moment variation for various facing with respect to nails was studied and it was calculated by using Eqn. 4.1 as given by Shaw-Shong, 2005[140]

$$T_{FN} = C_F\left(M_{v,neg} + M_{v,pos}\right)(8S_hS_v) \qquad \text{Eqn. 4.1}$$

T_{FN}: Critical nail head strength,

C_F: Flexure pressure factor (from Table 4.1);

$M_{v,neg}$ and M_{vpos} : Vertical nominal unit moment resistance at the nail head and mid-span;

S_h & S_v: Horizontal and vertical nail spacings

Table 4.1 Values for Flexural pressure factor Punching Shear factor[140]

Facings Thickness (mm)	Temporary Facings		Permanent Facings	
	C_F	C_S	C_F	C_S
100	2.0	2.5	1.0	1.0
150	1.5	2.0	1.0	1.0
200	1.0	1.0	1.0	1.0

The variation of bending moment for various nails is depicted below:

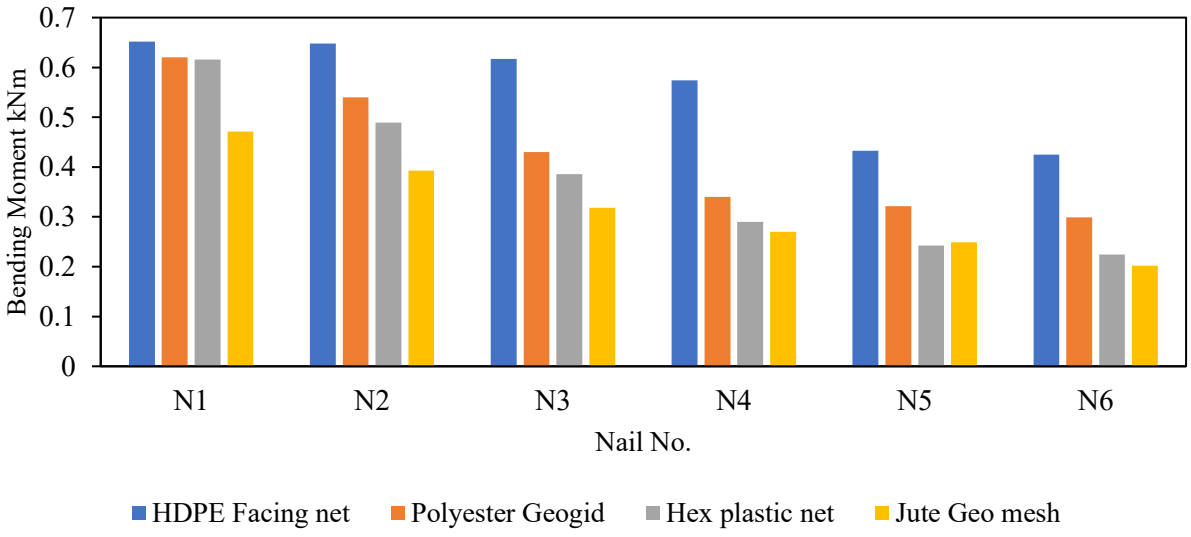

Figure 4.32 Variation of Bending Moment for various facing

The bending moment is higher in the upper set of nails because the upper part of a soil nail wall frequently functions as the free end of a cantilever beam. This indicates that because of the soil mass's leverage effect behind it, it undergoes greater bending moments. Lower nails

have low bending moments than upper nails because the wall acts more like a fixed end towards lower end of wall. Due to its increased stiffness, HDPE facing net has higher bending moments because the material experiences higher internal stresses as a result of its stiffness. The bending moment was noticed higher in HDPE facing slope as compared to other flexible materials as it was 4.88%, 5.66% and 27.70% for Polyester geogrid, Hex plastic net and Jute Geomesh respectively.

4.13 Facing Punching mobilized stress variation for various facing with reference to Nails

When designing soil nail walls, punching shear—which focuses on the localized shear failure of the facing material as a result of concentrated loads from the nail heads or anchor plates—is an important factor to take into account. Making sure the facing is thick enough, employing the right reinforcement, distributing loads efficiently, and choosing the right facing materials are all necessary to prevent punching shear.

The Facing Punching mobilized stress for various facing with respect to nails was studied and it was calculated by using following equation given by Shaw-Shong, 2005[140].

$$T_{FN} = V_N \left(\frac{1}{1 - C_S(A_C - A_{GC}) \Big/ (S_h S_V - A_{GC})} \right) \quad \text{Eqn. 4.2}$$

C_s: Punching shear pressure factor,

A_c: Soil contact area of cone-shaped block;

A_{GC}: Cross sectional area of grout column,

V_N: Nominal internal facing punching mobilized stress.

The variation of Facing Punching mobilized stress for various nails is depicted below:

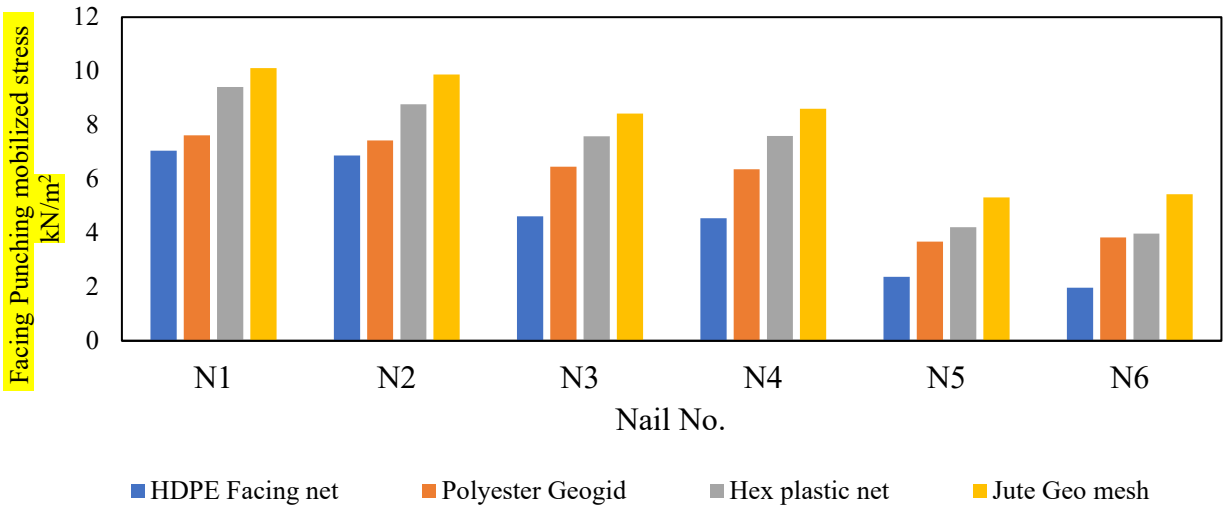

Figure 4.33 Facing Punching mobilized stress variation for various facing w.r.t Nails

The variation in Facing Punching mobilized stress with depth, despite identical nail and facing conditions, is due to increasing overburden pressure and active earth pressure at greater depths. This results in higher axial forces in the nails and greater stress concentrations around nail heads in the lower sections of the wall. Flexible facings deform under these stresses, redistributing loads and mobilizing higher resistance at greater depths. The observed variation arises from the interaction between soil pressure, nail forces, and facing deformation. Higher facing punching mobilized stress at these locations may result from these concentrated loads. Due to greater deformation, which produces greater shear forces around the points where the nails pierce the facing, the facing punching mobilized stress is higher in jute geomesh due to its lower strength. The Facing punching mobilized stress was found higher in Jute Geomesh and it was higher by 6.95%, 24.68% and 30.26% for hex plastic net, Polyester geogrid and HDPE facing net respectively.

4.14 Facing Stiffness Results and Equations Proposed

Soil nail walls behave and function under different loading scenarios requires an understanding of the stiffness of the facing material. The following results show how facing stiffness affects the total axial force, the bending moment, and the relative significance of bending moments on internal nail stresses. The equations have been suggested based on these results.

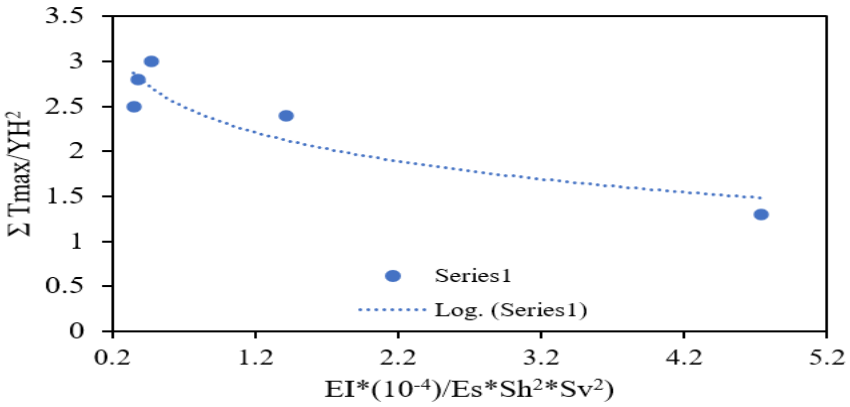

Figure 4.34 Influence of Facing Stiffness on Summation of Axial forces

Equation Proposed

Nail tensile forces per nail from facing stiffness (*EI*) and soil stiffness (E_s) can be calculated using Eqn 4.3

$$\Sigma T_{max} = \gamma H^2 / 1.22\ (\log EI*(10^{-4})/(Es*S_h{}^2*S_v{}^2)) - 0.363 \qquad \text{Eqn.4.3}$$

Where S_h – Horizontal Spacing of Nails

S_v- Vertical Spacing of Nails

γ- Unit weight of Soil

H- Height of soil nail wall

The proposed equation is site specific including surcharge load, distance from the facing, facing inclination, structure height, and the nails' axial and bending stiffness. However, the proposed equation holds good for estimating the nail tensile forces in soil nailed structures with Young's Modulus (*E*) varying between 1500 to 6000 MPa for flexible facing materials.

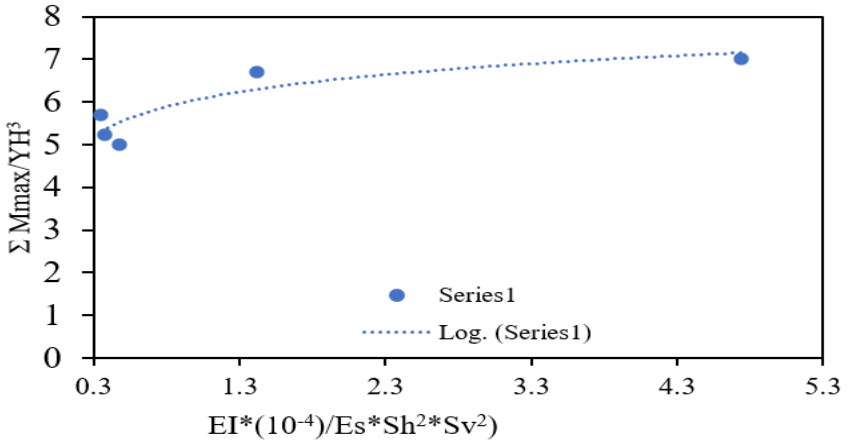

Figure 4.35 Influence of Facing Stiffness on Summation of Bending Moments

Equation Proposed

Bending Moment per nail from facing stiffness (EI) and soil stiffness (E_s) can be calculated using Eqn. 4.4

$$\Sigma M_{max} = \gamma H^3 /1.63(logEI*(10^{-4})/(Es* S_h{}^2*S_v{}^2))-0.781 \quad \text{Eqn. 4.4}$$

Based on the above equations Eqn.4.3 and Eqn.4.4 the relative importance of bending moment on nail internal stresses is related to index I_m as follow:

$$I_m = (6/e)\,\Sigma M_{max} / \Sigma T_{max} \quad [141] \quad \text{Eqn.4.5}$$

Where (e) is thickness of the facing.

The relative importance of the bending on soil nail stresses is shown in shown in Figure 4.36 below:

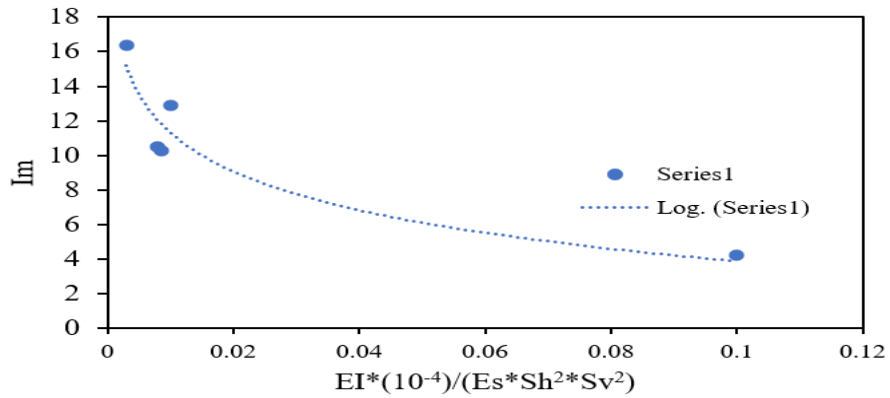

Figure 4.36 Influence of Facing Stiffness on nail internal stresses

So, from above figures 4.34 to 4.36, The soil yielding near the face is controlled by the facing stiffness, which also affected the nail bending moment. An important factor in the construction and functionality of soil-nailed walls is facing stiffness. It affects the internal stresses, bending moments, and axial force distribution and magnitude in the nails.

4.15 Lateral Slope Deformation with Surcharge

Increased lateral earth pressure and vertical settlement brought on by the surcharge have an impact on lateral slope deformation in soil nail walls. Setting deformation limits, improving wall stiffness and reinforcement, and analyzing these effects are all necessary for proper design. In order to guarantee the wall's stability and functionality under surcharge circumstances, monitoring and routine maintenance are essential. The impact of surcharge on lateral slope deformation was discussed in various flexible facing materials and for both the nail arrangements. The results for rectangular pattern are as under:

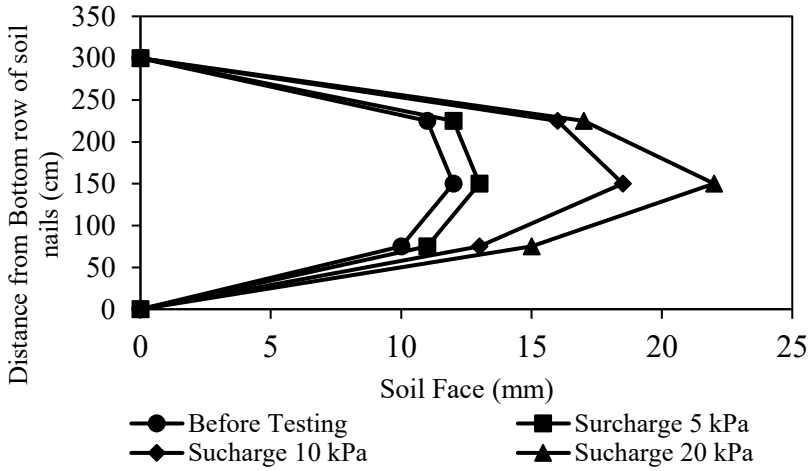

Figure 4.37 Lateral deformation for HDPE facing net

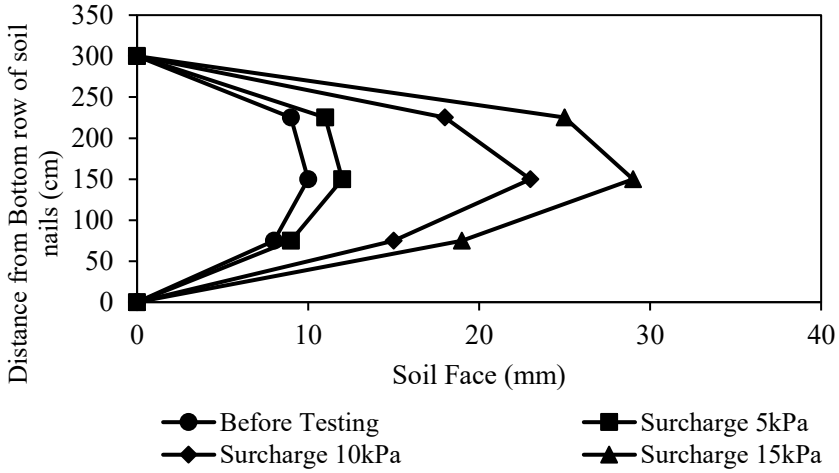

Figure 4.38 Lateral deformation for Polyester geogrid

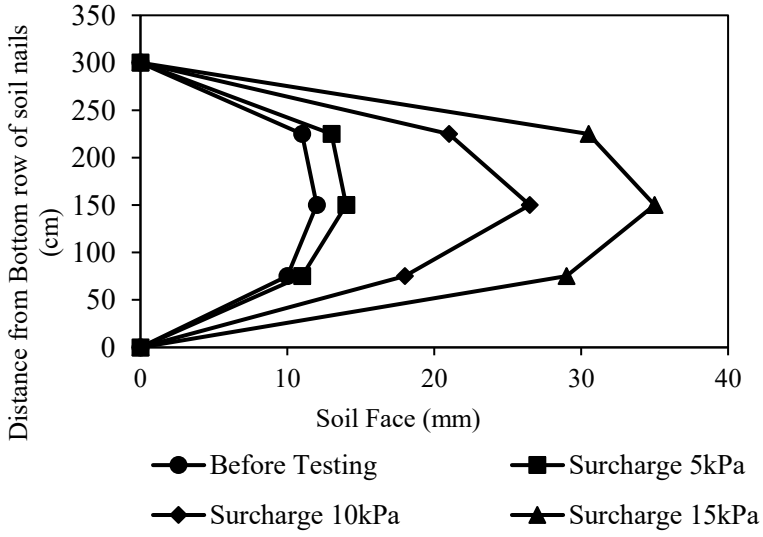

Figure 4.39 Lateral deformation for Hex plastic net

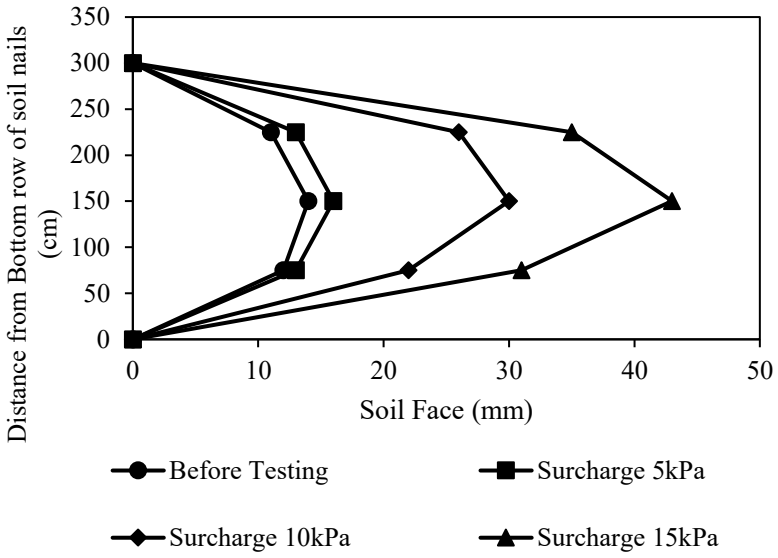

Figure 4.40 Lateral deformation for Jute Geomesh

As per the results mentioned in Figure 4.37 to 4.40 the HDPE facing has less deformation even at the higher surcharge pressure, this is due to the fact that HDPE facing is having higher stiffness as compared to other material and is able to take up the reasonable amount of stresses before its failure. Lateral facing displacement were maximum in Jute geomesh facing. As compared to lateral displacement of slope with hex plastic net, Polyester geogrid and HDPE facing, the lateral displacement of Jute geomesh was 18.60%, 32.55% and 48.83% higher. Similarly, the results were studied for staggered pattern as well which are depicted below:

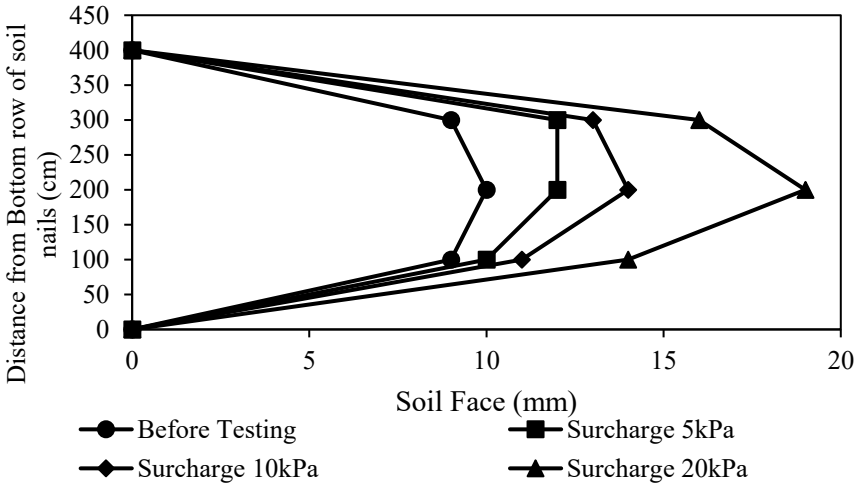

Figure 4.41 Lateral deformation for HDPE facing net

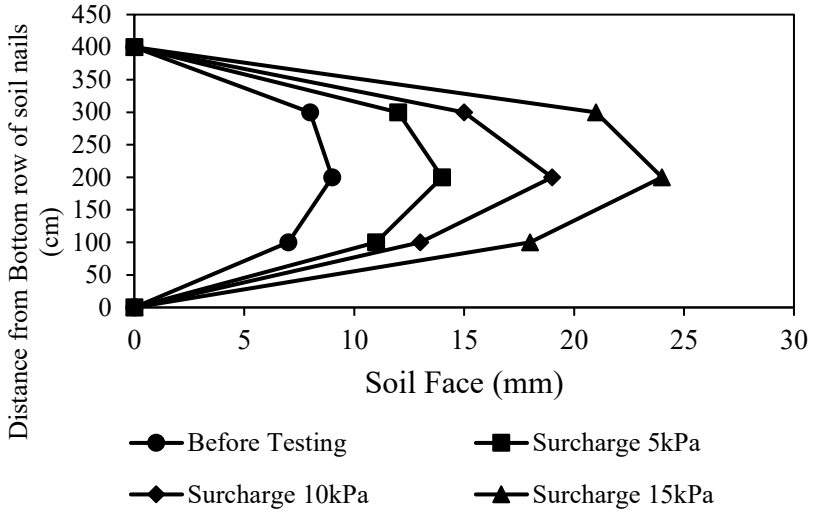

Figure 4.42 Lateral deformation for Polyester Geogrid

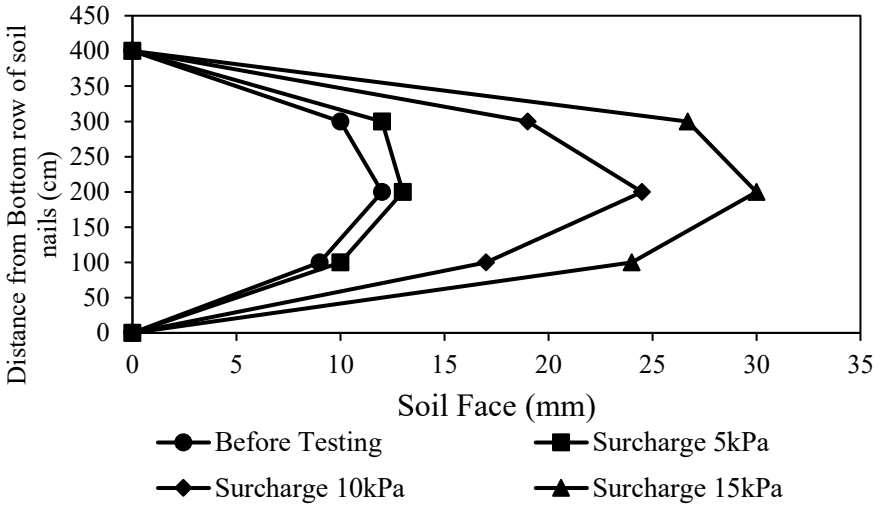

Figure 4.43 Lateral deformation for Hex plastic net

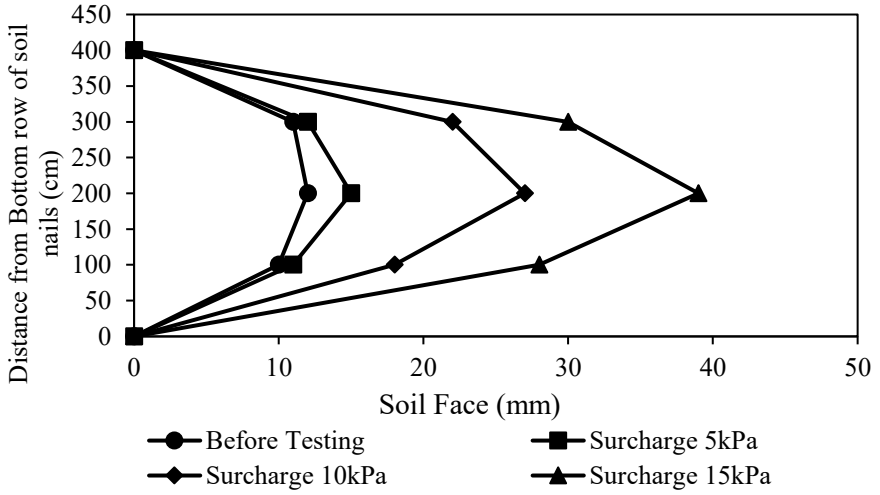

Figure 4.44 Lateral deformation for Jute geomesh

As per the results mentioned in Figure 4.41 to 4.44 the HDPE facing has less deformation even at the higher surcharge pressure, this is due to the fact that HDPE facing is having higher stiffness as compared to other material and is able to take up the reasonable amount of stresses before its failure. The similar trend was observed as in the rectangular pattern. Lateral facing displacement were maximum in Jute geomesh facing for staggered arrangement and were found to be higher by 23.07%, 38.46% and 51.28% for hex plastic net, Polyester geogrid and HDPE facing net respectively as compared to Jute Geomesh facing.

4.16 Vertical Deformation with Surcharge

The vertical displacement increased in tandem with the surcharge due to a number of factors including higher loads, soil settlement, increased lateral pressure, material deformation properties, and long-term effects like creep. The displacement was examined in relation to the variation in surcharge.

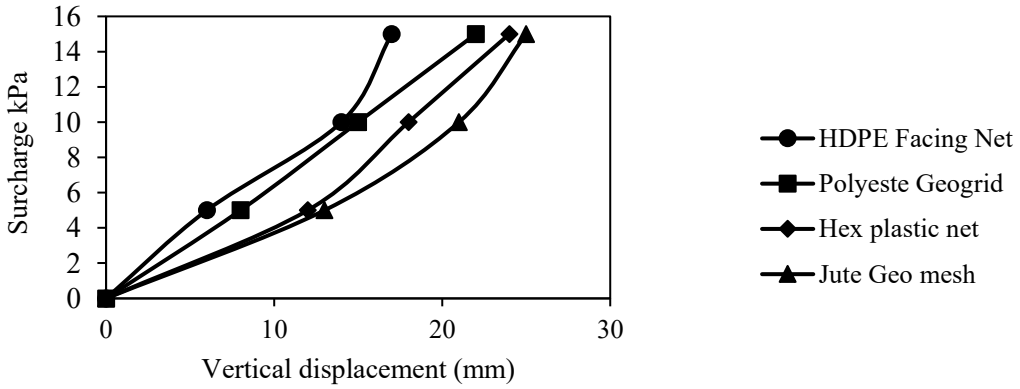

Figure 4.45 Comparison of Vertical Deformation with Surcharge in Rectangular arrangement

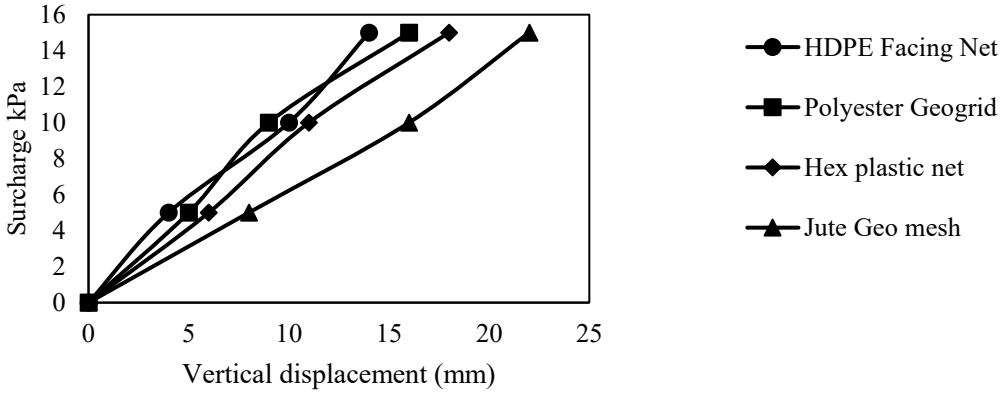

Figure 4.46 Comparison of Vertical Deformation with Surcharge in Staggered arrangement

The vertical displacements are higher in Jute geomesh due to its lower strength and stiffness and the displacements are lower in the staggered arrangement due to higher no. of nails in the

staggered pattern. Vertical Settlements were higher for Jute geomesh by 4%,12%, and 32% as compared with hex plastic net, Polyester Geogrid and HDPE facing net respectively in rectangular arrangement. In the case of staggered arrangement, they were higher for Jute geomesh by 18.18%, 27.27% and 36.36% as compared with hex plastic net, Polyester Geogrid and HDPE facing net respectively.

4.17 Drainage Assessment of Flexible Facing

The pore water pressure within the slope was measured by using PPTs (Pore Pressure Transducers) and the figure below shows the variation of measured pore water pressure within the soil due to the seepage of water in the slope. As mentioned earlier three PPTs were used in the test and the recording was done till 900 seconds.

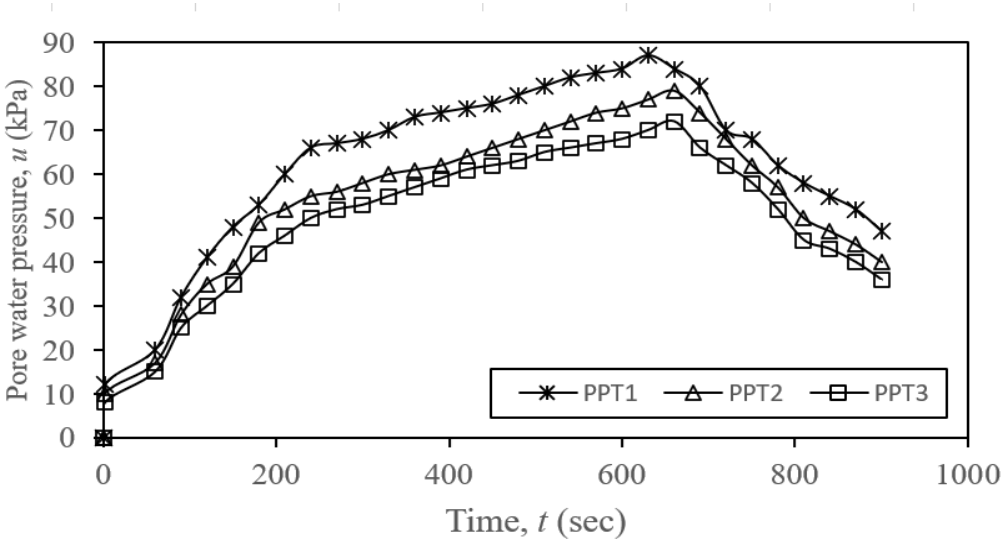

Figure 4.47 Variation of Pore Water Pressure with time

The variation of pore pressure was studied by utilizing three pore pressure transducers and it was found that PPT 1 has developed higher pore pressure as it is near to the bottom of the tank while others were away as depicted in schematic diagram. The values for pressure were in increasing order till 660 seconds and after that decreasing trend was followed for all the PPTs.

The variation of surface settlement with respect to lateral distance at various values of normalized pore water pressure i.e (u/YH) for Pore pressure transducer, PPT 2 are shown below. The normalized pore water pressure is essentially the ratio of the bulk unit weight of model soil divided by the slope height H to the pore water pressure as measured by PPT at the midpoint from the slope's crest. Surface settlements increase together with an increase in seepage. The variation of lateral distance from crest of slope w.r.t Surface settlement was

studied at six different values of u/YH for all the facing materials. The graphs below demonstrate how surface settlements vary with lateral distance from slope crest.

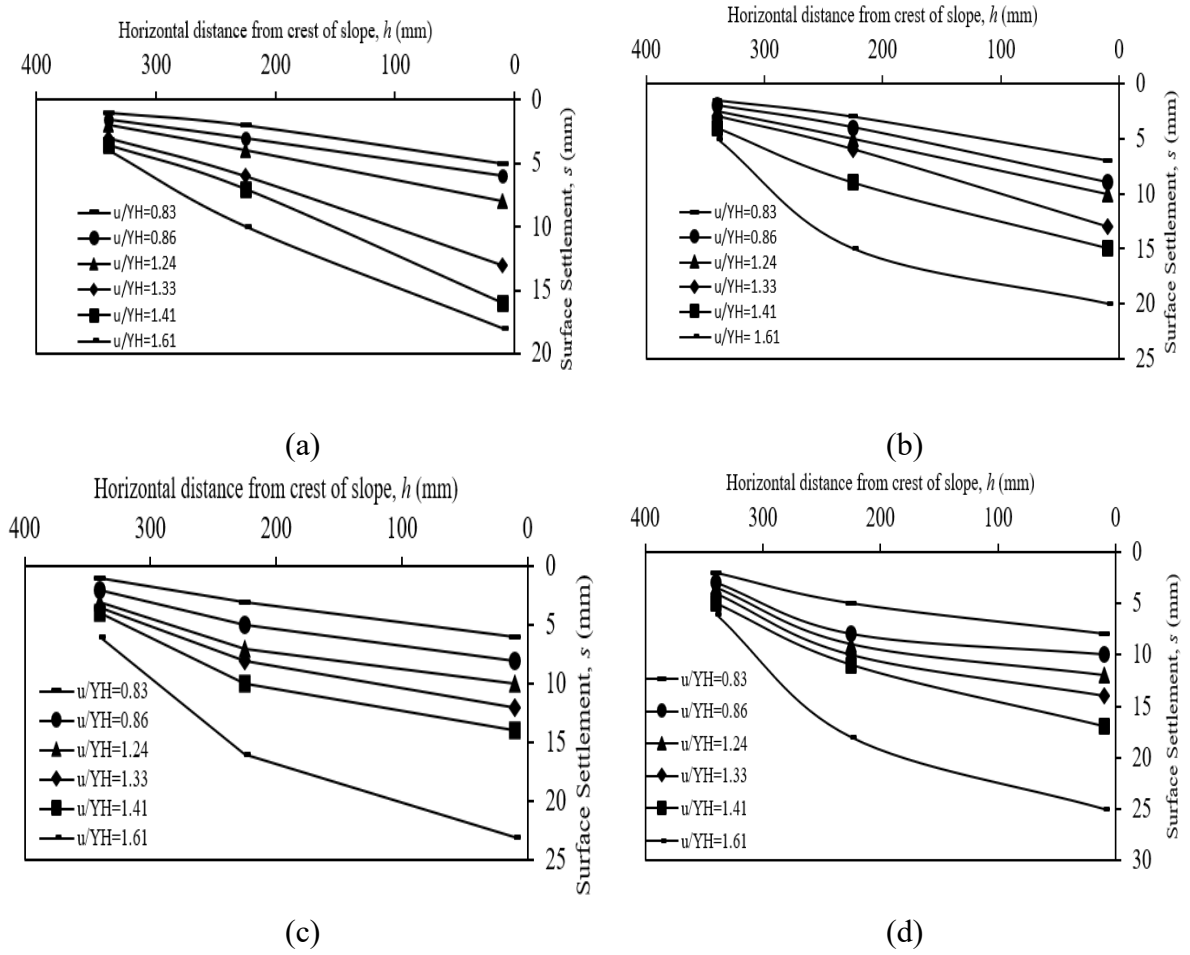

Figure 4.48 Variations in surface settlements with horizontal distance from Slope crest and Normalized Pore water Pressure for (a) HDPE facing, (b) Polyester Geogrid, (c) Hex plastic net (d)Jute geomesh

Similarly, the variation was also studied for the staggered arrangements and the results are depicted below for the same.

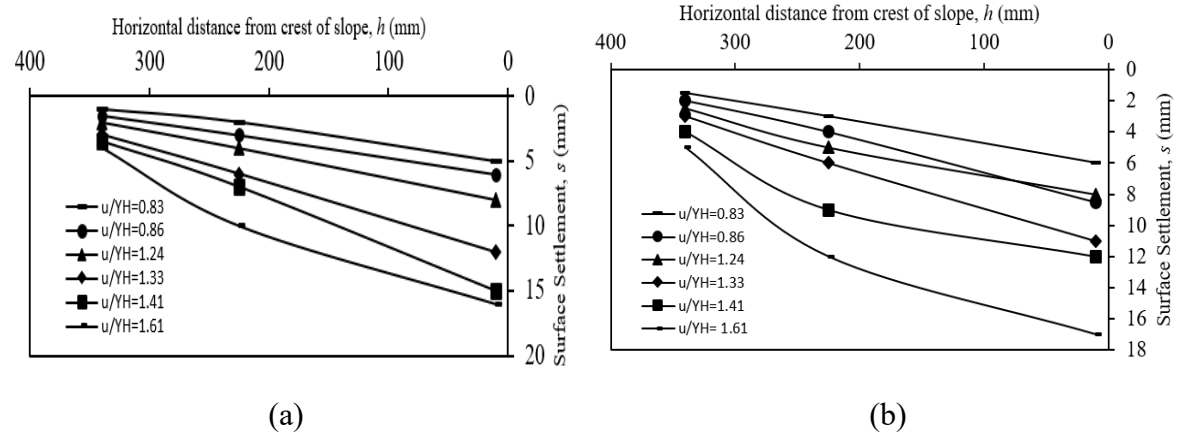

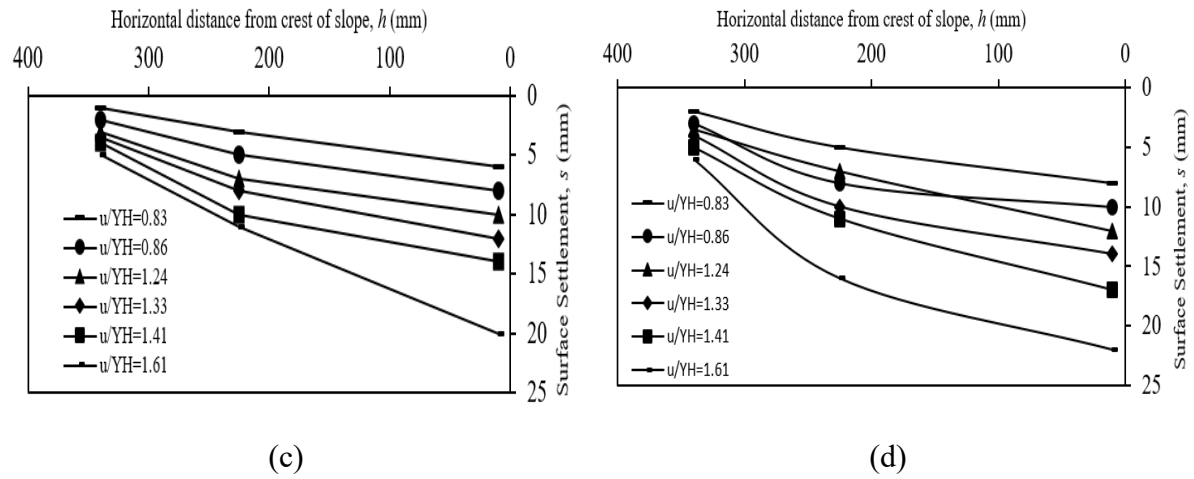

Figure 4.49 Variations of surface settlements with horizontal distance from Slope crest and Normalized Pore water Pressure for (a) HDPE facing, (b) Polyester Geogrid, (c) Hex plastic net (d)Jute geomesh

As per the results depicted in Figure 4.48 and Figure 4.49, the Surface settlements are higher for Jute geomesh for both cases but for staggered case the surface settlements are lower than rectangular arrangement for all the flexible materials. The difference in surface settlements between the staggered and rectangular nail arrangements is directly influenced by the number of nails and their spacing. The staggered arrangement, with 8 nails, provides better load distribution and increased stability, resulting in lower surface settlements for all types of flexible materials, including Jute Geomesh. In contrast, the rectangular arrangement, with only 6 nails, offers less reinforcement, leading to higher surface settlements, especially for more flexible materials like Jute Geomesh. These findings support the need for and impact of stiffness facing on the behaviour of seepage-prone soil-nailed slopes. This suggests that one of the most crucial elements of a soil-nailed slope is the slope facing, which also helps to improve the stability and deformation behaviour when the seepage occurs. The settlements were higher for u/YH= 1.61, because of the fact that there is higher pore water pressure at the said value that leads to the higher settlement.

The surface settlements during drainage were higher near the crest of slope as compared to other points and were higher for Jute geomesh in both cases by 8%, 13.04% and 21.73% and 56.52 % as compared to hex plastic net, Polyester geogrid and HDPE facing net respectively for rectangular arrangement and were higher by 9.09%, 22.72% and 27.27% respectively for staggered arrangement.

4.18 Finite Element Modelling Results

After performing the testing on the physical model and obtaining the results from the model, the FEM analysis was performed for the validation of the results using the Plaxis 3D software. The Boundary Condition were considered similar to those in the physical model.

4.18.1 Tensile Nail Force Diagrams

To comprehend the distribution of loads along soil nails, verify design assumptions, and guarantee structural integrity, tensile nail force diagrams in PLAXIS are indispensable. The results were compared for tensile forces among various types of facing material. The Figures shown below depict the tensile force diagrams. The results were obtained for rectangular pattern which shows forces in all the nails and the nails are represented from top to bottom nails.

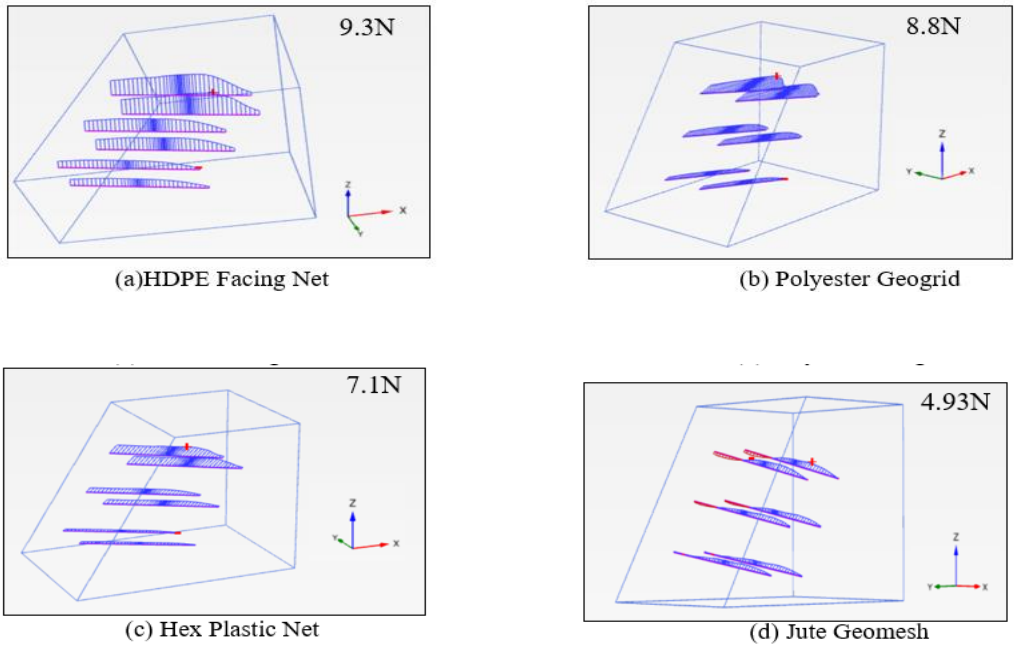

(a)HDPE Facing Net (b) Polyester Geogrid

(c) Hex Plastic Net (d) Jute Geomesh

Figure 4.50 Variations of Nail forces for (a) HDPE facing, (b) Polyester Geogrid, (c) Hex plastic net (d)Jute geomesh

As per the nail forces diagrams Figure 4.50, it can be concluded that the maximum nail tensile forces are in upper set of nails in all the cases. Due to the proximity of the external load (with limited width, i.e., non-infinite distributed loading), the upper portion of the soil nailing mass experiences higher overburden stress than the lower layers. The external load also induces greater lateral movement at the top nails compared to those at the bottom, leading to higher loading in the top nail layers.

The maximum tensile forces are in HDPE Facing due to its higher tensile strength and it has to bear more load to compensate for the deformation and maintain the stability of the wall, resulting in higher forces in the nails. The maximum tensile nail forces were at the middle part of the nail as per FEM and Physical model test results.

4.18.2 Bending Moments Diagrams for nails

Bending moments have a significant impact on the structural integrity, stability, load-bearing capacity, crack prevention, and standard compliance of soil nail walls, making them an essential component of their design and analysis. An accurate analysis of bending moments guarantees that the wall can withstand additional loads and lateral earth pressures while still remaining serviceable and functioning dependably over time. The results were compared for Bending moment diagrams among various types of facing material. The Figures shown below depict the Bending moment diagrams for rectangular pattern.

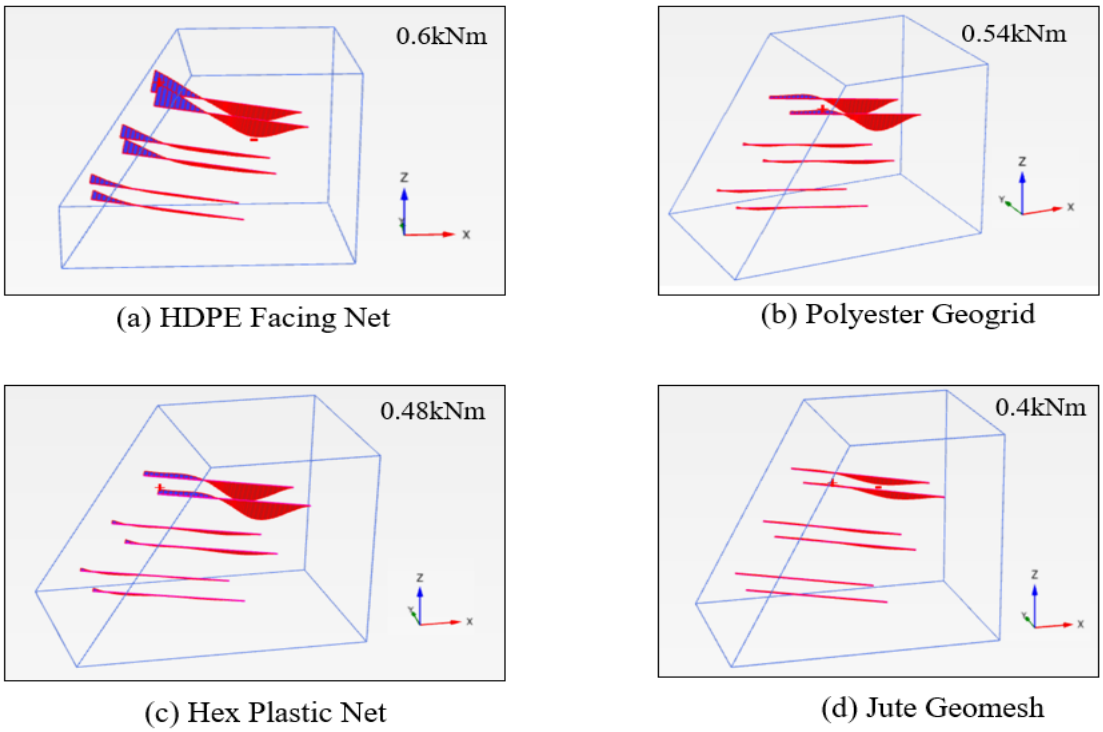

(a) HDPE Facing Net (b) Polyester Geogrid

(c) Hex Plastic Net (d) Jute Geomesh

Figure 4.51 Variations of Bending Moment for (a) HDPE facing, (b) Polyester Geogrid, (c) Hex plastic net (d)Jute geomesh

The bending moments are higher in HDPE facing material due to the fact that that it is stiffer and having higher strength than other materials and the interaction between the facing material and the retained soil plays a crucial role in determining the bending moment distribution.

Bending moment reported for HDPE facing was found to be higher as it had taken higher amount of load before the failure.

4.18.3 Vertical displacements in Soil nail walls

Monitoring and controlling vertical displacements in soil nail walls is essential to preserving the stability and integrity of the building as well as the surrounding area. Designing, building, and maintaining soil nail walls successfully depends on knowing the causes and effects of vertical displacement and using the right analysis techniques and control measures. The results were compared for Vertical displacements among various types of facing material. The Figures shown below depict the Vertical displacements for rectangular pattern.

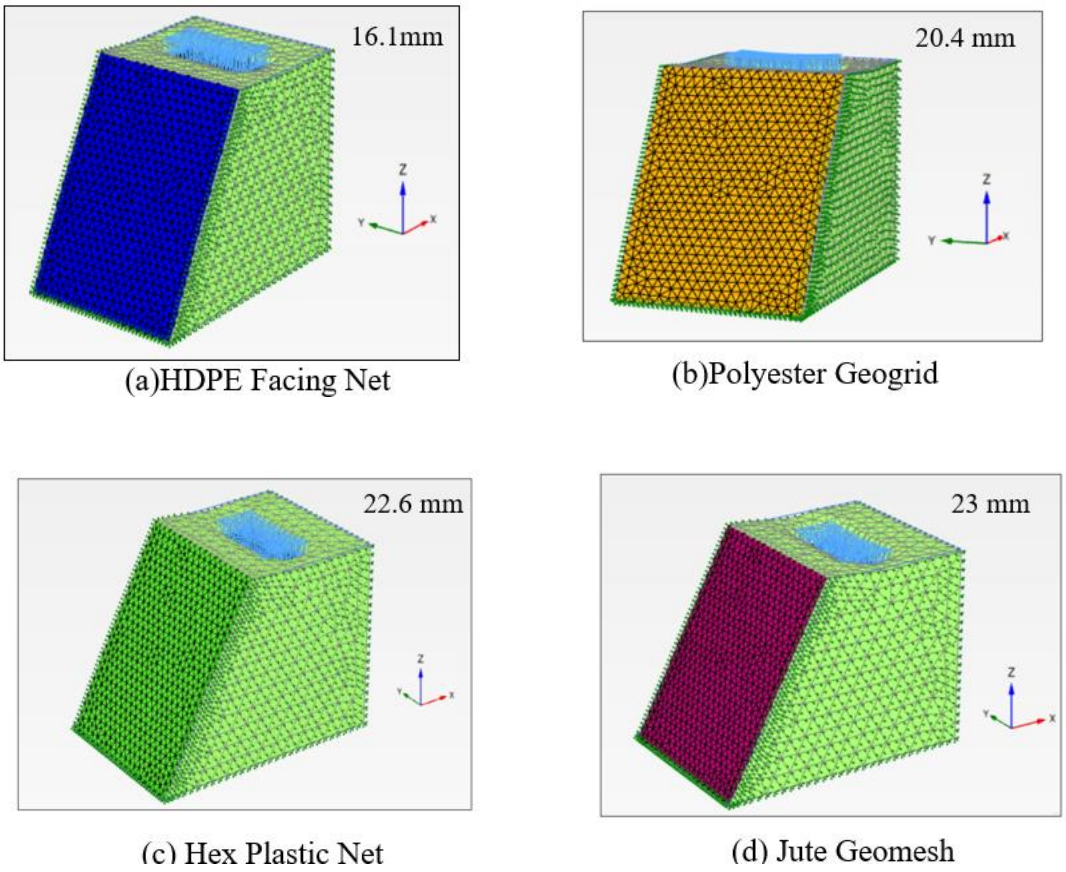

Figure 4.52 Variations of Vertical displacements for (a) HDPE facing, (b) Polyester Geogrid, (c) Hex plastic net (d)Jute geomesh

Maximum vertical settlement was reported in Jute Geomesh due to its lower strength and it was higher by 1.73%,11.30% and 30% as compared to Hex plastic net, Polyester geogrid and HDPE facing net. The displacements in the case of HDPE facing net are lower due to its higher tensile strength and stiffness as compared to the other materials and the results are in accordance with physical testing results as well.

4.18.4 Lateral Deformation of Slope

The lateral deformation of various flexible facing materials was studied in the plaxis 3D. The term "lateral deformation" describes the bending or sideways movement of the flexible facing in a soil nail wall as a result of forces acting on the retaining structure, such as surcharge loads and lateral earth pressures.

The figure below depicts the lateral deformation in various materials.

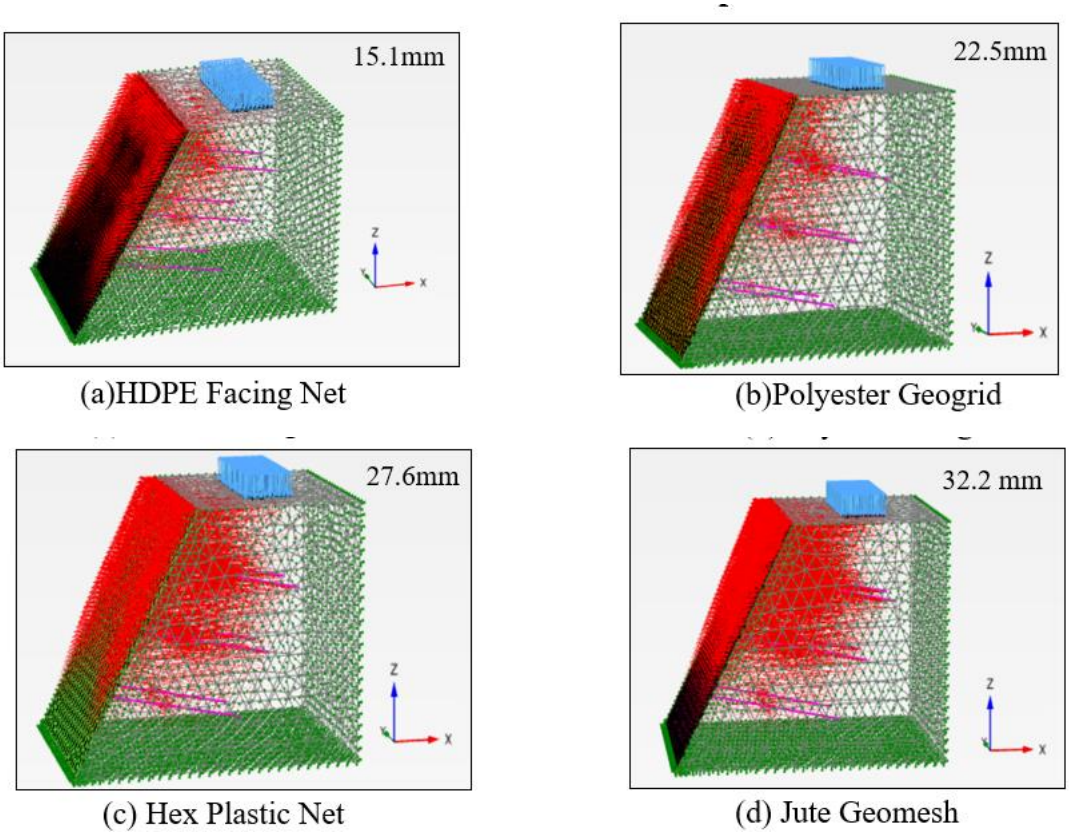

Figure 4.53 Variations of Lateral Deformation for (a) HDPE facing, (b) Polyester Geogrid, (c) Hex plastic net (d)Jute geomesh

Jute Geomesh exhibits higher lateral deformations mainly because of its natural flexibility, reduced stiffness, and soil movement compliance. The increased lateral deformation observed in the case of the Jute Geomesh is due to its lower stiffness and tensile strength compared to other materials. This greater deformation results in higher facing displacements, as the flexible nature of the Jute Geomesh offers less resistance to soil movement, allowing for more significant outward displacement of the facing. Consequently, the ability of the facing to limit deformation is reduced, leading to more pronounced displacement of the soil mass behind it. The lateral deformations were higher by 34.28%, 40%, and 51.42% as compared to Hex plastic net, Polyester geogrid and HDPE facing net.

4.18.5 Facing Displacements

In a soil nail wall, facing displacements are the result of movement or deformation of the facing material, the part of the retaining structure that is visible. The facing material's susceptibility to displacement is influenced by its tensile strength, flexibility, and stiffness. Compared to rigid materials, which could break or fail under extreme deformation, flexible facing materials might allow for greater movement. The Facing displacements for various materials are depicted as follow:

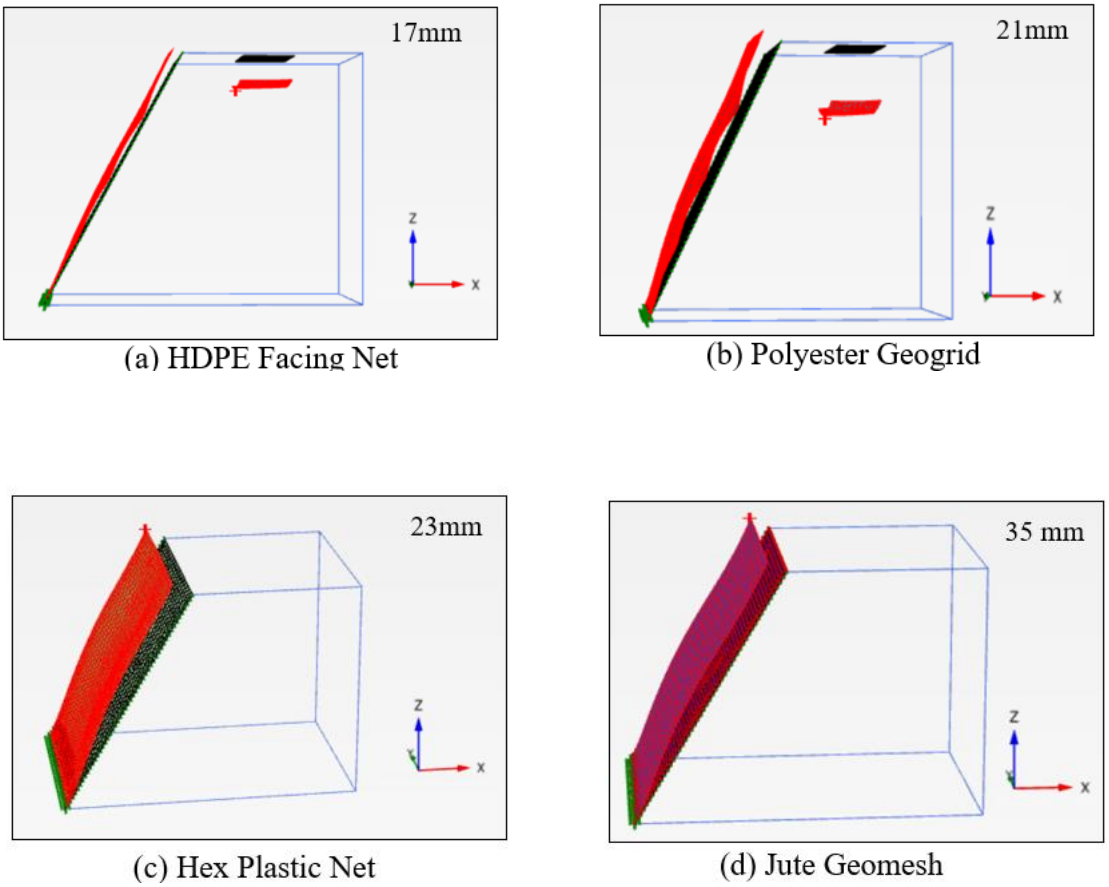

Figure 4.54 Variations of Facing Displacement for (a) HDPE facing, (b) Polyester Geogrid, (c) Hex plastic net (d)Jute geomesh

The Facing displacements were found to be high in the case of jute geomesh due to the fact that it has low stiffness and low tensile strength. Facing displacements are likewise increased as a result of higher lateral earth pressures caused by the retained soil.

4.18.6 Factor of Safety

The concept of factor of safety is used in PLAXIS 3D, a finite element analysis program frequently used for geotechnical engineering applications, to evaluate the safety margin against failure and determine the stability of soil structures. The ratio of the driving and resisting forces acting on the soil structure is known as the factor of safety, or FOS. A structure

is considered stable if its factor of safety is greater than one; instability or failure is suggested if the factor of safety is less than one[142], [143][144][105], [141], [145]–[147]. The input parameters from direct shear tests were used as a practical approximation, The adopted procedure of using input parameters from direct shear test led to a significant limitation in the performed numerical analyses, preventing them from fully representing real field conditions. The factor of safety for various materials is mentioned below in Table 4.2

Table 4.2 Factor of safety for various Flexible Materials

Soil Cohesion (kPa)	Angle of Internal Friction (°)	Nail Length (m)	Nail Spacing (m)	Surcharge Load (kPa)	Facing Material Type	Factor of Safety
2.1	37	0.46	0.15	5040	HDPE Facing net	1.85
2.1	37	0.46	0.15	5040	Polyester Geogrid	1.55
2.1	37	0.46	0.15	5040	Hex Plastic Net	1.35
2.1	37	0.46	0.15	5040	Jute Geomesh	1.2

Therefore, flexible facing materials for soil nail walls have a higher factor of safety due to their combination of material flexibility, load redistribution, conformity to soil movements, enhanced soil-structure interaction, and resistance to overturning and sliding. So as per the values of factor of safety compared in Table 4.2 it is observed that the HDPE facing net is having greater stability and low risk for the failure as compared to other materials. So, the HDPE facing material could be better utilized as compared to the other flexible materials considered in the study.

4.19 Performance Comparison Between Hard and Flexible Facing

A comparative study was carried out comparing different flexible materials with the rigid facing. Strong structural strength and stiffness are provided by rigid facing materials, such as welded wire mesh and shotcrete, which offer strong support against lateral earth pressure. Whereas flexible facing materials have a higher tensile strength and less stiffness, which enable them to deform without failing, they are appropriate for applications that call for minimal deformation and long-term stability.

4.19.1 Comparison of Vertical Settlement

The downward movement or compression of the wall structure caused by different factors like soil consolidation, loading, and environmental conditions is referred to as the vertical settlement of a soil nail wall. Vertical settlement may result in structural problems and have an impact on the soil nail wall's stability and performance. The comparison between facing materials is described as below:

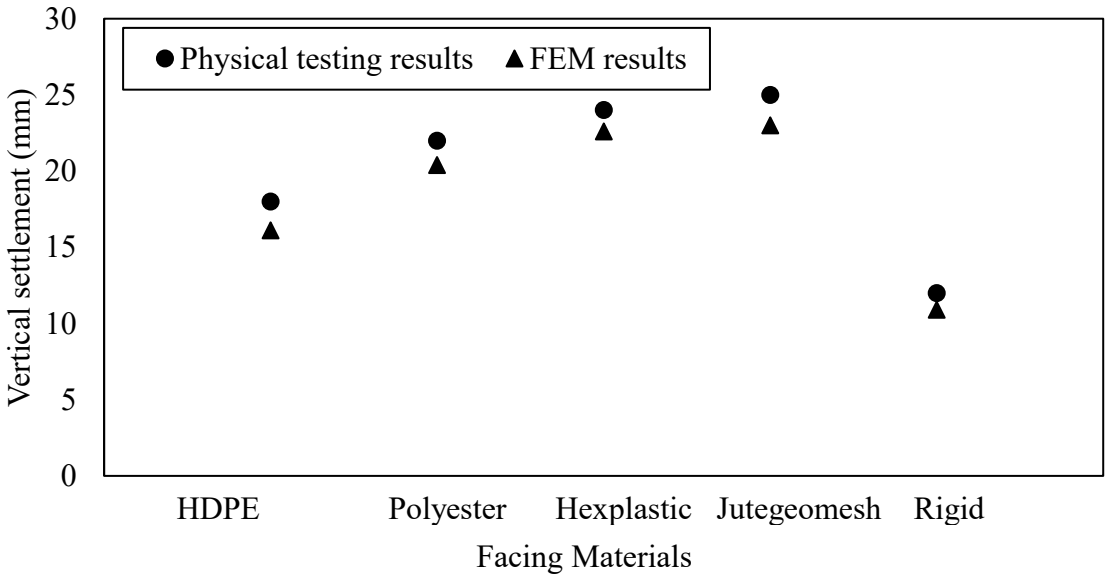

Figure 4.55 Comparison of vertical settlement for Physical model results and FEM results

Rigid materials distribute applied loads more evenly across the entire surface, flexible facing has higher vertical displacements than rigid facing. This even dispersion minimizes vertical settlement, lessens localized stress concentrations, and Loads may be concentrated at particular locations by flexible materials, increasing localized stresses and increasing vertical displacements. The Vertical displacements in Jute geomesh were higher by 4%, 12%, 28%, and 52% for Hex plastic net, polyester geogrid, HDPE facing net and Rigid facing respectively. The variation of physical model testing results with FEM results where vertical displacement was 10.55%, 7.27%, 5.83%,8% and 9.16% for HDPE facing, Polyester geogrid, Hex plastic net, Jute geomesh and rigid facing respectively.

4.19.2 Comparison of Facing displacement

In soil nail walls, facing displacement describes the movement or deformation of the facing material, which is the part of the retaining wall that is visible. The lateral earth pressure that the retained soil applies to the facing material is the main factor responsible for facing

displacement. The facing displacements were compared for rigid facing and all the flexible materials.

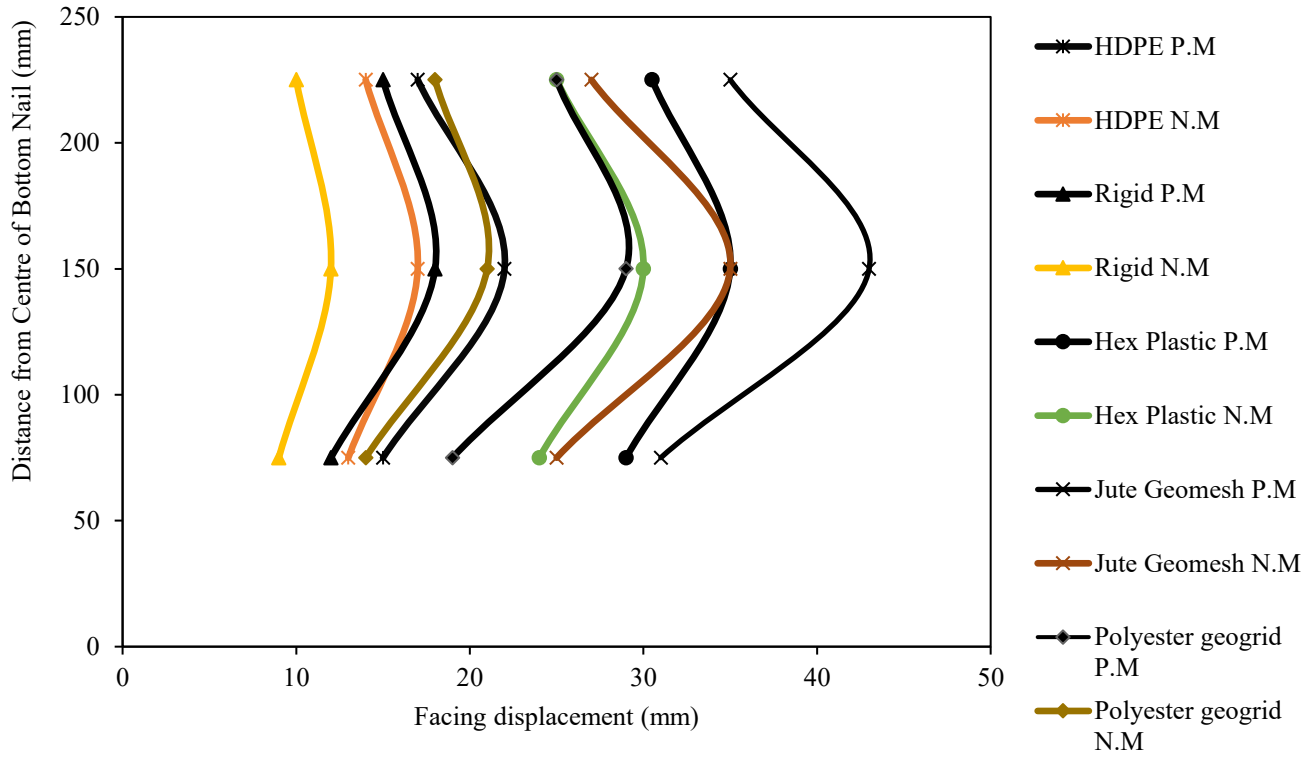

Figure 4.56 Comparison of Facing displacements for Physical model (P.M) results and FEM results (N.M)

Rigid facing materials have less flexibility and deformability than flexible facing materials, they are less likely to deform under load. This explains why the facing displacements in rigid facing were lower than those in flexible facing. Comparing this resistance to deformation to flexible materials—which can experience considerable stretching and deflection—we find that the facing displacements are reduced. The facing displacements were lower in rigid facing by 18.18% as compared to HDPE facing net. FEM depicts lower results due to stiffer modelling of facing.

4.19.3 Comparison of Tensile Nail Forces at Nail head

To comprehend the function of facing, comparisons were made between the tensile nail forces for different types of facing materials. Tensile nail forces are the forces applied to the soil nails as a result of the facing material being compressed laterally by the soil. The stability and structural integrity of the soil nail wall depend heavily on these forces. The figure below shows the comparison of tensile nail forces.

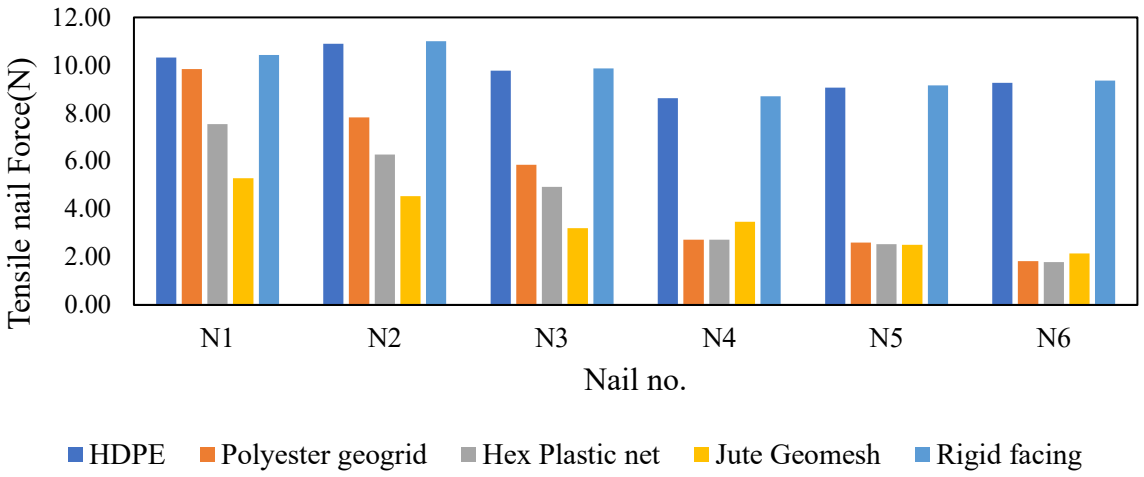

Figure 4.57 Comparison of Tensile nail force for various Facing Materials

Tensile nail forces are higher in rigid facing because rigid facing materials transmit a large amount of the load directly to the soil nails when they are subjected to lateral earth pressure. This causes the nails to experience higher tensile forces. The results for Physical model and numerical model of HDPE facing net and rigid facing were compared in order to validate the results, and are represented below:

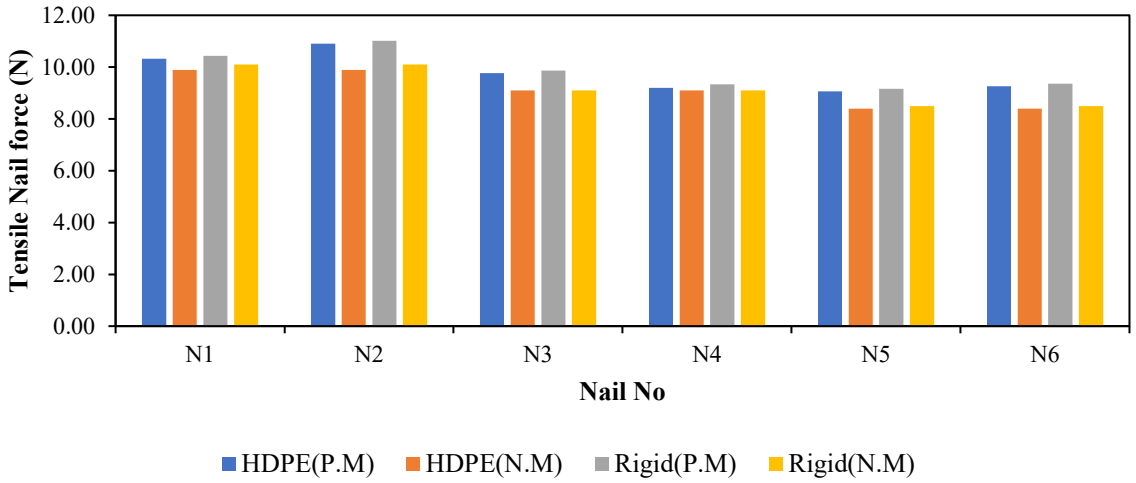

Figure 4.58 Comparison of Tensile Nail force for Physical model (P.M) results and FEM results (N.M)

As per the results obtained from figure 4.58, it is observed that Rigid facing is having higher tensile nail force as compared to HDPE facing for physical modelling results and FEM results due to higher rigidity and FEM depicts lower results due to stiffer modelling of facing. The variation may be accounted to the limitation of simulating the nail installation in Plaxis. In Plaxis analysis the nails are simulated using beam elements which are embedded in the soil domain whereas during the model testing the nails are installed after the soil slope has been

fabricated. Thus, the effects of nail installation are not accounted for in the finite element (FE) analysis. Similarly, the slope facing is simulated using plate element in FE analysis, which covers the complete slope face whereas facing type used in model testing as in case of polyester geogrid and hex plastic net have apertures which renders partial slope face cover. Thus, in FE analysis, additional constraint is applied to the slope face due to the plate element. During the FE analysis, simulation of the Perspex sheet which was used as boundaries for the slope model are not simulated. Thus, the difference in the boundary conditions between FE model and physical model influence the stress distribution, leading to variation in the nail forces observed. However, care is taken during simulation in FE analysis that the absorbent boundaries are distant enough to cause any boundary effect on the results. The variation in the recorded nail forces between experimental and Fe analysis can also be due to the limitation of Mohr-Coulomb soil model used. The soil model has limited efficiency in fully capturing the non-linear soil behavior for large displacement problems. The same are represented for Tensile nail force in the form of Percentage variation and Coefficient of variance in Table 4.3

Table 4.3 Variation of Tensile Nail force for Experimental results and FEM results (Plaxis)

Nail no	Facing material	Experimental results (Tensile nail force in 'N')	FEM Plaxis results (Tensile nail force in 'N')	Percentage variation (%)	Coefficient of variance (CoV) (%)
Nail 1	HDPE	10.33	9.89	4.22	2.16
	Rigid	10.43	10.10	3.16	1.61
Nail 2	HDPE	10.90	9.89	9.27	4.86
	Rigid	11.01	10.10	8.27	4.31
Nail 3	HDPE	9.77	9.10	6.87	3.56
	Rigid	9.87	9.10	7.80	4.06
Nail 4	HDPE	9.20	9.10	1.09	0.55
	Rigid	9.34	9.10	2.57	1.30
Nail 5	HDPE	9.07	8.40	7.37	3.83
	Rigid	9.16	8.50	7.21	3.74
Nail 6	HDPE	9.27	8.40	9.35	4.90

	Rigid	9.36	8.50	9.19	4.82

This could be due to various reasons such as Numerical models often involve simplifications, such as idealized soil properties and boundary conditions, which do not fully capture the complexity and variability of real-world scenarios present in physical models. Additionally, construction imperfections, and inherent variability in soil properties contribute to discrepancies. Numerical approximations, such as mesh sensitivity, and potential non-linear or time-dependent soil behaviour in physical models further widen the gap. Lastly, differences in measurement accuracy between physical and numerical approaches also play a role in this variation. These factors collectively explain the observed differences in performance between the two modelling approaches.

4.19.4 Comparison of Bending moment of Flexible materials with Rigid facing

The lateral earth pressure acting on the facing material and the resistance offered by the soil nails are the main causes of bending moments. The bending moment values for various materials are depicted in figure below:

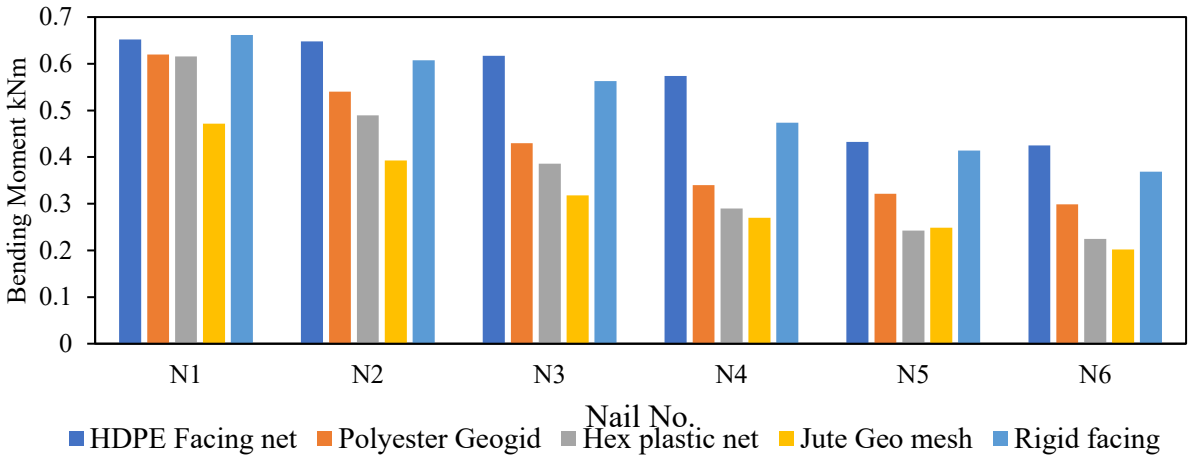

Figure 4.59 Comparison of Bending Moment for various Facing Materials

Even though HDPE facing nets are flexible, their tensile strength and anchorage to the soil nails allow them to offer considerable resistance to bending moments. Welded wire mesh with shotcrete and other rigid facing materials can effectively withstand bending moments through various mechanisms. Due to their ability to disperse moments along their lengths, both materials have similar bending characteristics.

Further the bending moment was compared for Physical model which were calculated using Eqn 4.1 and numerical model of HDPE facing net and rigid facing in order to validate the results, and are represented below:

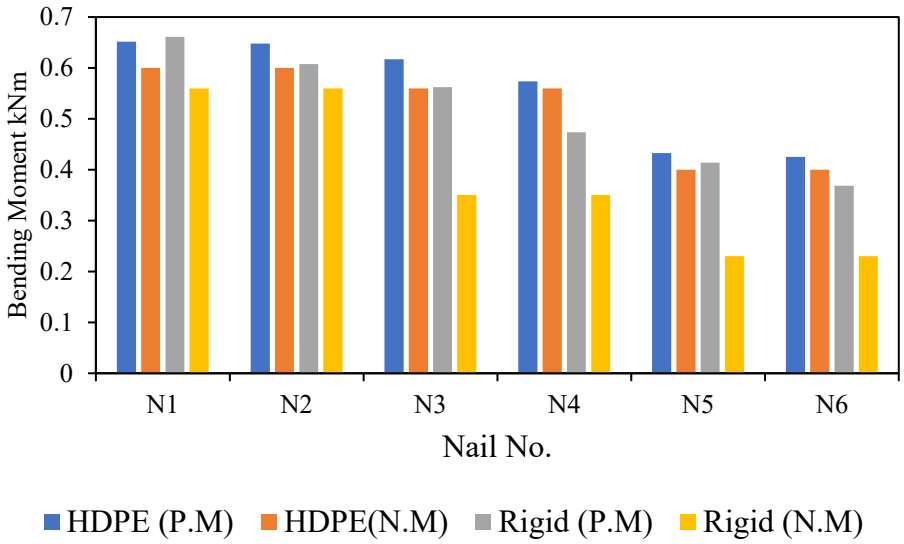

Figure 4.60 Comparison of Bending Moment for Physical model results and FEM results

As per the results obtained from figure 4.60, it is observed that Rigid facing is having comparable bending moment in the upper nails as compared with the HDPE facing net rigid facings and HDPE walls are designed to effectively withstand lateral earth pressures, so that's why the bending moments in these types of walls are comparable and FEM depicts lower results due to stiffer modelling of facing.

4.19.5 Comparison of Facing Punching mobilized stress of Flexible materials with Rigid facing

Punching shear, which occurs when concentrated loads or pressure points cause the facing material of a soil nail wall to undergo shear stresses, is a localized failure mechanism. Where the soil nails are anchored to the facing material in those conditions' failure is most common. The comparison of facing punching mobilized stress is depicted in the figure below:

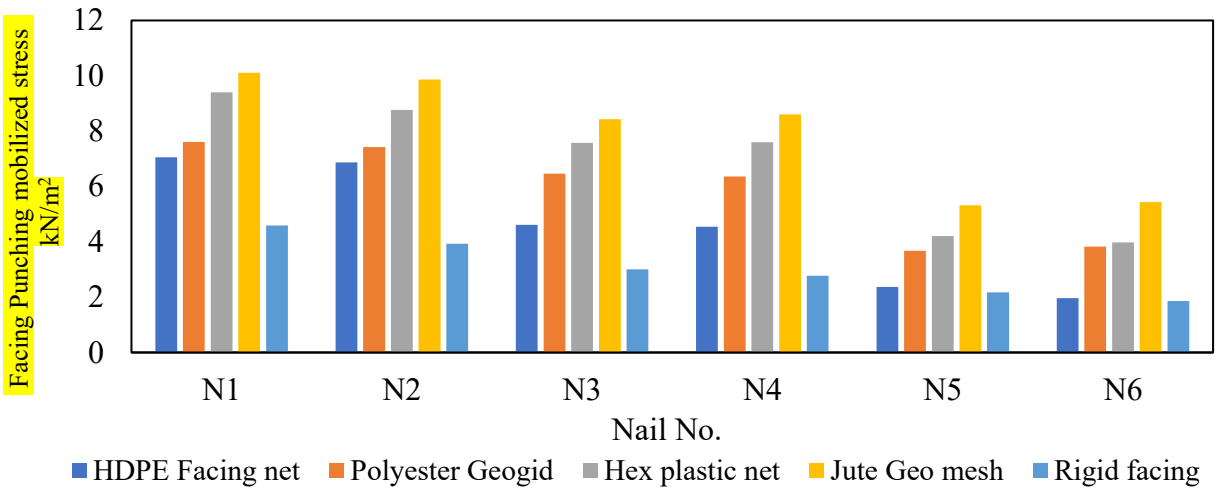

Figure 4.61 Comparison of Facing Punching mobilized stress for various Facing Materials

Rigid facing materials are more stiff and rigid than flexible facing materials, the facing punching mobilized stress is lower in rigid facing materials as determined from Eqn no. 4.2. They reduce localized stress concentrations and punch shear at connection points by spreading applied loads more equally and establishing larger load transfer zones.

Further the facing punching mobilized stress was compared for Physical model and numerical model of HDPE facing net and rigid facing in order to validate the results, and are represented below:

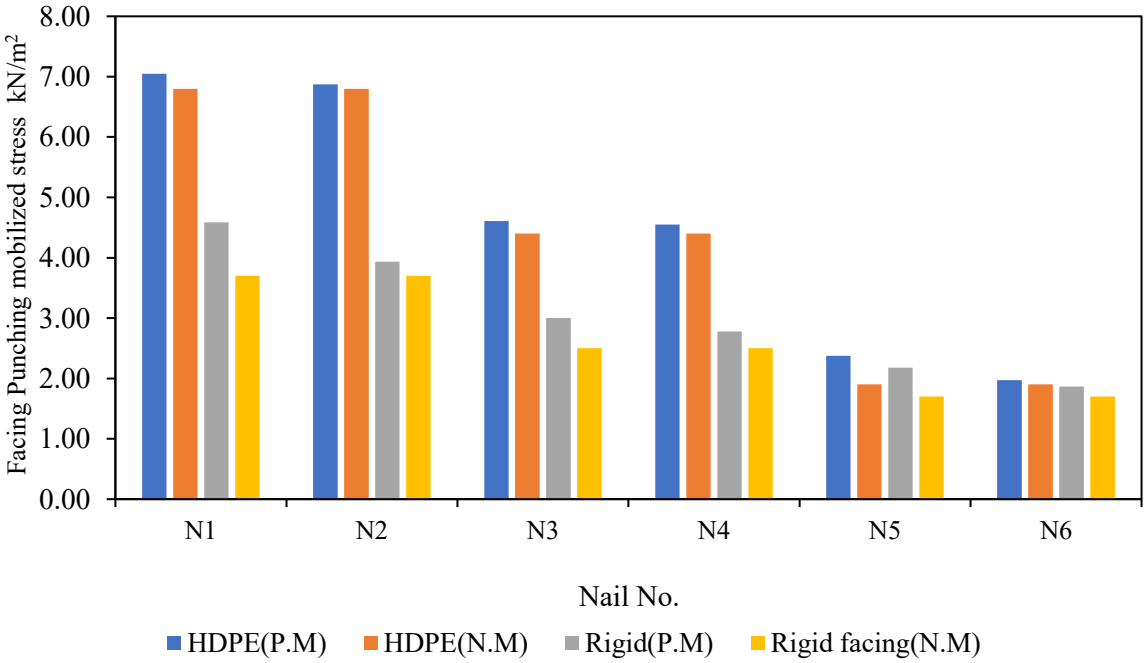

Figure 4.62 Comparison of Facing Punching mobilized stress for Physical model (P.M) results and FEM (N.M) results

The similar trend was noticed on comparison of physical model test results and Numerical model test results; the values of Facing Punching mobilized stress were higher for HDPE facing as compared to Rigid facing due to flexible nature of HDPE facing which leads to the validation of the results and FEM depicts lower results due to stiffer modelling of facing.

The choice between these facing materials depends heavily on the balance between cost and required performance. Rigid facings provide excellent structural integrity but are expensive, while flexible facings like HDPE nets and Jute Geomesh are cost-effective for temporary or low-stress conditions. Polyester geogrids strike a good balance for moderate demands. Therefore, the decision should be project-specific, considering both the expected load conditions and the budget. Further the cost comparison was done for HDPE facing net and Rigid facing as described below:

Rigid Facing

- Material cost:
  The cost of shotcrete in India typically ranges between ₹5,500 to ₹7,000 per m^3 (Maccaferri, 2023).
  For a 1 m^2 area with a 0.1 m thick layer of shotcrete, the required volume is 0.1 m^3.

  Material cost (shotcrete) = ₹5,500 to ₹7,000 × 0.1 = ₹550 to ₹700 per m^2.

- Labor cost:
  The labor cost for shotcrete application in India is around ₹1,000 to ₹2,500 per m^2.

- Total cost for rigid facing:

  Material + Labor cost = ₹550 to ₹700 + ₹1,000 to ₹2,500 = ₹1,550 to ₹3,200 per m^2.

HDPE Facing Net Material cost:
HDPE nets typically cost around ₹150 to ₹500 per m^2 in India, depending on the quality and type of net. (Maccaferri, 2023).

- Labor cost:
  The labor for installing HDPE nets is usually around ₹200 to ₹500 per m^2.

- Total cost for HDPE facing net:

Material + Labor cost = ₹150 to ₹500 + ₹200 to ₹500 = ₹350 to ₹1,000 per m^2.

Cost Comparison Summary (in INR):

Rigid Facing: ₹1,550 to ₹3,200 per m²

HDPE Facing Net: ₹350 to ₹1,000 per m²

The HDPE facing net is significantly cheaper, ranging from ₹350 to ₹1,000 per m², while rigid facing costs ₹1,550 to ₹3,200 per m², making HDPE approximately 3 to 5 times more economical than rigid facing for the same area.

5. Conclusions

5.1 General

The behaviour of soil nail slopes that are exposed to various facing materials is discussed in the present research. The following inferences from the current investigation may be made based on the results of the physical model and after validating the results with Plaxis 3D:

5.2 Conclusions

1. The maximum surcharge pressure was taken up by HDPE Facing net for both the nail arrangement. HDPE has taken up 18.80%, 30.18% and 46.43% more surcharge than Polyester geogrid, Hex plastic net and Jute Geomesh respectively in rectangular arrangement. In case of staggered Pattern HDPE has taken up 19.20%, 28.70% and 38.21% more surcharge pressure than Polyester geogrid, Hex plastic net and Jute Geomesh respectively. On comparison of Surcharge pressure for both the arrangement the increase in surcharge was 9.56%, 9.03%, 11.08% and 26.38% for HDPE facing net, Polyester geogrid, Hex plastic net and Jute Geomesh respectively for staggered arrangements.
2. The nail forces were higher in the case of HDPE facing and it was found to be 14.42%, 26.33% and 48.28% higher for Polyester geogrid, Hex plastic net and Jute Geomesh respectively in rectangular arrangement. Similarly for the staggered pattern, HDPE facing nail forces were found to be 17.55%, 19.55% and 45.72% higher for Polyester geogrid, Hex plastic net and Jute Geomesh respectively.
3. The facing strain increases with the increase of surcharge and are found to be higher in upper set of nails and similar trend is found with respect to height. The facing forces were found to be higher in the HDPE facing net, they were higher by 17.53%, 35.54% and 54.15% as compared Polyester geogrid, Hex plastic net and Jute Geomesh respectively in rectangular arrangement.In case of staggered pattern, the facing forces in rigid facing were higher by 22.09%, 32.01%, and 54.95% for Polyester geogrid, Hex plastic net and Jute Geomesh respectively.
4. The bending moment was noticed higher in HDPE facing slope as compared to other flexible materials as it was 4.88%, 5.66% and 27.70% for Polyester geogrid, Hex plastic net and Jute Geomesh respectively.

5. The facing punching mobilized stress was found higher in Jute Geomesh and it was higher by 6.95%, 24.68% and 30.26% for hex plastic net, Polyester geogrid and HDPE facing net respectively.
6. Lateral facing displacement were maximum in Jute geomesh facing. As compared to lateral displacement of slope with hex plastic net, Polyester geogrid and HDPE facing, the lateral displacement of Jute geomesh was 18.60%, 32.55% and 48.83% higher. The facing displacement follow similar trend as stated above for staggered arrangement and were found to be higher by 23.07%, 38.46% and 51.28% for hex plastic net, Polyester geogrid and HDPE facing net respectively as compared to Jute Geomesh facing.
7. Vertical Settlements were higher for Jute geomesh by 4%,12%, and 32% as compared with hex plastic net, Polyester Geogrid and HDPE facing net respectively in rectangular arrangement. Vertical Settlements were higher for Jute geomesh by 18.18%, 27.27% and 36.36% as compared with hex plastic net, Polyester Geogrid and HDPE facing net respectively in Staggered arrangement.
8. The surface settlements during drainage were higher near the crest of slope as compared to other points and were higher for Jute geomesh in both cases by 8%, 13.04% and 21.73% and 56.52 % as compared to hex plastic net, Polyester geogrid and HDPE facing net respectively for rectangular arrangement and were higher by 9.09%, 22.72% and 27.27% respectively for staggered arrangement.
9. The Vertical displacements in Jute geomesh were higher by 4%, 12%, 28%, and 52% for Hex plastic net, polyester geogrid, HDPE facing net and Rigid facing respectively.
10. The variation of physical model testing results with FEM results for vertical displacement were 10.55%, 7.27%, 5.83%,8% and 9.16% for HDPE facing, Polyester geogrid, Hex plastic net, Jute geomesh and rigid facing respectively.
11. The facing displacements were lower in rigid facing by 18.18% as compared to HDPE facing net. The nail tensile forces were higher in rigid facing by 12.63% as compared to HDPE facing net.
12. Based on Parametric assessment, strain in nails with surcharge, strain on facing with surcharge, strains with variation in spacing, HDPE facing Net is most suitable flexible facing material among Polyester geogrid, Hex plastic Net and Jute Geomesh.
13. Based on the results of facing stiffness, the bending moments were higher in HDPE facing and Facing Punching mobilized stress was higher in Jute geomesh and internal nail stresses decrease with increase in Bending moment.

14. Validation of experiment results are FEM are in accordance, though FEM depicts lower results due to stiffer modelling of facing.
15. On comparison of Flexible facing materials with rigid facing, HDPE is best facing which could be utilized in the field for steep slopes ranging from 60° to 70°.

5.3 Limitations and Future Scope

1. Head plate size- The nail head plate needs to be the right size to minimize local instability between soil nails and punching failure of the facing. It should also prevent bearing failure and encourage soil arching.
2. Embedment of facing edges-Side anchorage enhances the stability of the soil nail wall by providing additional lateral resistance. This reduces the wall deflection and also prevents sliding and overturning.
3. Excavation staged Modelling- In the field the excavation is done from top to bottom and it's done in stages but in the case of physical testing the slope construction and insertion of nail was not according to the field conditions.
4. The physical boundary conditions influence stress distributions due to the friction between the soil and the tank Perspex sheet boundaries, which are difficult to simulate keeping in view the defined boundary condition options available in the Plaxis software. Moreover, the interface modelling of the soil – nail and nail – facing interfaces are done using the R_{inter} value which only encompasses the reduction in the shear strength parameters of the interface. However, during physical testing the installation effects, the nail to facing connection and placement of facing also governs the soil – nail and nail – facing interaction. This can be done with more sophisticated modelling.
5. The proposed equation 4.3 cannot be applied to all the field condition as its validation is limited only to the condition of present model.
6. **Non – usage of advance constitutive soil models**: The adopted Mohr-Coulomb (M - C) constitutive soil model uses a bilinear elastoplastic approach. The M-C model requires only single linear elastic stiffness value, taken as secant stiffness at 50% of failure stress (E50). The model assumes the stiffness to be constant throughout the elastic zone, until the stress state reaches the plastic (failure) zone. However, in reality, the soil behaves non - linearly, representing that the soil stiffness is never constant. Furthermore, the stiffness changes with the stress level within the soil mass. Since Mohr Coulomb model uses only a single stiffness value, it fails to cater for realistic deformations, overestimates bottom heave, and may predict unrealistic soil heave

behind the wall. Alternatively, the actual soil stress-strain behavior in non – linear under loading condition. With the increase in loading, the stiffness modulus of the soil decreases gradually. This non-linear stress strain behavior can be approximated by hyperbolic model developed by Duncan & Chang, 1970 known as Hardening Soil model (HS model). The soil behavior below excavation behaves within the unloading/reloading stiffness, even soils behind wall behaves between unloading/reloading stiffness and secant stiffness at 50% of failure stress (E50). Therefore, Hardening Soil (HS) model is recommended for soil under isotropic loading, shearing and unloading-reloading and is found to predict more realistic wall deformations, bottom heave, and settlement behind wall. An improved version of HS model is the Small Strain Hardening Soil Model (HSS model). The HSS model is used for simulating far field small strain behavior, yielding much more realistic (narrower and deeper) settlement behind the soil nailed walls.

7. **Non – simulation of installation of soil nails:** In PLAXIS 3D, soil nails are modelled using embedded beam elements (wished – in – place), which do not simulate the installation sequence typically used in practice. The simulation of pre – drilled bore holes followed with insertion of soil nail tendon and consequent grouting process was not carried out. This numerical modelling simplification induces the necessary stiffness into the soil domain but fails to model the soil stress variations that occurs due to installation disturbances, thereby overestimating the interaction between the soil and reinforcement (Lazarte et al. 2015).
8. **Use of Plate element for modelling the soil nailed slope facing:** The facing was modelled as a continuous plate element in the FEM analysis, applying uniform constraints along the slope surface. However, during field application of flexible facings using geosynthetics or hexagonal nets, the slope face is only partial covered due to the open apertures of the geogrids/geonets. The plate element forms a continuous plate which fails to model the joints or allow for relative displacements, which are important for realistic deformation predictions. Thus, modelling additional restraint in the numerical model, which potentially overestimates the nail force mobilization and reduced slope displacement (Lazarte et al., 2015).

6 REFERENCES

[1] N. T. Pham, P. Bing, and N. V. Nguyen, "Study on the effect of some parameters of soil nails on the stability of vertical slopes," *J. Min. Earth Sci.*, vol. 61, no. 6, pp. 30–37, 2020, doi: 10.46326/jmes.2020.61(6).04.

[2] V. P. Singh and G. L. S. Babu, "2D Numerical simulations of soil nail walls," *Geotech. Geol. Eng.*, vol. 28, no. 4, pp. 299–309, 2010, doi: 10.1007/s10706-009-9292-x.

[3] G. Di Flora, A. Fonzo, M. V. Nicotera, G. Manfredi, and A. Prota, "Some remarks on the effect of soil-nail interface stress state on the determination of pullout resistance of driven nails," *Proc. 17th Int. Conf. Soil Mech. Geotech. Eng. Acad. Pract. Geotech. Eng.*, vol. 2, no. 3, pp. 1150–1154, 2009, doi: 10.3233/978-1-60750-031-5-1150.

[4] Sanvitale N, Simonini P, Bisson A, and Cola S, "Role of the facing on the behaviour of soil-nailed slopes under surcharge loading Rôle du parement sur le comportement des pentes de sol cloué sous surcharge," pp. 2091–2094.

[5] H. J. Lengkeek and E. Bruijn, "Soil nailing in clay for dike reinforcement," *Proc. 17th Int. Conf. Soil Mech. Geotech. Eng. Acad. Pract. Geotech. Eng.*, vol. 2, pp. 1586–1589, 2009, doi: 10.3233/978-1-60750-031-5-1586.

[6] A. Perera, S. D. Mudannayake, H. M. Azamathulla, and U. Rathnayake, "Recent climatic trends in Trinidad and Tobago, West Indies," *Asia-Pacific J. Sci. Technol.*, vol. 25, no. 2, pp. 1–11, 2020.

[7] S. Sahoo, B. Manna, and K. G. Sharma, "Seismic Stability Analysis of Un-Reinforced and Reinforced Soil Slopes," vol. 3, pp. 74–81, 2016, doi: 10.1061/9780784480007.009.

[8] S. Sahoo, B. Manna, and K. G. Sharma, "Stability analysis of steep nailed slopes under seismic condition using 3-D finite element method," *Int. J. Geotech. Eng.*, vol. 9, no. 5, pp. 536–540, 2015, doi: 10.1179/1939787914Y.0000000084.

[9] B. Manna, S. Rawat, R. Zodinpuii, and K. G. Sharma, "Effect of surcharge load on stability of slopes - testing and analysis," *Electron. J. Geotech. Eng.*, vol. 19 N, no. October 2017, pp. 3397–3410, 2014.

[10] S. Rawat, R. Zodinpuii, B. Manna, and K. G. Sharma, "Investigation on failure mechanism of nailed soil slopes under surcharge loading: testing and analysis," *Geomech. Geoengin.*, vol. 9, no. 1, pp. 18–35, 2014, doi: 10.1080/17486025.2013.804211.

[11] FHWA, "Soil Nail Walls Reference Manual," *Geotech. Eng. Circ. NO. 7 - Soil Nail Walls Ref. Man.*, no. 132085, p. 425, 2015, [Online]. Available: https://www.fhwa.dot.gov/engineering/geotech/pubs/nhi14007.pdf.

[12] C. C. Meng and Y.-C. Tan, "Soil Nail Design : A Malaysian Perspective," *Int. Conf. Slopes*, pp. 379–400, 2006.

[13] J. Liu, K. Shang, and X. Wu, "Stability Analysis and Performance of Soil-Nailing Retaining System of Excavation during Construction Period," *J. Perform. Constr.*

Facil., vol. 30, no. 1, 2016, doi: 10.1061/(asce)cf.1943-5509.0000640.

[14] A. K. Kokane, V. A. Sawant, and J. P. Sahoo, "Seismic stability analysis of nailed vertical cut using modified pseudo-dynamic method," *Soil Dyn. Earthq. Eng.*, vol. 137, no. May, p. 106294, 2020, doi: 10.1016/j.soildyn.2020.106294.

[15] B. R. A. Jewell and M. J. Pedley, "Analysis for s o i l reinforcement with bending stiffness," vol. 118, no. 10, pp. 1505–1528, 1993.

[16] W. K. Pun, W. M. Cheung, and K. W. Shum, "Geoguide 7 - Guide to Soil Nail Design and Construction," *Proc. 17th Int. Conf. Soil Mech. Geotech. Eng. Acad. Pract. Geotech. Eng.*, vol. 2, pp. 1465–1468, 2009, doi: 10.3233/978-1-60750-031-5-1465.

[17] Carlos A. Lazarte et al, "Geotechnical Engineering Circular No. 7," *Tech. Man.*, no. FHWA0-IF-03–017, 2003.

[18] S. Suman, S. Z. Khan, S. K. Das, and S. K. Chand, "Slope stability analysis using artificial intelligence techniques," *Nat. Hazards*, vol. 84, no. 2, pp. 727–748, 2016, doi: 10.1007/s11069-016-2454-2.

[19] A. Chebrolu, S. K. Sasmal, R. N. Behera, and S. K. Das, "Prediction of Factor of Safety For Slope Stability Using Advanced Artificial Intelligence Techniques," *Adv. Intell. Syst. Comput.*, vol. 949, pp. 173–181, 2020, doi: 10.1007/978-981-13-8196-6_16.

[20] S. K. Das, R. K. Biswal, N. Sivakugan, and B. Das, "Classification of slopes and prediction of factor of safety using differential evolution neural networks," *Environ. Earth Sci.*, vol. 64, no. 1, pp. 201–210, 2011, doi: 10.1007/s12665-010-0839-1.

[21] H. Imam *et al.*, "Shallow Landslide Site Characterization using Electrical Resistivity Technique (ERT) at Balukhali Rohingya Refugee Camps of Ukhiya, Cox's Bazar, Bangladesh," *Eur. J. Eng. Technol. Res.*, vol. 8, no. 1, pp. 46–53, 2023, doi: 10.24018/ejeng.2023.8.1.2932.

[22] E. U. Pahlowan and A. T. M. S. Hossain, "Jamuna river erosional hazards, accretion & annual water discharge-A remote sensing & GIS approach," *Int. Arch. Photogramm. Remote Sens. Spat. Inf. Sci. - ISPRS Arch.*, vol. 40, no. 7W3, pp. 831–835, 2015, doi: 10.5194/isprsarchives-XL-7-W3-831-2015.

[23] A. Burman, S. P. Acharya, R. R. Sahay, and D. Maity, "A Comparative Study of Slope Stability Analysis Using Traditional Limit Equilibrium Method and Finite Element Method.," *ASIAN J. Civ. Eng.*, vol. 16, no. 4, pp. 467–492, 2015.

[24] V. Kumar and S. Kumari, "Impact on slopes with development of shear band," *Int. J. Adv. Technol. Eng. Explor.*, vol. 9, no. 94, pp. 1260–1275, 2022, doi: 10.19101/IJATEE.2021.875841.

[25] A. Sengupta and A. Upadhyay, "Locating the critical failure surface in a slope stability analysis by genetic algorithm," *Appl. Soft Comput. J.*, vol. 9, no. 1, pp. 387–392, 2009, doi: 10.1016/j.asoc.2008.04.015.

[26] D. Giri and A. Sengupta, "Dynamic behavior of small scale nailed soil slopes," *Geotech. Geol. Eng.*, vol. 27, no. 6, pp. 687–698, 2009, doi: 10.1007/s10706-009-9268-x.

[27] N. Himanshu, V. Kumar, A. Burman, D. Maity, and B. Gordan, "Grey wolf

optimization approach for searching critical failure surface in soil slopes," *Eng. Comput.*, vol. 37, no. 3, pp. 2059–2072, 2021, doi: 10.1007/s00366-019-00927-6.

[28] S. Q. Luo, S. A. Tan, W. Cheang, and K. Y. Yong, "Elastoplastic analysis of pull-out resistance of soil nails in dilatant soils," *Proc. Inst. Civ. Eng. - Gr. Improv.*, vol. 6, no. 4, pp. 153–161, 2002, doi: 10.1680/grim.2002.6.4.153.

[29] S. Rawat and A. K. Gupta, "Numerical modelling of pullout of helical soil nail," *J. Rock Mech. Geotech. Eng.*, vol. 9, no. 4, pp. 648–658, 2017, doi: 10.1016/j.jrmge.2017.01.007.

[30] S. Rawat and A. K. Gupta, "Testing and modelling of screw nailed soil slopes," *Indian Geotech. J.*, vol. 48, no. 1, pp. 52–71, 2018, doi: 10.1007/s40098-017-0229-7.

[31] S. Rawat and A. K. Gupta, "An experimental and analytical study of slope stability by soil nailing," *Electron. J. Geotech. Eng.*, vol. 21, no. 17, pp. 5577–5597, 2016.

[32] A. Pant, M. Datta, and G. V. Ramana, "Bottom ash as a backfill material in reinforced soil structures," *Geotext. Geomembranes*, vol. 47, no. 4, pp. 514–521, 2019, doi: 10.1016/j.geotexmem.2019.01.018.

[33] G. Brunet and P. Bertolo, "Flexible facing analysis for soil nailing," no. August, pp. 1–20, 2010.

[34] K. Tei, R. Neil Taylor, and G. W. E. Milligan, "Centrifuge model tests of nailed soil slopes," *Soils Found.*, vol. 38, no. 2, pp. 165–177, 1998, doi: 10.3208/sandf.38.2_165.

[35] P. Sharma, S. Rawat, and A. K. Gupta, "Laboratory investigation of pullout behavior of hollow and solid shaft helical nail in frictional soil," *Acta Geotech.*, vol. 16, no. 4, pp. 1205–1230, 2021, doi: 10.1007/s11440-020-01069-6.

[36] P. Sharma, *Behavior Of Helical Soil Nails: An Experimental And Theoretical Behavior of Helical Soil Nails : An Experimental and Theoretical Study*, no. Ph.D thesis, Department of Civil Engineering, Jaypee University of Information Technology Solan. 2021.

[37] P. Sharma, S. Rawat, and A. K. Gupta, "Force–Displacement Characteristics of Helical Soil Nail under Monotonic Pullout Loading: Experimental and Theoretical Study," *Indian Geotech. J.*, vol. 51, no. 4, pp. 757–772, 2021, doi: 10.1007/s40098-021-00515-w.

[38] H. Rahardjo, Y. Kim, N. Gofar, E. C. Leong, C. L. Wang, and J. L. H. Wong, "Field instrumentations and monitoring of GeoBarrier System for steep slope protection," *Transp. Geotech.*, vol. 16, no. June, pp. 29–42, 2018, doi: 10.1016/j.trgeo.2018.06.006.

[39] Y. Sutejo and N. Gofar, "Effect of area development on the stability of cut slopes," *Procedia Eng.*, vol. 125, pp. 331–337, 2015, doi: 10.1016/j.proeng.2015.11.071.

[40] C. Kolay, A. Prashant, and S. K. Jain, "Nonlinear dynamic analysis and seismic coefficient for abutments and retaining walls," *Earthq. Spectra*, vol. 29, no. 2, pp. 427–451, 2013, doi: 10.1193/1.4000141.

[41] D. Chavan, G. Mondal, and A. Prashant, "Seismic analysis of nailed soil slope considering interface effects," *Soil Dyn. Earthq. Eng.*, vol. 100, no. October 2015, pp. 480–491, 2017, doi: 10.1016/j.soildyn.2017.06.024.

[42] B. Pradhan, L. G. Tham, Z. Q. Yue, S. M. Junaideen, and C. F. Lee, “Soil – Nail Pullout Interaction in Loose Fill Materials,” vol. 6, no. 4, pp. 238–247, 2007.

[43] Q. Wang, W. Ahmad, A. Ahmad, F. Aslam, A. Mohamed, and N. I. Vatin, “Application of Soft Computing Techniques to Predict the Strength of Geopolymer Composites,” *Polymers (Basel).*, vol. 14, no. 6, 2022, doi: 10.3390/polym14061074.

[44] S. R. Abid, G. Murali, M. Amran, N. Vatin, R. Fediuk, and M. Karelina, “Evaluation of mode II fracture toughness of hybrid fibrous geopolymer composites,” *Materials (Basel).*, vol. 14, no. 2, pp. 1–14, 2021, doi: 10.3390/ma14020349.

[45] J. P. Turner and W. G. Jensen, “Landslide Stabilization Using Soil Nail and Mechanically Stabilized Earth Walls: Case Study,” *J. Geotech. Geoenvironmental Eng.*, vol. 131, no. 2, pp. 141–150, 2005, doi: 10.1061/(asce)1090-0241(2005)131:2(141).

[46] S. J. Vitton, W. W. Harris, M. F. Whitman, and R. Y. Liang, “Application of anchored geosynthetic systems for in situ slope stabilization of fine-grained soils,” *Transp. Res. Rec.*, no. 1633, pp. 94–101, 1998, doi: 10.3141/1633-12.

[47] Y. Hu and P. Lin, “Probabilistic Prediction of Maximum Tensile Loads in Soil Nails,” *Adv. Civ. Eng.*, vol. 2018, pp. 10–13, 2018, doi: 10.1155/2018/3410146.

[48] B. Khirwadkar and R. Mahajan, “Numerical analysis of shored reinforced soils walls,” *11th Int. Conf. Geosynth. 2018, ICG 2018*, vol. 3, no. September, pp. 2012–2019, 2018.

[49] B. Joshi, “Behavior of Calculated Nail Head Strength in Soil-Nailed Structures,” *J. Geotech. Geoenvironmental Eng.*, vol. 129, no. 9, pp. 819–828, 2003, doi: 10.1061/(asce)1090-0241(2003)129:9(819).

[50] H. Liu, L. Tang, P. Lin, and G. Mei, “Accuracy assessment of default and modified federal highway administration (FHWA) simplified models for estimation of facing tensile forces of soil nail walls,” *Can. Geotech. J.*, vol. 55, no. 8, pp. 1104–1115, 2018, doi: 10.1139/cgj-2017-0237.

[51] J. Liu, X. Rong, and P. Lin, “Numerical simulation of wave propagation along a soil nail,” *68e Conférence Can. Géotechnique 7e Conférence Can. sur le Pergélisol, 20 au 23 Sept. 2015, Québec, Québec.*, no. September, 2015.

[52] J. S. dan S. ITS, “BS EN 14490:2010 Execution of special geotechnical works-Soil nailing,” vol. 6, no. 1, pp. 51–66, 2010.

[53] J. C. Jimenez Fernandez *et al.*, “3D numerical simulation of slope-flexible system interaction using a mixed FEM-SPH model,” *Ain Shams Eng. J.*, vol. 13, no. 2, p. 101592, 2022, doi: 10.1016/j.asej.2021.09.019.

[54] M. A. Naveed, Z. Ali, A. Qadir, U. N. Latif, S. Hamid, and U. Sarwar, “Geotechnical forensic investigation of a slope failure on silty clay soil—A case study,” *Front. Struct. Civ. Eng.*, vol. 14, no. 2, pp. 501–517, 2020, doi: 10.1007/s11709-020-0610-y.

[55] T. T. Bui, M. Bost, A. Limam, J. P. Rajot, and P. Robit, “Modular precast concrete facing for soil-nailed retaining walls: laboratory study and in situ validation,” *Innov. Infrastruct. Solut.*, vol. 5, no. 1, 2020, doi: 10.1007/s41062-019-0250-z.

[56] M. Cala, M. Stolz, P. Baraniak, A. Rist, and A. Roduner, “Large scale field tests for

slope stabilizations made with flexible facings," *ISRM Int. Symp. - EUROCK 2013*, no. February 2018, pp. 659–662, 2013, doi: 10.1201/b15683-111.

[57] S.-X. I. S. On Landslides and C. Cartagena, "Results of large-scale testing of high-tensile steel meshes and soil nails for ground surface support and validation of modelling software," *Int. Soc. Soil Mech. Geotech. Eng.*, no. June 2020, 2021.

[58] J. Wang, W. Zhong, Z. Lin, and Y. Tang, "Dynamic Response and Geogrid Strain Analysis of GRS Retaining Wall," *Appl. Sci.*, vol. 12, no. 19, 2022, doi: 10.3390/app12199930.

[59] N. Sanvitale, P. Simonini, A. Bisson, and S. Cola, "Role of the facing on the behaviour of soil-nailed slopes under surcharge loading," *18th Int. Conf. Soil Mech. Geotech. Eng. Challenges Innov. Geotech. ICSMGE 2013*, vol. 3, no. September, pp. 2091–2094, 2013.

[60] V. M. Rotte and B. V. S. Viswanadham, "Centrifuge and Numerical Model Studies on the Behaviour of Soil-Nailed Slopes with and without Slope Facing," no. 1996, pp. 581–591, 2014, doi: 10.1061/9780784413449.056.

[61] S. Pokharel, D. Ph, I. Willems, and M. Pierson, "Use of Flexible Facing for Soil Nail Walls," *Transportation (Amst).*, no. November, 2011.

[62] L. M. L. Megal, "High Capacity Reinforced Flexible Systems for Slope Stabilization: An Outstanding Technology, Not Well Known.," pp. 1694–1703, 2013, doi: 10.1061/9780784412787.170.

[63] P. Bertolo, C. Oggeri, and D. Peila, "Full-scale testing of draped nets for rock fall protection," *Can. Geotech. J.*, vol. 46, no. 3, pp. 306–317, 2009, doi: 10.1139/T08-126.

[64] C. Balg and Lopamudra Dutta, "Flexible Slope Stabilization Systems Made From Hightensile Steel Wire," 2016.

[65] A. Pol and F. Gabrieli, "Anchor plate bearing capacity in flexible mesh facings," *Soils Found.*, vol. 62, no. 6, p. 101222, 2022, doi: 10.1016/j.sandf.2022.101222.

[66] D. Cheer and G. Giacchetti, "Rock and soil slope protection using a high stiffness geocomposite mesh system," pp. 1273–1284, 2013, doi: 10.36487/acg_rep/1308_90_cheer.

[67] Geoguide 7, "Guide to Soil Nail Design and Construction," *Guid. To Soil Nail Des. Constr.*, p. 100, 2008.

[68] W. K. Pun and Y. K. Shiu, "Design Practice and Technical Developments of Soil Nailing in Hong Kong," *HKIE Geotech. Div. 27th Annu. Semin. Geotech. Adv. Hong Kong Since 1970s*, pp. 197–212, 2007.

[69] Y. K. Shiu and G. W. K. Chang, "Soil Nail Head Review Geo Report No. 175 Geotechnical Engineering Office Civil Engineering and Development Department the Government Of The Hong Kong Special Administrative Region," no. 175.

[70] Y. K. Shiu and G. W. K. Chang, "Effects of Inclination, Length Pattern and Bending Stiffness of Soil Nails on Behaviour of Nailed Structures, GEO Report No. 197, Geotechnical Engineering Office, Hong Kong.," no. 197, 2005.

[71] R. B. J. Brinkgrere, “Copyright ASCE 2005 69 Soil Constitutive Models Evaluation, Selection, and Calibration,” *Geo-Frontiers Congr. 2005*, pp. 69–98, 2005.

[72] R. C. H. Koo and J. S. H. Kwan, “A Numerical Study of Dynamic Responses of Two Selected Flexible Barriers Subject to Punching and Areal Loads,” no. 323, p. 48, 2016.

[73] V. M. Rotte and B. V. S. Viswanadham, “Influence of nail inclination and facing material type on soil-nailed slopes,” *Proc. Inst. Civ. Eng. Gr. Improv.*, vol. 166, no. 2, pp. 86–107, 2013, doi: 10.1680/grim.11.00026.

[74] V. Bvs and R. Vm, “Effect of facing type on the behaviour of soil-nailed slopes: centrifuge and numerical study,” *Discovery*, vol. 46, no. 215, pp. 214–223, 2015, [Online]. Available: www.discoveryjournals.com.

[75] V. M. Rotte, B. V. S. Viswanadham, and D. Chourasia, “Influence of slope geometry and nail parameters on the stability of soil-nailed slopes,” *Int. J. Geotech. Eng.*, vol. 5, no. 3, pp. 267–281, 2011, doi: 10.3328/IJGE.2011.05.03.267-281.

[76] M. H. Mohamed, M. Ahmed, J. Mallick, and S. AlQadhi, “Finite Element Modeling of the Soil-Nailing Process in Nailed-Soil Slopes,” *Appl. Sci.*, vol. 13, no. 4, 2023, doi: 10.3390/app13042139.

[77] T. Yang, J. F. Zou, and Q. J. Pan, “Three-dimensional seismic stability of slopes reinforced by soil nails,” *Comput. Geotech.*, vol. 127, no. June, p. 103768, 2020, doi: 10.1016/j.compgeo.2020.103768.

[78] V. Kumar, H. M. Azamathulla, K. V. Sharma, D. J. Mehta, and K. T. Maharaj, “The State of the Art in Deep Learning Applications, Challenges, and Future Prospects: A Comprehensive Review of Flood Forecasting and Management,” *Sustain.*, vol. 15, no. 13, 2023, doi: 10.3390/su151310543.

[79] P. Paul and K. Tota-Maharaj, “Laboratory Studies on Granular Filters and Their Relationship to Geotextiles for Stormwater Pollutant Reduction,” *Water (Switzerland)*, vol. 7, no. 4, pp. 1595–1609, 2015, doi: 10.3390/w7041595.

[80] K. H. Yang, J. N. Thuo, J. W. Chen, and C. N. Liu, “Failure investigation of a geosynthetic-reinforced soil slope subjected to rainfall,” *Geosynth. Int.*, vol. 26, no. 1, pp. 42–65, 2019, doi: 10.1680/jgein.18.00035.

[81] I. Juran, “Nailed-Soil Retaining Structures: Design and Practice.,” *Transp. Res. Rec.*, pp. 139–150, 1987.

[82] S. Firat, “Stability analysis of pile-slope system,” *Sci. Res. Essays*, vol. 4, no. 9, pp. 842–852, 2009.

[83] A. Pol and F. Gabrieli, “Discrete element simulation of wire-mesh retaining systems: An insight into the mechanical behaviour,” *Comput. Geotech.*, vol. 134, no. March, p. 104076, 2021, doi: 10.1016/j.compgeo.2021.104076.

[84] A. Sheikhbahaei, A. M. Halabian, and S. H. Hashemolhosseini, “Lateral Earth Pressure Analysis of Soil-Nailed Walls under Static Conditions using Finite Difference Method,” *GeoHalifax*, pp. 353–360, 2009.

[85] Q. B. Bui, T. T. Bui, M. Jaffré, and L. Teytu, “Steel nail embedded in rammed earth wall to support vertical loads: An investigation,” *Constr. Build. Mater.*, vol. 234, p. 117836, 2020, doi: 10.1016/j.conbuildmat.2019.117836.

[86] C.-Y. Hong, J.-H. Yin, W.-H. Zhou, and H.-F. Pei, “Analytical Study on Progressive Pullout Behavior of a Soil Nail,” *J. Geotech. Geoenvironmental Eng.*, vol. 138, no. 4, pp. 500–507, 2012, doi: 10.1061/(asce)gt.1943-5606.0000610.

[87] T. Nalgire, D. P. P, M. A.A, and H. P.D, “Slope Stability Analysis by GeoSlope,” *Helix*, vol. 10, no. 1, pp. 71–75, 2020, doi: 10.29042/2020-10-1-71-75.

[88] Z. Dai, C. Zhao, C. Guo, and P. Lin, “System Reliability Analysis of Soil Nail Walls against Facing Failures,” *Int. J. Geomech.*, vol. 21, no. 9, pp. 1–18, 2021, doi: 10.1061/(asce)gm.1943-5622.0002134.

[89] M. Sharma, M. Samanta, and S. Sarkar, “Soil nailing: An effective slope stabilization technique,” *Adv. Nat. Technol. Hazards Res.*, vol. 50, pp. 173–199, 2019, doi: 10.1007/978-3-319-77377-3_9.

[90] A. Srivastava and G. L. S. Babu, “Effect of soil variability on the bearing capacity of clay and in slope stability problems,” *Eng. Geol.*, vol. 108, no. 1–2, pp. 142–152, 2009, doi: 10.1016/j.enggeo.2009.06.023.

[91] P. Lin, P. Ni, C. Guo, and G. Mei, “Mapping soil nail loads using federal highway administration (FHWA) simplified models and artificial neural network technique,” *Can. Geotech. J.*, vol. 57, no. 10, pp. 1453–1471, 2020, doi: 10.1139/cgj-2019-0440.

[92] T. T. T. Phan and M. W. Gui, “Soil nailing behaviour for slope stabilization: A case study,” *IOP Conf. Ser. Mater. Sci. Eng.*, vol. 527, no. 1, 2019, doi: 10.1088/1757-899X/527/1/012037.

[93] C. Alston, “Construction of a Geogrid-and Geocomposite-Faced Soil-Nailed Slope Reinforcement Project in Eastern Canada,” *Transp. Res. Rec.*, vol. 1330, p. 87, 1991.

[94] Z. Xu, Y. Ding, L. Yao, and Q. Li, “Application of the soil nailing wall on foundation engineering,” *Adv. Mater. Res.*, vol. 418–420, pp. 739–743, 2012, doi: 10.4028/www.scientific.net/AMR.418-420.739.

[95] H. Taek kim Hong, Kwon young ho, cho yong, “An Experimental Study of the Soil Nailed Wall Behavior with Front Plate Rigidity.” .

[96] Y.-C. Tan and C.-M. Chow, “Slope Stabilization Using Soil Nails : Design Assumptions and Construction Realities,” *Malaysia-Japan Symp. Geohazards*, pp. 2277–2280, 2004, [Online]. Available: http://gnpgeo.com.my/download/publication/2004_11.pdf.

[97] G. L. S. Babu and V. P. Singh, “Simulation of Soil Nail Structures Using PLAXIS 2D,PLAXIS Bulletin, Spring Issue,” *Plaxis Bull.*, no. December, pp. 16–21, 2009.

[98] A. G. L. Sivakumar, B. Associate, and V. Pratap, “Simulation of Soil Nail Structures using PLAXIS 2D,” no. December, pp. 16–21, 2009.

[99] M. Yazdandoust, “Experimental study on seismic response of soil-nailed walls with permanent facing,” *Soil Dyn. Earthq. Eng.*, vol. 98, no. April, pp. 101–119, 2017, doi: 10.1016/j.soildyn.2017.04.009.

[100] S. Ghareh, “Parametric assessment of soil-nailing retaining structures; strain absorption in anchors,” *Int. J. Eng. Technol. Sci.*, vol. 03, no. 02, pp. 101–111, 2015.

[101] S. S. Chowdhury, K. Deb, and A. Sengupta, “Estimation of Design Parameters for

Braced Excavation: Numerical Study," *Int. J. Geomech.*, vol. 13, no. 3, pp. 234–247, 2013, doi: 10.1061/(asce)gm.1943-5622.0000207.

[102] V. Deepa and B. V. S. Viswanadham, "Centrifuge model tests on soil-nailed slopes subjected to seepage," *Proc. Inst. Civ. Eng. Gr. Improv.*, vol. 162, no. 3, pp. 133–144, 2009, doi: 10.1680/grim.2009.162.3.133.

[103] M. Moradi, A. P. Babaki, and M. Sabermahani, "Effect of Nail Arrangement on the Behavior of Convex Corner Soil-Nailed Walls," vol. 146, no. 5, pp. 1–12, 2020, doi: 10.1061/(ASCE)GT.1943-5606.0002235.

[104] N. N. S. Chou, T.-Y. Liu, P.-H. Chen, C.-C. Fan, and J. Zhang, "Failure Investigation and Sustainable Renovation for Slope at National Chi Nan University in Taiwan," *J. Perform. Constr. Facil.*, vol. 34, no. 5, p. 04020085, 2020, doi: 10.1061/(asce)cf.1943-5509.0001459.

[105] R. M. Linhares, S. H. Mirmoradi, and M. Ehrlich, "Evaluation of the effect of surcharge on the behavior of geosynthetic-reinforced soil walls," *Transp. Geotech.*, vol. 31, no. June, p. 100634, 2021, doi: 10.1016/j.trgeo.2021.100634.

[106] I. P. Damians, R. J. Bathurst, A. Josa, A. Lloret, and P. J. R. Albuquerque, "Vertical-Facing Loads in Steel-Reinforced Soil Walls," *J. Geotech. Geoenvironmental Eng.*, vol. 139, no. 9, pp. 1419–1432, 2013, doi: 10.1061/(asce)gt.1943-5606.0000874.

[107] J. Lehn, M. Sc, and D.-I. habil Ernö Biczók, "Numerical modelling of soil nailing combined with flexible facing for slope stabilization."

[108] R. J. Bathurst, N. Vlachopoulos, D. L. Walters, P. G. Burgess, and T. M. Allen, "The influence of facing stiffness on the performance of two geosynthetic reinforced soil retaining walls," *Can. Geotech. J.*, vol. 43, no. 12, pp. 1225–1237, 2006, doi: 10.1139/T06-076.

[109] S. Farrand and A. Teen, "Seismically induced landslide mitigation using flexible slope stabilisation systems," *2008 New Zeal. Eathquake Eng. …*, no. 55, 2008, [Online]. Available: https://citeseerx.ist.psu.edu/viewdoc/download?doi=10.1.1.524.1761&rep=rep1&type=pdf.

[110] M. Rabie, "Performance of hybrid MSE/Soil Nail walls using numerical analysis and limit equilibrium approaches," *HBRC J.*, vol. 12, no. 1, pp. 63–70, 2016, doi: 10.1016/j.hbrcj.2014.06.012.

[111] H. Hu and P. Lin, "Model Uncertainty in Predicting Facing Tensile Forces of Soil Nail Walls Using Bayesian Approach," *Math. Probl. Eng.*, vol. 2019, 2019, doi: 10.1155/2019/5076438.

[112] A. Johari, A. K. Hajivand, and S. M. Binesh, "System reliability analysis of soil nail wall using random finite element method," *Bull. Eng. Geol. Environ.*, vol. 79, no. 6, pp. 2777–2798, 2020, doi: 10.1007/s10064-020-01740-y.

[113] A. D. Barley, "Soil nailing case histories and developments," *Retaining Struct. Proc. Conf. Cambridge, 1992*, pp. 559–573, 1993.

[114] T. T. Bui *et al.*, "Modular precast concrete facing for soil nailed retaining walls : Laboratory study and in situ validation To cite this version : HAL Id : hal-02415778," 2019.

[115] C. Mosser, “Numerical Study on the Behaviour of Soil Nails,” no. May, pp. 1–116, 2016.

[116] C. C. Fan and J. H. Luo, “Numerical study on the optimum layout of soil-nailed slopes,” *Comput. Geotech.*, vol. 35, no. 4, pp. 585–599, 2008, doi: 10.1016/j.compgeo.2007.09.002.

[117] T. S. Ann, W. Cheang, O. P. Hai, and D. Tan, “Finite Element Analysis of A Soil Nailed Slope-Some Recent Experience,” *3rd Asian Reg. Conf. Geosynth. GeoAsia*, pp. 183–192, 2004.

[118] E. Guler, M. Hamderi, and M. M. Demirkan, “Numerical analysis of reinforced soil-retaining wall structures with cohesive and granular backfills,” *Geosynth. Int.*, vol. 14, no. 6, pp. 330–345, 2007, doi: 10.1680/gein.2007.14.6.330.

[119] R.B.J. Brinkgreve and W. Broere, “Plaxis 3D Foundation Reference Manual,” vol. 58, no. 2, pp. 243–249, 2015.

[120] V. Jaya, J. Annie, and M. T. Student, “a Numerical Investigation of Nailed Vertical Soil Wall Using Pseudo-Static Approach,” no. 1996, pp. 0–3, 2011.

[121] S. Zamiran, H. Ghojavand, and H. Saba, “Numerical analysis of soil nail walls under seismic condition in 3D form excavations,” *Appl. Mech. Mater.*, vol. 204–208, pp. 2671–2676, 2012, doi: 10.4028/www.scientific.net/AMM.204-208.2671.

[122] X. T. H. Tang, “Plaxis Finite Element Modeling And Analysis Of Soil Nailing Support For Deep Foundation Pit,” vol. 1, no. 3, pp. 135–139, doi: 10.25236/FSST.20190321.

[123] M. Moradi, A. Pooresmaeili Babaki, M. Sabermahani, A. P. Babaki, and M. Sabermahani, “Effect of Nail Arrangement on the Behavior of Convex Corner Soil-Nailed Walls,” *J. Geotech. Geoenvironmental Eng.*, vol. 146, no. 5, pp. 1–12, 2020, doi: 10.1061/(asce)gt.1943-5606.0002235.

[124] R. C. and M. S. (2021) Ehrlich M, “Effect of construction and design factors on the behaviour of nailed-soil structures,” *Proc. Inst. Civ. Eng. Geotech. Eng.*, vol. 175, no. 6, pp. 618–630, 2021, doi: 10.1680/jgeen.20.00139.

[125] J. A. Schiavon, C. D. H. C. Tsuha, and L. Thorel, “Scale effect in centrifuge tests of helical anchors in sand,” *Int. J. Phys. Model. Geotech.*, vol. 16, no. 4, pp. 185–196, 2016, doi: 10.1680/jphmg.15.00047.

[126] P. Lin and J. Liu, “Evaluation and calibration of ultimate bond strength models for soil nails using maximum likelihood method,” *Acta Geotech.*, vol. 15, no. 7, pp. 1993–2015, 2020, doi: 10.1007/s11440-019-00883-x.

[127] J. Lehn, E. Biczók, and A. Roduner, “Investigations on load-bearing behavior of soil nailing combined with flexible facing for slope stabilization,” *IOP Conf. Ser. Earth Environ. Sci.*, vol. 710, no. 1, 2021, doi: 10.1088/1755-1315/710/1/012027.

[128] A. Ismail *et al.*, “Application of combined terrestrial laser scanning and unmanned aerial vehicle digital photogrammetry method in high rock slope stability analysis: A case study,” *Meas. J. Int. Meas. Confed.*, vol. 195, no. April, p. 111161, 2022, doi: 10.1016/j.measurement.2022.111161.

[129] A. Kassim, N. Gofar, L. M. Lee, and H. Rahardjo, “Modeling of suction distributions in an unsaturated heterogeneous residual soil slope,” *Eng. Geol.*, vol. 131–132, pp. 70–

82, 2012, doi: 10.1016/j.enggeo.2012.02.005.

[130] N. Saadatkhah, A. Kassim, L. M. Lee, and J. Rahnamarad, “Spatiotemporal regional modeling of rainfall-induced slope failure in Hulu Kelang, Malaysia,” *Environ. Earth Sci.*, vol. 73, no. 12, pp. 8425–8441, 2015, doi: 10.1007/s12665-014-4002-2.

[131] R. A. Jewell, “Application of revised design charts for steep reinforced slopes,” *Geotext. Geomembranes*, vol. 10, no. 3, pp. 203–233, 1991, doi: 10.1016/0266-1144(91)90056-3.

[132] P. Jelušič, B. Žlender, and B. Dolinar, “NLP Optimization Model as a Failure Mechanism for Geosynthetic Reinforced Slopes Subjected to Pore-Water Pressure,” *Int. J. Geomech.*, vol. 16, no. 5, pp. 1–6, 2016, doi: 10.1061/(asce)gm.1943-5622.0000604.

[133] P. Sharma, B. Mouli, R. S. Jakka, and V. A. Sawant, “Economical Design of Reinforced Slope Using Geosynthetics,” *Geotech. Geol. Eng.*, vol. 38, no. 2, pp. 1631–1637, 2020, doi: 10.1007/s10706-019-01118-2.

[134] Y. Modulus and T. Analysis, “The determination of Youngs modulus from the direct shear test,” *Int. J. Rock Mech. Min. Sci. Geomech. Abstr.*, vol. 11, no. 1, p. A5, 1974, doi: 10.1016/0148-9062(74)92243-8.

[135] K. Tei, “A Study of Soil Nailing in Sand,” *Thesis sumitted degree Dr. Philos. Univ. oxford*, 1993.

[136] H. G. Poulos and L. T. Chen, “Pile Response Due to Excavation-Induced Lateral Soil Movement,” *J. Geotech. Geoenvironmental Eng.*, vol. 123, no. 2, pp. 94–99, 1997, doi: 10.1061/(asce)1090-0241(1997)123:2(94).

[137] Kenny and Kawai, “The effect of of bending stiffness of soil nails on wall deformation,” *Earth Reinf. Ochiai*, pp. 6–9, 1996.

[138] G. L. S. Babu and V. P. Singh, “Reliability analysis of soil nail walls,” *Georisk*, vol. 3, no. 1, pp. 44–54, 2009, doi: 10.1080/17499510802541425.

[139] United States. Federal Highway Administration. and French National Research Project CLOUTERRE., *Recommendations clouterre 1991 = Soil nailing recommendations--1991 : for designing, calculating, constructing and inspecting earth support systems using soil nailing*. 1993.

[140] L. Shaw-shong, “Soil Nailing for Slope Strengthening,” *Geotech. Eng.*, no. May, pp. 1–9, 2005.

[141] A. M. L. EHRLICH, M.; ALMEIDA, M. S. S.; LIMA, “Parametric Numerical analyses of soil nailing systems,” *2nd Int. Conf. Soil Reinf.*, no. 2nd International Conference on Soil Reinforcement ,1996.

[142] P. Samui, R. Kumar, U. Yadav, S. Kumari, and D. T. Bui, “Reliability Analysis of Slope Safety Factor by Using GPR and GP,” *Geotech. Geol. Eng.*, vol. 37, no. 3, pp. 2245–2254, 2019, doi: 10.1007/s10706-018-0697-2.

[143] M. Mishra, V. R. Gunturi, and D. Maity, “Teaching–learning-based optimisation algorithm and its application in capturing critical slip surface in slope stability analysis,” *Soft Comput.*, vol. 24, no. 4, pp. 2969–2982, 2020, doi: 10.1007/s00500-019-04075-3.

[144] E. Guler, “Seismic stability of reinforced soil walls Seismic stability of reinforced soil walls,” no. January 2006, 2014.

[145] M. Ehrlich and S. H. Mirmoradi, “Evaluation of the effects of facing stiffness and toe resistance on the behavior of GRS walls,” *Geotext. Geomembranes*, vol. 40, pp. 28–36, 2013, doi: 10.1016/j.geotexmem.2013.07.012.

[146] S. H. Mirmoradi and M. Ehrlich, “Modeling of the compaction-induced stress on reinforced soil walls,” *Geotext. Geomembranes*, vol. 43, no. 1, pp. 82–88, 2015, doi: 10.1016/j.geotexmem.2014.11.001.

[147] G. Nascimento, M. Ehrlich, and S. H. Mirmoradi, “Numerical- simulation of compaction-induced stress for the analysis of RS walls under surcharge loading,” *Geotext. Geomembranes*, vol. 48, no. 4, pp. 532–538, 2020, doi: 10.1016/j.geotexmem.2020.02.011.

List of Publications

Journal Publications

1. **A. Tangri and S. Rawat, "Experimental and Analytical Investigation of Wall Strengthened with Soil Nail Facing: An approach to enhance Soil Stability",** *Int. J. of Sc., Mathematics and Tech. Learning***, vol. 31, no. 2, pp. 780- 791, Dec. 2023.** https://doi.org/10.5281/zenodo.10276414

   (Scopus Indexed, ISSN: 2327-7971 (Print))

2. **A. Tangri and S. Rawat, "**An experimental and analytical study of slope stability utilizing Flexible facing for Soil nail wall", *J. of Harbin Engg Univ***.,** vol 44, no. 12, pp. 321-330, Dec. 2023. **(Scopus Indexed, ISSN: 1006-7043)**

Conference Publications

1. A. Tangri, and S. Rawat, "Study of stress-strain behaviour in soil nail wall using flexible facing." In *IOP Conference Series: Earth and Environmental Science*, vol. 795, no. 1, p. 012039. IOP Publishing, 2021. **(Scopus Indexed)**
2. A. Tangri, and S. Rawat, "Study of Slope Stability Using Flexible Facing." *In Advances in Construction Materials and Sustainable Environment: Select Proceedings of ICCME 2020*, Book vol. Lecture Notes in Civil Engineering, Springer Singapore pp. 747-755., 2022. **(Scopus Indexed)**
3. A. Tangri, and S. Rawat, "Strength Comparison of Flexible Materials for Stability of Slope." *In Earthquake Geotechnics: Select Proceedings of 7th ICRAGEE 2021*, Book vol. Lecture Notes in Civil Engineering, Springer Singapore pp. 373-383, 2022.

   (**Scopus Indexed**)